Wind Turbines for the Power Supply for Offshore Fish Farms

A Case Study for the Norwegian West Coast

ANDREA ASPENES JUSTAD

SUPERVISOR

Prof. Hans Georg Beyer

Abstract

In this thesis the power consumption of a fish farm is set in relation to the expected power production from a wind turbine in order to assess the feasibility of this combination. The fish farm, called Rataren, is located in Sør-Trøndelag and hourly data on power consumption is available in the period 1st February 2016 until 31st August 2016, as a result of change in energy source from diesel generators to the onshore power grid. This is one of Norway's largest fish farms and has 14 cages during the studied period. There are some minor data losses that are removed from the data sets. Wind speed, air and water temperatures at 2.5 masl and 1 mbsl are measured by a Seawatch Midi 185 Buoy at the location, and the data are supplied by SINTEF Ocean. In view of the estimation of the power output of a wind turbine the data on wind speed have to be extrapolated from measuring height to turbine hub height. For this the atmospheric stability, estimated here by the temperature difference between the air and the sea, is taken into account. The classifications used are unstable, slightly unstable, near-neutral, slightly stable and stable, and are characterized by limits of the temperature differences set to -3°C, -1°C, 1°C and 3°C.

Two methods of extrapolating wind speed from measuring height to hub height are considered; the logarithmic law with corrections according to stability and the power law parametrized according to stability. For both methods the complete calculation of key variables requires information that is unavailable in this case of study. The problems faced when using the log law were the determination of stability parameter z/L, but also variation in friction velocity or roughness height. When using the log law in combination with different values for the variables based on literature, there were inconsistencies in the results indicated by unreasonable wind profiles. The more simplified method, the power law, is therefore concluded as the best approximation when this many parameters are unknown. The power law exponents that are used to correspond to each of the atmospheric conditions mentioned are set to 0.07, 0.09, 0.11, 0.13 and 0.15. Hourly mean wind speeds were then calculated using the power law with the exponent for the stability class found to occur at that particular hour. The results show an average wind speed of 7.04 m/s at 65 meters, compared to a measured average of 5.01 m/s at 2.5 meters height.

The hourly power production at site by a Hywind Demo 2.3 MW turbine and a GWP 750 kW turbine was estimated. To analyse the sensitivity of the results to the relation of consumption and production, the hourly consumption is also multiplied by three and by six in two other cases, while being compared to the power production by the Hywind turbine. The production by a wind farm of three GWP turbines are estimated and compared to the other cases, which is similar in capacity to the one Hywind turbine. The 750 kW turbines are considered to be slightly more favourable, as the ratio of energy import to export to the onshore power grid is lower. In all, the results show that wind turbine is not suitable without energy storage or additional power sources. Hence, it is not possible to make a firm conclusion of which turbine is most suitable without further investigations.

Abbreviations

RES = Renewable Energy Sources
O&M = Operation and Maintenance
PV = Photovoltaic (Solar Cell)
MUP = Multi-Use Platform
MOST = Monin-Obukhov Similarity Theory
HAWT = Horizontal Axis Wind Turbine
AEP = Annual Energy Production
RNA = Rotor-Nacelle Assembly
PBL = Planetary Boundary Layer
SL = Surface Layer
Masl = Meters above sea level
Mbsl = Meters below sea level

Nomenclature

z_0 : Roughness height [m]
z : Height [m]
z_r : Reference height [m]
α : Power law exponent [-]
$U(z)$: Wind speed at height z [m/s]
$U(z_r)$: Wind speed at reference height [m/s]
ρ : Air density [kg/m^3]
u^* : Friction velocity [m/s]
k : von Kàrmàn constant [-]
τ_0 : Surface shear stress [N/m^2]
L : Monin-Obukhov length [m]
ζ : Stability parameter [-]
$\overline{\theta_v}$: Mean virtual potential temperature [K]
g : Acceleration due to gravity [m/s^2]
$\overline{(w'\theta')}_s$: Surface virtual potential heat flux [m×K/s]
A_C : Charnock parameter [-]
H_S : Significant wave height [m]
L_P : Peak period wavelength [m]
A : Area [m^2]
v : Wind speed [m/s]
A_b : Blade area [m^2]
D : Drag force [N]
L : Lift force [N]
C_d : Drag coefficient [-]
C_l : Lift coefficient [-]
C_f : Capacity factor [-]
C_p : Power coefficient [-]
a : Axial induction factor [-]
λ : Tip speed ratio [-]

Preface

This is a master thesis submitted in fulfilment of the requirements for the degree of Master of Science in renewable energy at the Department of Engineering Sciences, University of Agder. The work has been conducted under the supervision of Prof. Hans Georg Beyer. The main objective has been to study the possibility of wind turbine as power supply for an offshore fish farm. In the thesis data from Rataren fish farm in Trøndelag, Norway, are examined. The wind resource at site has been extrapolated with the purpose of estimate the power production by Statoil's Hywind Demo 2.3 MW turbine and a GWP 750 kW turbine as accurate as possible.

Andrea Aspenes Justad,
Bergen, Norway,
May 2017.

Table of Contents

List of Figures

List of Tables

1. Introduction

The utilization of wind turbine as power supply for a fish farm will be examined in this thesis. This chapter will present the background and context for the problem, the problem statement, limitations and assumptions, literature review, solution approach, methods and finally the outline of the report.

1.1 Background and Context

Aquaculture is one of the most important industries in Norway but many facilities experience challenges with the environmental impact, partly because they traditionally run on diesel generators and the farms have a high energy consumption. Simultaneously the offshore wind industry is experiencing rapid growth. This subchapter will provide the background for the problem solution by introducing the situation and trends of offshore wind turbines and fish farming industry, and why a possible synergy could be beneficial.

1.1.1 Status and Trends for Wind Turbines

According to WindEurope's report on offshore wind for 2016, Europe had an installed capacity of 12 631 MW from 3 589 wind turbines connected to the grid in 10 countries by the end of the year (WindEurope, 2017a). In comparison, the installed capacity for onshore wind turbines in EU was 141.1 GW, making a total capacity of 153.7 GW combined. Thus, wind energy is now the second largest form of power generation capacity worldwide, replacing coal (now third) and with natural gas fired power stations being the very largest form of power generation capacity. There were investments of 27.5 billion euros in wind onshore and offshore during 2016 in the 28 EU countries. UK had the largest share of this, with investments of 12.7 billion euros (WindEurope, 2017b). As seen from Figure 1 below, the amount of new, offshore installed capacity was much lower in 2016 than in 2015. However, there were a lot of installations done in 2014 that was not connected until 2015. The cumulative capacity is noticeable increasing and will continue to do so for at least the next two years, which is evident if one looks at the number of projects that have currently started construction. It is projected that offshore wind will have a total installed capacity of 24.6 GW by 2020, which is a doubling from today over the next four years (WindEurope, 2017a).
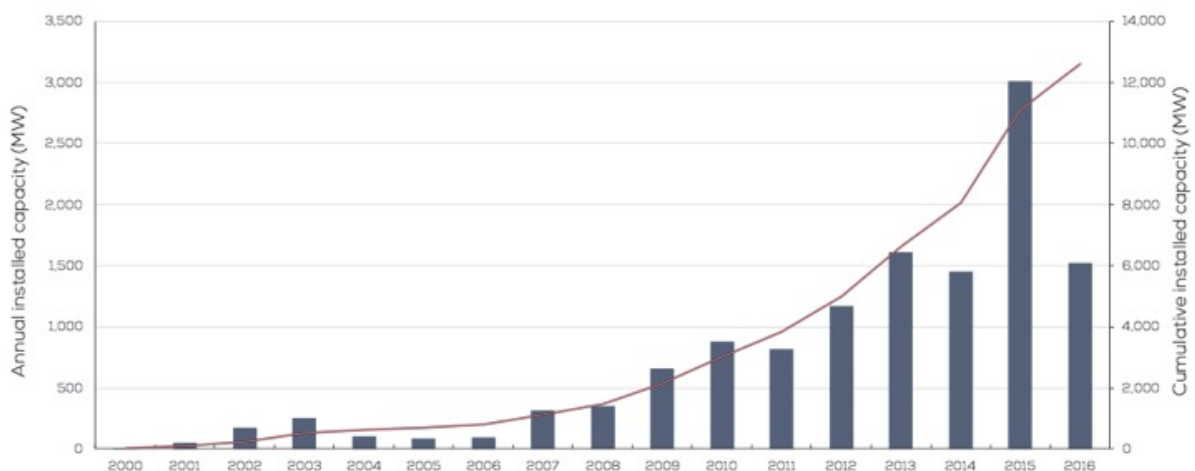
Figure 1: Cumulative and annual offshore wind installations Europe the recent years. Source: WindEurope (2017a).

In 2016, the sea basin where 96.4% of all net capacity had been installed was the North Sea due to its high wind energy availability (Mermaid, 2016), however not in Norwegian waters. One of the reasons are that there is a very uneven distribution of wind energy available in Europe, with very high resources in the North Sea, the Atlantic ocean, and some parts of the Mediterranean and Baltic sea (WindEurope, 2017a). The countries having the most installed capacity offshore in total are United Kingdom, Germany, Denmark and the Netherlands. Norway is the 10th largest on offshore installations, with one floating Hywind Demo Turbine at 2.3 MW installed outside Karmøy (WindEurope, 2017a). From WindEurope's report for offshore wind for 2016, Figure 2 shows the depths and distance from shore (fetch) for bottom-fixed wind farms, where the size of the circle indicates the overall capacity. It is prominent that installations continue to be not much more than at 45-meter water depths, however distance from shore is planned to increase in the near future (WindEurope, 2017a).
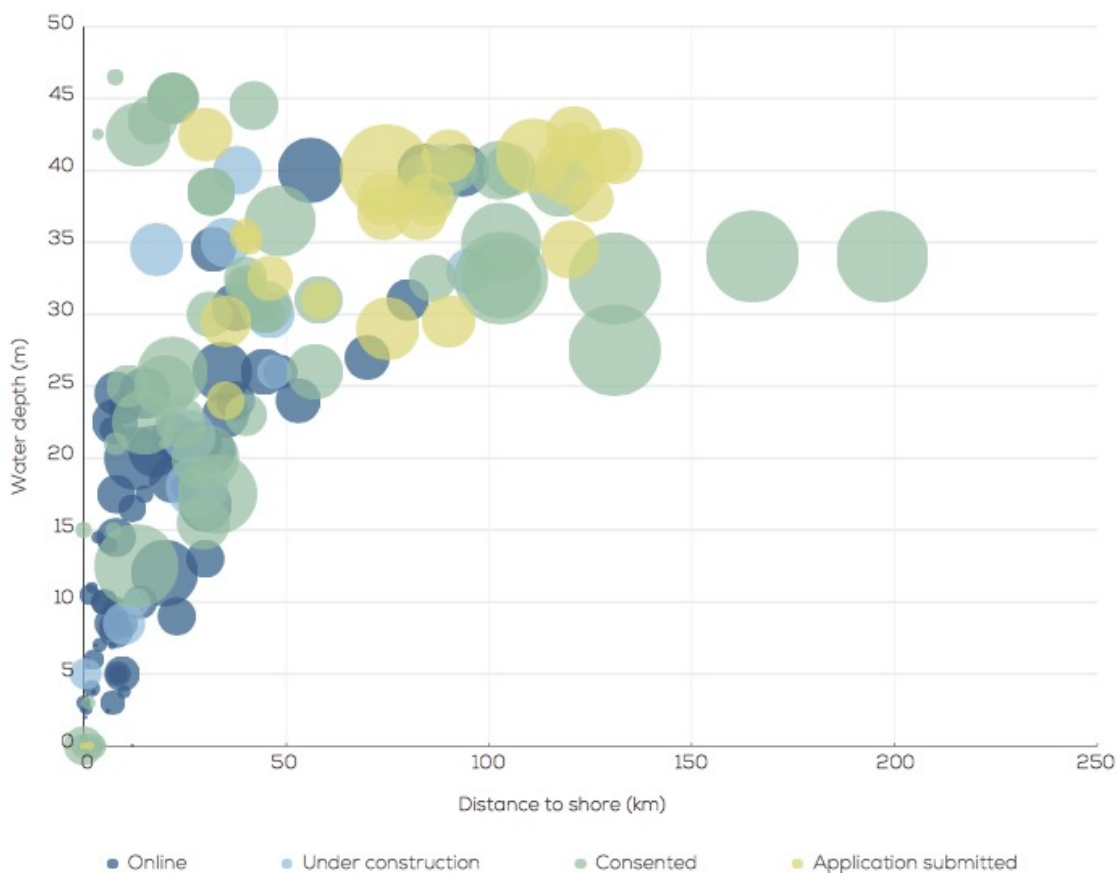
Figure 2: Offshore wind farms distance from shore and water depths per 2016. Source: WindEurope (2017a).

The development of floating turbines recent years makes it possible to install in much deeper waters, and it gives possibilities of expanded use also for stand-alone offshore installations and platforms that are self-dependent in terms of power. Statoil has since 2002 developed a floating wind turbine called Hywind. Its support structure is a spar buoy, i.e. closed cylindrical tube that floats upright in the water. It has a ballast of a few tonnes (depending on the power capacity) at the bottom of the spar that counteract the thrust loads and the weight of the RNA, therefore resisting overturning. There are mooring lines and anchors securing it to the seabed (Manwell, 2009). In 2009 the Hywind Demo turbine with rated power of 2.3 MW, was installed outside Karmøy in south-west of Norway. It has since then produced more power than expected and is very successful. In late 2017 the world's first floating wind park

will start to operate in Scotland, the installation of the five 6 MW turbines is currently ongoing and will constitute the Hywind Pilot Park. The total installed capacity of 30 MW is enough to power around 20 000 UK homes. The cost reduction for the wind park is 60-70% from the Hywind Demo project (Moxnes, 2017). As utilizing much deeper waters becomes possible, the technical potential of wind resource exploitation can increase significantly.

One of the downsides of offshore wind farms is the very large areas of use; to reduce the interference on other turbines' production, the length of 7-8 rotor diameters is often needed as spacing between each turbine. This can result in many square kilometres per farm, even up to 100 km^2 – in comparison to around 2.5 km^2 for fish farms (Mermaid, 2016). Wind farms typically get exclusive rights to areas offshore, making very large areas unusable for other purposes for decades.

1.1.2   The Fish Farming Industry

Over-population is causing a substantial pressure on food production and distribution, among other challenges. A part of the solution can be to rely more on the sea in the future as the earth's surface is composed of 71% water, however many challenges must be overcome. At some coastlines the sea food production is already reaching its maximum capacity limits. Every day the Norwegian seafood industry delivers 38 million meals all over the world alone, this makes it one of the country's most important export products after oil and gas (SjømatNorge, 2017). Only in 2012 the Norwegian aquaculture production reached a first-hand value of 31.4 billion NOK (Myrseth, 2016).

The industry causes a lot of emissions due to the traditional use of diesel generators at the offshore facilities, along with a large power consumption. The most important loads are feeding lines (compressors), light in the cages and operation of the barges. In addition, there are some equipment such as cranes etc. (Næss, 2017). There is now a shift in use of energy source in the fish farm industry in Norway, where Enova has subsidised approximately 10 companies at 30 locations for connecting to the onshore grid by cables as per January 2017 (Knain, 2017). Nevertheless, the installations are costly as the cables can be very long and substations are needed and so on.

Vision 3 of the European Energy plan is to place the power source close to the demand (ECF, 2010). The amount of power transferred on the electricity grids in Europe are pushing their capacity limits, therefore the power source should be located close to the loads where this is possible and stand-alone systems are favourable. DNV GL states: "In the longer term, the offshore wind industry should become integrated with other associated industries such as fishing and aquaculture and thereby share resources and assets that will further reduce operation and maintenance (O&M) costs" (Bosma, 2014). The aquaculture industry has also proclaimed prospects of utilization of renewable energy sources (RES) in the future (Flathagen, 2016b). Getting involved with renewable energy would give the industry a progressive and sustainable profile. Food and Agriculture Organization (FAO) of the United Nations has stated that technological development is one of the major deal breakers for the future development and growth of the aquaculture industry (Subasinghe, 2003).

The available areas closer to shore are becoming few due to conflicting interest between fisheries, tourism and the rapid growth in the fish farming industry. Large areas in Norway are already utilized - some thinks this has reached a critical load on the coastline (SINTEF, 2011). As a consequence, the industry's interest for utilizing exposed areas further offshore is

increasing. Aquaculture in exposed areas is more challenging, not only because of the remoteness (and therefore the costs and time of vessel transport), but also the strong current, high waves and varying and severe wind conditions. This is causing large challenges and enhancing the issues experienced closer to shore.

Because of severe weather conditions and longer distances to shore, power supply failures are more likely to happen. In addition, this is more serious at exposed locations because there are more autonomous operations as human presence may be inhibited or undesirable. Autonomous operations are strongly dependent on reliable power supply. Examples of these operations are feeding, size grading and distribution for best stocking densities, monitoring fish welfare and water quality, net cleaning and structural maintenance. In addition, the regularities of these tasks are important for maintaining sustainable and profitable production (Bjelland, 2015). Hence, it is crucial to ensure that core operations remain uninterrupted by power downtime i.e. caused by severe weather conditions. The trend has been to up-scale traditional cage systems as they are moved further away from shore, and some are also researching and developing closed or semi-closed cages (SINTEFOcean (2015), HaugeAqua (2017), Aquafarm (2017)). This affects the energy demand and ratio of autonomous operations to human labour.

Because of the costs of cables, Zanuttigha (2016) concludes that it is cheaper with stand-alone system than transferring the power to shore by subsea cables, and thereby store the generated power on site or use it for other purposes. Potential advantages by stand-alone configuration listed by Zanuttigha (2016) are firstly the avoidance of substation and export cables, which reduces the environmental impact and significantly decreases the costs, and second, the boost of blue-growth – EUs long term strategy for sustainable growth in the maritime environment and sector – by using renewables instead of diesel generators that are an alternative for some fish farms. There is not a direct income from selling power to the grid but there are savings in avoiding the mainland connection.

According to aPoint, a company who consults the industry on energy measures, a typical fish farm in Norway uses 4-500 000 kWh per year. Demand varies from 200 000 kWh for the smaller and up to 800 000 kWh for the largest farms (Næss, 2017). Compared to diesel generators, where the fuel use can be 70 000 litres diesel per generator per year and the efficiency is about 35%, there are significant benefits to depending on RES instead (Flakne, 2015). Among the benefits of RES compared to diesel generators are no continuous expenses for fuel and fuel transportation, no fuel storage needed at the facility, absence of environmental disadvantages, i.e. emissions, noise and risks regarding spill.

1.2 Problem Statement

Norwegian economy strongly depend on exporting fish and holds a lot of knowledge about offshore operations from oil and gas industry. Hence, innovative work on multiuse on these subjects can have value for the Norwegian offshore industry, that is primarily based on petroleum, because many companies seek to transfer their knowledge to new provident objectives. Statoil – a Norwegian energy company and the world's largest offshore operator – is investing a lot in wind energy and is gaining much experience under the processes of being operators of the Dudgeon wind farm and being involved in several projects in UK and now also in Germany in cooperation with EON. Other international oil and gas companies are also involved with offshore wind, i.e. Shell in the Netherlands.

Focussing on the power consumption side, the world is likely to be more dependent of the sea as source for food, and as the food production industry in general causes massive emissions and harm to the environment, it is essential to have focus on a sustainable growth. For the global view it is crucial to transition from fossil energy sources to renewable energy where this is possible. Research and innovation will spark more research and innovation, and provide more insight in how to combine technologies and in turn more optimization of design. It is important to demonstrate with research that new areas of use are possible to save emissions where there would otherwise generally be diesel generators or other fossil sources for energy, and also that synergies and cooperation between industries can be a win-win situation.

This report should focus on a case study investigating in the possible wind power supply of a fish farm. Fish farming is in the thesis defined as the grow-out phase for the fish that is taking place in cages at sea, located in floating farms moored to the seabed or the shore. A somewhat exposed location would be a benefit due to the suitability of a turbine and wind conditions, and because the trend is to move fish farms further offshore.

The main goal of the thesis is to examine how a wind turbine can supply the electrical load of an offshore fish farm and how well the energy consumption will be covered by the energy supply in the case of study. Wind turbines could possibly produce the power required but the main adverse consequence is the difference in production and consumption – it is not necessarily needed when available and vice versa. This thesis will examine how great this difference will be. In doing so, a crucial task also becomes to extrapolate the wind speed by utilizing the most suitable method. The wind speed distribution at the location is essential for the power production, hence methods of extrapolation of its magnitude from sea level to the height of the generator will be emphasized. The effect of changing unknown variables in methods regarding this will be examined, as these are implemented with some uncertainties.

The power production from a GWP 750 kW turbine and a Hywind Demo 2.3 MW turbine is calculated and compared to the power consumption of a specific fish farms offshore. One of the challenges will be how to get the best match in power supply and demand. Meeting the power consumption requirements at the facility will result in a very low utilization of the amount of power produced, hence an over-dimensioned turbine. Turbine will however, always have hours without sufficient production no matter the size. A lower surplus is likely to be more suitable for a system including energy storage. Because of these contradictions it is not expected to find an optimum solution without regards to energy storage calculations. In the case of a facility supplied by the onshore power grid, it will be studied how much energy can be delivered to the grid. Energy storage is preferable, and will be included if time.

For the specific facility chosen, main questions to be answered in the thesis are:
- How can wind speed be extrapolated between recorded measure height and assumed turbine hub height in the most realistic manner for offshore sites?
- How does the power production compare to the consumption of the fish farm, and what is likely to be the best match of turbine for the fish farm facility chosen?
- How does the key findings change when the ratio of power consumption to turbine capacity becomes different?

1.3 Limitations and Assumptions

This work is mainly limited to be valid only for the site chosen, with its energy consumption during a specific period, the related weather and its time pattern. However, the methods and approach is general and could be transferrable to other sites. The actual possibility of placing a turbine of this size at the site will not be evaluated, neither the structure and complexity of such a hybrid facility. This work will not include economical evaluations. The emphasis is neither on energy storage, however, this is a very important aspect that will be investigated if time. It is important to note that the power demand at a fish farm is changing by season and year, and is depending on where in the growth phase the fish are. Not basing results on data that include different seasons is therefore a limitation in itself. The study may also be limited by the availability of meteorological data. As the wind resources are so rapidly changing, there would ideally be an infinite number of intervals of data on power production and consumption, over a very large timescale. The availability of various data will have a great effect on how comprehensive and realistic the calculations can be.

In the thesis it is assumed no down time for the turbines due to maintenance or other service operations, because this would have to be at an arbitrary chosen time, affecting the production in a non-realistic way. The turbines are assumed to be preforming at their theoretical characteristics; the power curves are assumed to give the realistic output power. Some simplifications are made for the power extraction for the turbines, hereby the assumption that the pitching of the blades and the yaw regulation are instant. The latter is more reasonable when there is only one turbine because there is no big impact of changing wind direction. Wind speed at turbine height is calculated based on assumptions of the unknown parameters in the methods, which gives a simplification to the calculations and hence, an uncertainty to the results as the power in the wind is strongly dependent on the wind velocity. Regarding the power consumption at the fish farm, there are some periods in the data that show zero consumption. In conversation with aPoint, these are regarded as measurement failures and the periods its regarding are excluded from the calculations. Other than that, the data are assumed to be very reliable. The calculations are done in Excel and may have some human error which could affect the results.

1.4 Literature Review

A literature review reveals that there is not much discussion worldwide on the combination of aquaculture within offshore wind farms. According to Wever (2015), the number of events discussed have been increasing each year until 2012, when the number of events were approximately 12. The article states that it is believed that it could offer significant benefits in terms of minimizing the impact on the environment, economics and optimizing spatial planning. However, nearly no experience exists demonstrating the potential impacts of multiple offshore wind energy and aquaculture installations. A few studies were found were the power produced by wind turbines is utilized by the fish farm, however, these systems are very small compared to the ones in this thesis. Also studies were found for very large combining systems of a round 1000 MW in turbine farm capacity, with these sizes the main purpose is to deliver the power to the onshore grid and not only to be used at the fish farm. Both types of studies are presented here.

Michalis (2013) presented the case of a very small size RES system to be applied on offshore aquaculture sites to enable remote monitoring of the feeding management system. The capacity was based on that the power was considered to cover a sea current profiler, a

temperature sensor and an oxygen sensor. Energy consumption from the feeding management system was therefore only 16 Wh per day. The hybrid RES system was decided to include a wind turbine with nominal power of 200W and two photovoltaic (PV) solar cell units of 80Wp each, supplying power to a battery bank. There were two batteries connected in parallel with 90 Ah capacity each and nominal voltage of 12V.

In Toner (2002), a number of different RES are discussed for power supply to aquaculture, including small wind turbines of less than 4.5 kW. Total energy consumption per week for a Pacific oyster farm was 79.3 kWh, for rainbow trout farm it was 280.7 kWh, and for marine recirc farm it was 13 767 kWh. Based on an estimated average wind speed, it was found that it is feasible for oyster farm, but not economic for the rainbow trout farm or marine recirc. It is stated in the report that energy costs are a significant part of operating costs, even though it's often less than salary, feed and stock costs. It is concluded that wind turbines may have a part to play in aquaculture and its solely site dependent, and it's worth exploring if the site has wind speed of 6 m/s or higher (Toner, 2002).

There have been many EU projects under "the oceans of tomorrow" initiative regarding multi-use platforms (MUPs) with purpose of developing multidisciplinary approaches to marine and maritime challenges. This is platforms with a large number of energy conversion units, and hence, main purpose is delivering power to the onshore grid. MUPs are foreseen to be the marine infrastructure of the future as a way of minimizing the impact on environment and the costs of offshore operations. Mermaid (2012-2015) was one of the projects for developing innovative multi-purpose offshore platforms. Four pilot study sites were chosen to be able to make real contributions to design concepts and industrial applications. The final report points to differences between wind farms and aquaculture farms, among them cost characteristics, area sizing, and operational nature. Nevertheless, there can be some common interest regarding the forecast and warning systems, accommodation platforms – although this is most necessary for the fish farm, and possibly sharing of staff. Each industry has however a high focus on their own needs and possibilities, and this is seen as one of the main barriers for MUPs to be realized according to (Christensen, 2016). Regarding one of the sites for MERMAID with wind turbines and aquaculture combined, they state that there are major concerns about unwanted impacts on the ecosystem. Also the costs and environmental effects are very uncertain, and therefore has dominated the discussions to some degree.

In addition to MERMAID, other similar research projects founded by EU are H2OCEAN (2012-2014) and TROPOS (2012-2015), which also have all been a part of the "Ocean of tomorrow" initiative from 2011. In the project H2OCEAN studies were done on the possibility of harvesting wind and wave power and partly using the energy for multiple applications on-site. This would include hydrogen production to be stored and shipped to shore or refuelling at the platform, and for multi-trophic aquaculture farm. (H2OCEAN, 2014). Further it is stated that the energy from wind and wave also would be used in the form of electricity, in addition to hydraulic power, to feed the other energy demanding activities on the platform (H2OCEAN, 2016).

As part of MERMAID, there has been done theoretical case studies on MUPs with a 1000 MW wind farm integrated with both wave farm and fish farm, concluding that there are economic benefits with sharing the infrastructure, installation and O&M. However, the technologies are in developing stages (W. He, Weissenberger, J., et. al. (2011), W. He, Yttervik, R., et. al. (2013)).

In a paper by Zanuttigha (2016), the purpose is to provide a new multi-criteria methodology for the initial design and the selection of the uses of MUPs, and further the methods for the design optimization of projects at specific sites. Evaluation is done by experts on the possible solutions for MUPs with different combinations of wind turbines, wave power and aquaculture, being connected to the onshore grid or as stand-alone system at an area outside Alghero, Sardinia Island, Italy. According to Zanuttigha (2016) there were only a few studies dealing with co-location of aquaculture and wind farms as per January 2016. It is stated that fostering the development of synergies with other activities such as fish farms, transportation and gas platforms are desirable. Different combinations for MUPs are scored and compared, where wind and aquaculture together as a stand-alone system gets good scores on complexity of the installation type, exploitation potential, environmental impact and costs. On total scores, only one solution gets better results, that is if also wave is implemented to the stand-alone wind and aquaculture platform (Zanuttigha, 2016).

Christian Michelsens Research (CMR) Prototec is developing a concept called Green Fish Farming (GFF) where units of RES are incorporated to the fish farm for production of oxygen for the fish and hydrogen for the vessels, among other purposes (Myrseth, 2016).

In a thesis from Haugesund University College in Norway, different RESs and combinations for powering a fish farm are evaluated. It was concluded that the wind was not strong enough at the site, with a mean wind speed of 5.86 m/s, for the one 800 kW wind turbine to supply enough power alone for the very roughly estimated energy consumption of 2416 kWh per 24 hours. However, it was suggested that the wind turbine could be sufficient in combination with fuel cell or battery storage (Haakull, 2016).

The Blauwdruk project had the main objective to study the feasibility of the combination of offshore wind energy production and offshore production of mussels on the Dutch Continental Shelf. There are done scenario analyses with the main purpose to demonstrate the economic feasibility of this combination. The project also evaluates the possibility of the same employees can manage both the wind farm and aquaculture farm. With the conclusion that the "lost hours" for the workers on site can be reduced from 50% to 25 %, resulting in large cost reductions (Lagerveld, 2014).

1.5 The Scheme Applied for Problem Solution

The main steps to cope with the problems stated are as follows. Firstly, collecting power consumption data with as frequent measurements as possible from a specific fish farm is essential. When the site is final, as many data on weather conditions as possible must be collected from the same period, preferably also for different heights. The wind speeds must then be extrapolated from the recorded height to the wind turbine height. The most frequently used methods for this are the logarithmic law (log law) and the power law, both will be presented in the following chapters. The atmospheric stability is essential for wind profile determination and can be estimated based on temperature difference between the sea and the air if these data are available. Each measurement interval of the period will be related to one of five atmospheric stability classes; unstable, slightly unstable, near-neutral, slightly stable or stable conditions. The calculated wind speeds at turbine hub height will then have variations based on stability class and wind speed at measured height. The combination of the datasets gives the background for calculating the possible power production at the site, based on the power curves for a GWP 750 kW turbine and Hywind Demo 2.3 MW turbine. The Hywind turbine is chosen because of its relevance in newer technology; it is floating and can be placed

further offshore for exposed fish farms locations. Excel is chosen as the software for all the computations, however, e.g. Matlab could also be used.

1.6 Report Outline

Chapter 1 has been an introduction to the thesis, in chapter 2 the theoretical background for the work will be presented. Chapter 3 is regarding the methods for the problem solution and in Chapter 4 the results of the study is presented. The results are further compared and discussed in Chapter 5, followed by conclusion and proposals for further work in Chapter 6. References are then listed in Chapter 7 and is followed by appendices.

2. Theoretical Background

In this chapter wind resources, aerodynamics, turbines and wind shear profile will be presented, as they are considered essential theoretical aspects of the thesis. There are many possibilities of wind energy extraction but only what is found most relevant for this work is introduced. Main focus is therefore on three bladed, horizontal axis turbines and offshore specifications. Methods for extrapolating wind speed between different altitudes is of great importance in the thesis and is therefore emphasised.

2.1 Wind Resources and Aerodynamics

The origin of the global wind systems is that the sun heats up the earth's surface and atmosphere unevenly because of the spherical shape of the earth. As air gets warmer its density is reduced and it will rise, which causes differences in atmospheric pressure over the surfaces. Hence, there are movements of air masses from higher pressure to lower pressure areas. Along with the Coriolis force, centrifugal force, gravity and friction forces, this results in the global wind systems. On a smaller scale the winds are affected by the topography and combinations of land and sea, and difference in direction of the heat transport between day and night, which also creates high and low pressure areas (Boyle, 2012). Land and sea breeze occur partly because water has a higher specific heat capacity and is therefore heated at a slower rate than land. As the air over land gets warmer it rises and creates a low pressure that is replaced by the air over the sea, called sea breeze, this cycle is reversed during night. In daily variation there are normally lower wind speeds from midnight to sunrise than during the day. Generally, there are stronger winds during winter season (Manwell, 2009).

The higher the wind speed, the more kinetic energy it holds. When combining the equations for kinetic energy and mass transport per unit of time, the power density of the wind can be written as:

$$\frac{P}{A} = \frac{1}{2}\rho v^3 \quad [\text{W/m}^2] \tag{2.1}$$

A : Area [m^2]
ρ : Air density (kg/m^3]
v : Velocity of the air [m/s]

Air density is a function of both temperature and pressure, and is given as 1.225 kg/m^3 at 15°C and atmospheric pressure at sea level. Equation 2.1 shows the importance of the wind velocity, v, because the wind power is very sensitive to this value as to a power of three. Hence, careful measurements and calculations over a long period of time is a necessity when predicting the available wind power at a site.

Drag and lift are the two forces generated on an object in an air flow. Lift forces are perpendicular to the air flow direction, and turbine devices that are based on lift are the most efficient and therefore the most used (Boyle, 2012). The design of the blades is crucial for the generation of lift forces and determine to a large extent the conversion efficiency of the turbine. The turbine blade design is shown by the cross section in Figure 3, with a convex upper surface, forcing the airflow to accelerate and therefore causing a large reduction in pressure which results in a suction-effect that is called the lift force. In turn, this produces a net positive torque on the rotating shaft of the turbine.
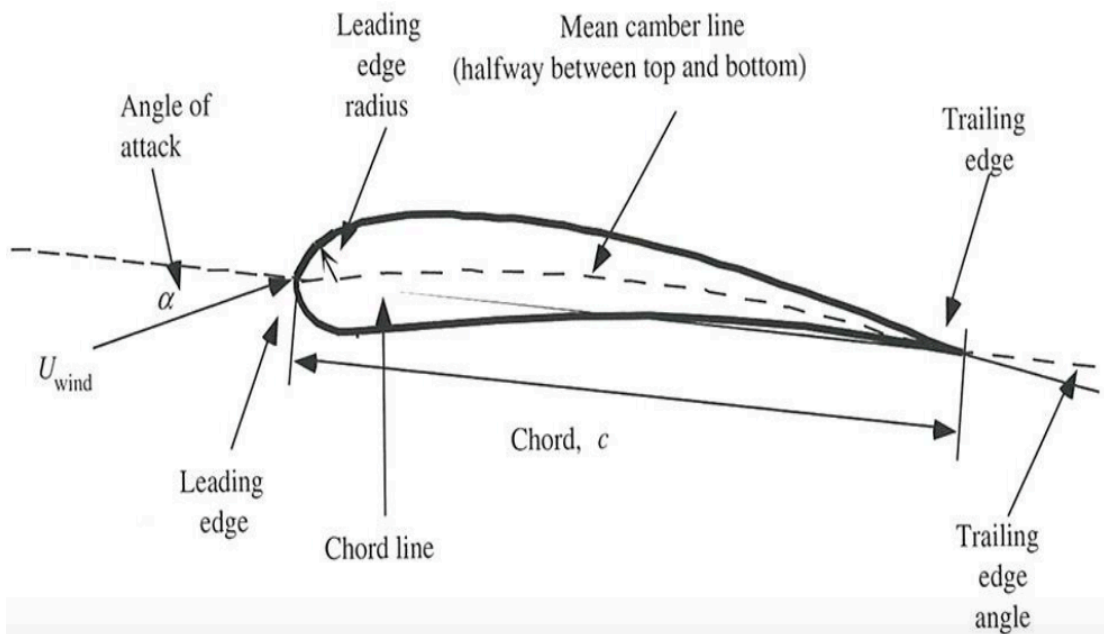
Figure 3: Airfoil nomenclature. Source: Nielsen (2016a).

The lift force is only sustained if the airflow leaves the blade smoothly at the trailing edge, and the low pressure at the upper surface is not cancelled out by the high pressure air moving around the trailing edge. The situation when turbulence occur at the upper surface is called stall, and is a consequence of a too steep angle of attack between the chord and the airflows direction. This is illustrated in Figure 4. Stall causes a large loss in lift forces and increase in drag forces.
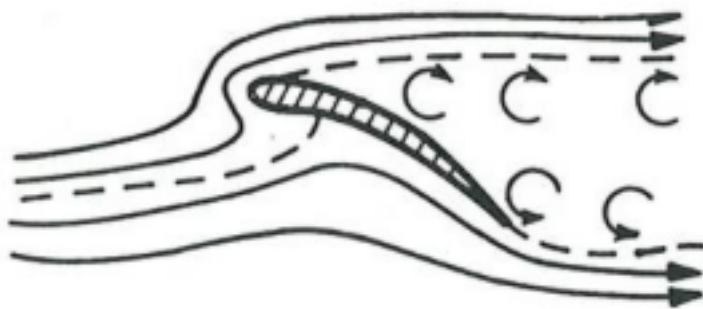
Figure 4: Stall on an airfoil because of an angle of attack that is too steep. Source: Nielsen (2016a).

Many studies have measured and catalogued lift and drag forces for different angle of attacks for a variety of aerofoil shapes. Drag and lift are often described by the coefficients, C_d and C_l, that can be written as shown in the following two equations, where the blade area is equal to the chord length multiplied by the length of the blade.

$$C_d = \frac{D}{0.5 * \rho * v^2 * A_b} \quad [-] \tag{2.2}$$

C_d : Drag coefficient [-]

D : Drag force [N]
A_b : Blade area [m^2]

$$C_l = \frac{L}{0.5 * \rho * v^2 * A_b} \quad [\text{-}]$$

(2.3)

C_l : Lift coefficient [-]
L : Lift force [N]

As shown, lift and drag are both proportional to the energy in the wind and are dependent on the shape of the blade, orientation of the blade relative to the airflow, and also on whether the flow is laminar or turbulent. It is typical to use the ratio between the lift and drag to describe their values, where the maximum value of the ratio then characterizes high lift and low drag, and therefore the most efficient setting of the blades. There have of course been done a lot of work to optimize the design to make the turbine most efficient, and specially developed software is used (Boyle, 2012).

2.2 Wind Turbines

Wind turbines are converting the kinetic energy in the wind into mechanical energy by the rotor and further to electrical energy by the generator. This occurs instantaneously, and is intermittent, the resource cannot be stored for electricity production later on without other units. It must also be converted to electricity at the location of the turbine. However, power lines make the power transportable to some extent, and also energy storage may compensate more for this in the future (Manwell, 2009).

Turbines can vary a lot in design and operation and therefore be classified by different criteria such as the number of blades, energy extraction mechanism and axis orientation. More blades are costlier, cause slower rotational speed and therefore need a larger gear ratio. For several reasons, together with its dynamic balance, the result has been that three blades are the most tested and used. The most dominant type today and the most successful type offshore is three bladed, horizontal axis wind turbine (HAWT), also called propeller turbine. Its main components are tower, nacelle, rotor – which include the blades and the hub, the drive train and the yaw system (Mermaid, 2016).

The yaw regulation is rotation around the vertical axis and enables the turbine to turn towards the direction of the wind. It may be a free (passive) or driven (active) yaw, which means that either the wind forces are utilized in order to adjust the orientation of the nacelle, or there are some torque producing device that rotates the nacelle. Inside the nacelle there are normally a generator, gearbox, control system with break, cables and conversion components. Gear system is implemented because the turbine rotates at relatively slow speeds, which is boosted to drive the generator at higher speeds. There is an ongoing development towards direct drive permanent magnet machines in very large sizes, which means no gear system is required and the operations are simplified (Mohan, 2012).

The offshore wind turbines consist of rotor-nacelle assembly (RNA) and support structure, which in turn consists of tower, substructure and foundation. The most common type of support structure is the monopiles, varying in diameter from 2.5 to 4.5 m and are driven 10-20 meters into the seabed (Manwell, 2009). However, this is changing as the turbines get larger in size. The second most common type is the gravity structure were the total weight of the

turbine and the large base area makes the stability achievable (Manwell, 2009). Multimember support structure is also common, this includes tripod and the jacket, respectively with three and four legs. These are suitable for greater depths and don't need seabed preparation as comprehensive as the two previous mentioned structures.

Design of RNA of offshore turbines are similar to onshore, however the tower and subsystem can be very different. Turbines operating offshore are affected by large forces on the construction, not only wind, but also waves and tides. Waves impact on a structure may be critical because it can have a regular cycle and produces both viscous drag and inertia forces on the structure (Manwell, 2009). In addition, there has to be a clearance between the highest expected sea and the blades, so this has to be taken into consideration in tower design. Offshore turbines are more challenging and costly to access and operate, the trends are to install them further offshore and towards deeper waters, the same trend that was experienced with oil rigs. One of the reasons for the decrease in cost is the prospects of further rotor dimensions expanding, and hence also increase in rated power capacity per turbine. This causes the number of turbines to be reduced for the same wind farm capacity, resulting in substantially reduction of installation costs per MW. However, both the turbine size and park size are increasing (Nielsen, 2016b).

The turbines have a limited operational range regarding wind speeds; power production starts at wind speeds higher than what is called cut-in wind speed due to overcoming losses and stops the production above shut-down wind speed for safety reasons (Mathew, 2011). Cut-in wind speed is typically at around 3 m/s and shut-down wind speeds are typically at around 25 m/s. The amount of power a turbine can extract is thereby higher if it has lower cut-in wind speed and higher shut-down wind speed, as the turbine will extract power from a broader spectre of wind velocities. The graph for the produced power at different wind speeds, i.e. power curve, is also characterized by the rated wind speed at which the turbines maximum power production is reached.

As mentioned, the angle of attack has a large effect on the lift force that drives the rotor around. By changing the angle of the blades in relation to the wind direction, i.e. pitching, the speed of the turbine can be regulated. Pitching the blades are used when the wind speed is between rated and shut-down values, with intention to minimize the effective angle of attack between the blades and the direction of the wind, and therefore to maximize the extracted power. Pitching is also very useful for breaking when shut-down wind speed is exceeded. There is also a mechanical break on the gear to be used to complete the shut down when the speed of the turbine has decreased sufficiently.

There can be very large differences between the actual power production and the rated power of the turbine due to the operational limitations and power curve, maintenance on the turbine and so on. The turbine also uses time to set the pitch and yaw to extract the most power at all times due to the irregularity of the wind direction and speed. The measure of actual annual energy production (AEP) divided by the maximum possible power production over one year gives the capacity factor, C_f. Typically, capacity factor ranges from 0.25-0.35 onshore and 0.35-0.45 offshore (Nielsen, 2016b).

The power coefficient, C_p, is an indicator of how efficient a turbine can extract power for different wind speeds, and as so, ideally it would be operating at maximum C_p at all times. For a modern wind turbine its value is close to 0.5, which is where they become commercially viable (Mathew, 2011). Power coefficient is generally assumed to be a function of pitch angle

and tip speed ratio, λ. Tip speed ratio is the ratio between rotational speed of the blades multiplied by their length (rotor radius), to the free wind speed. Optimal tip speed ratio is often 6-7, but in literature also varies between 6-20 (Boyle, 2012).

Because of continuity in the air mass flow across the turbine, there is a maximum amount of power that can be extracted by the turbine before the air downstream will decreased so much in speed that is blocks the transportation of new air masses. The power coefficient at this maximum transportation level is called the Betz limit and can be written as:

$$C_{P,max} = \left(\frac{P_{extracted}}{P_{wind}}\right)_{max} = \frac{16}{27} = 0.593 \hspace{2cm} (2.4)$$

This is the maximum portion of the winds kinetic energy that can be converted to mechanical energy by the rotor in a theoretical situation, and is not regarding wake (turbulence) rotation. Power coefficient is therefore not to be confused with efficiency. At this level of power extraction, the wind speed downstream of the rotor is slowed down by 2/3 compared to the upstream free speed of the wind. This variable is called the axial induction factor, a. The idealized model used to calculate the Betz limit is not valid when the axial induction factor exceeds the value of 0.5. Figure 5 shows the power coefficient curve and axial induction factor for an ideal turbine.
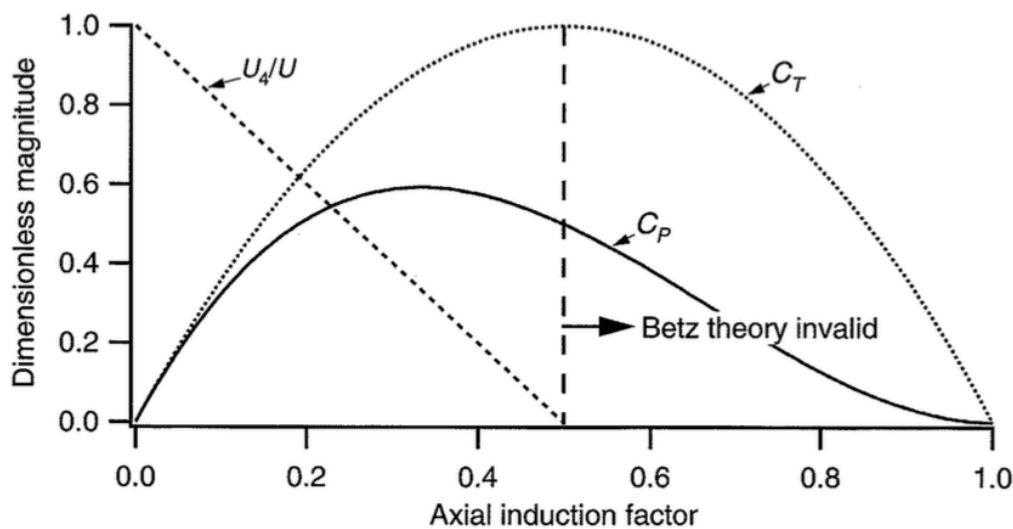
Figure 5: Power coefficient curve for an ideal turbine. Source: Manwell (2009).

Manwell (2009) mentions three reasons why the actual power extraction must be lower than Betz theoretical limit, namely:
-   Rotation of the wake downstream
-   A finite number of blades and their tip losses
-   An aerodynamic drag that is higher than zero

If including the consideration of wake rotation, the Glauert limit can be found, see Figure 6. However, this is still only theoretical, as its including an infinite number of blades and no drag forces. When the theoretical limits are accounted as maximum, the efficiency of modern turbines can be 80% or more (Mathew, 2011).
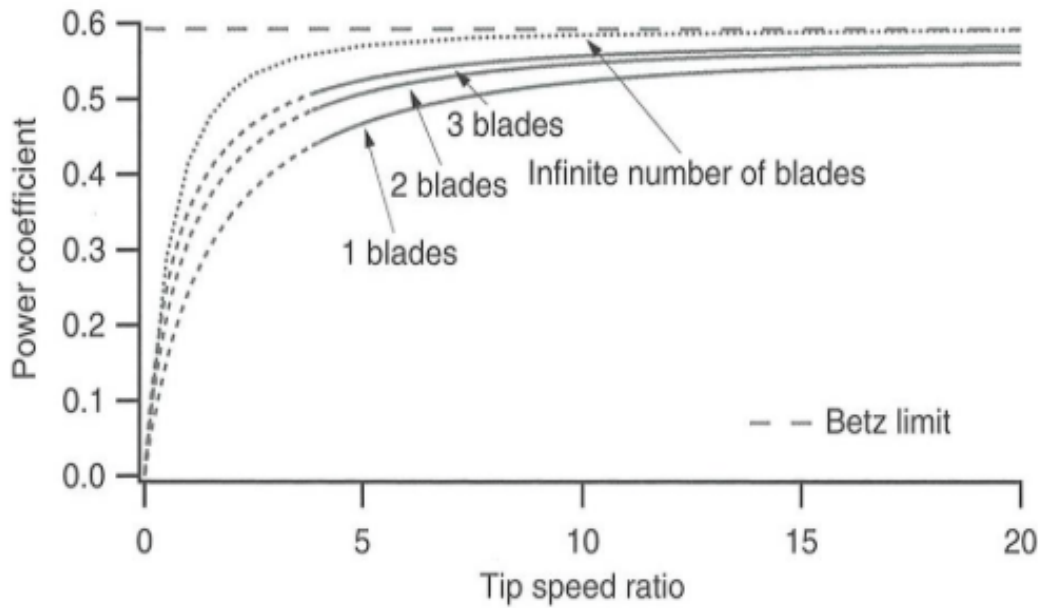
Figure 6: Maximum achievable power coefficients as a function of number of blades, no drag. Source: Manwell (2009).

2.3 Wind Shear and Atmospheric Condition

The lowest part of the atmosphere is called the Planetary Boundary Layer (PBL), where the air is considered turbulent due to the contact with the surface and hence the frictional resistance created. The wind may therefore have a very different velocity at different heights above the ground, i.e. wind shear profile. Roughly the lowest 10 % of the PBL is often referred to as the Surface Layer (SL), where the vertical increase in wind speed is nearly logarithmic (Stull, 1988). The wind shear profile is very difficult to estimate as it is constantly varying and affected by a number of parameters. Wind changes in speed and direction around its mean profile because of turbulence. The wind at any given time can then be written as u=U+û, where û is the turbulence and U is the mean wind speed. This is demonstrated in Figure 7 below, together with the increase in mean speed with height. For very rough terrains, a displacement height can also be taken into account such that the log profile does not start at ground. It is worth noting that wind speed can also decrease with height, called an inverse wind profile.
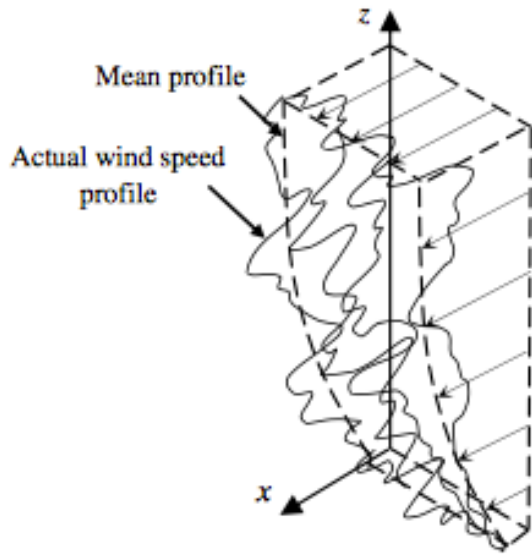
Figure 7: Momentary representation of a typical wind speed distribution with height above ground along z-axis. Source: van der Tempel (2006).

The atmospheric stability and the surface roughness height, z_0, are two variables that can strongly affect the vertical wind shear, and over sea they both change continuously. At any given time, roughness height varies with wave height and so it is a depends on wind speed and fetch. DNV (2010) lists typical values for roughness height for various terrain types, these are given in Table 1 and based on Panofsky (1984), Simiu (1978), JCSS (2001) and Dyrbye (1997). In literature the roughness height for offshore sites can vary a lot, it is often accepted as approximately 0.0002 meters for coastal areas and for calm open sea (Manwell, 2009).

Table 1: Terrain types with typical roughness parameter and power law exponent. Source: DNV (2010).

Terrain type	Roughness parameter z_0 [m]	Power law exponent α [-]
Plane ice	0.00001 – 0.0001	
Open sea without waves	0.0001	
Open sea with waves	0.0001 – 0.01	0.12
Coastal areas with onshore wind	0.001 – 0.01	
Snow surface	0.001 – 0.006	
Open country without significant buildings and vegetation	0.01	
Mown grass	0.01	
Fallow field	0.02-0.03	
Long glass, rocky ground	0.05	
Cultivated land with scattered buildings	0.05	0.16
Pasture land	0.2	
Forests and suburbs	0.3	0.30
City centres	1-10	0.40

Offshore conditions are mainly causing three related effects on the wind resource due to the smoothness of the sea compared to land. Winds over open water always higher, exhibit less shear, and are intrinsically less turbulent than over land (Manwell, 2009). Average wind speed increases with distance to shore, however, turbulence and shear decrease. Lower turbulence intensity in the undisturbed wind offshore is causing improved performance, but are also causing some negative effects. The downstream turbulence of a turbine takes longer time and distance to become as laminar as the upstream, undisturbed wind. This may increase the average intensity of the turbulence significantly, enhancing and enlarging the wake and therefore turbines need more spacing between them to not be too affected by the turbulent air flows of each other, adding to the already large area of use for wind farms. Turbulence offshore also decreases with height, so as the trends are bigger turbines, this problem becomes slightly less important (Manwell, 2009).

The atmospheric conditions can be determined based on how the temperature changes with altitude. Under atmospheric conditions where the temperature gradient for unsaturated air is 9.8°C per km, the atmosphere is considered to be neutral. If the temperature differs less than this, the atmosphere is considered stable as vertical movements are suppressed and velocity gradients are preserved. In the opposite case where the temperature differs more than 9.8°C per km, the atmosphere is unstable and vertical mixing of air masses is enhanced. The velocity gradients are therefore reduced. There are several reasons why the atmosphere will change, some of the processes that can create instability are (Ahrens, 2015):

- Radiation heating of lower altitudes and/or cooling in higher altitude
- Influx of hot air in the lower level
- Influx of moist air
- Rising of air that is cooled adiabatically

The effects of atmospheric stability on wind shear needs to be taken into account when extrapolating wind speed. Temperature can cause uncertainty because it can reinforce or diminish turbulence in the air. Wet air is generally less stable than dry air because the wet air gets cooled later. Pasquill (1961) established stability classes that are arranged from very unstable, A, to stable, F, where D corresponds to neutral conditions.

For offshore conditions, estimations on stability can be done by using the temperature difference between the sea and the air. The variation in stability with temperature differences and wind speed at 10 meters is demonstrated in Figure 8 by Hsu (1992). As seen, the neutral atmosphere assumption is reasonable when the hourly mean wind speed exceeds about 10 m/s. At this wind speed the turbulent mixing overpowers atmospheric instability. When the air is warmer than the sea, stable conditions often apply. This makes it more typical for the summer months. If the atmosphere is strongly stable, inversion is likely to happen.
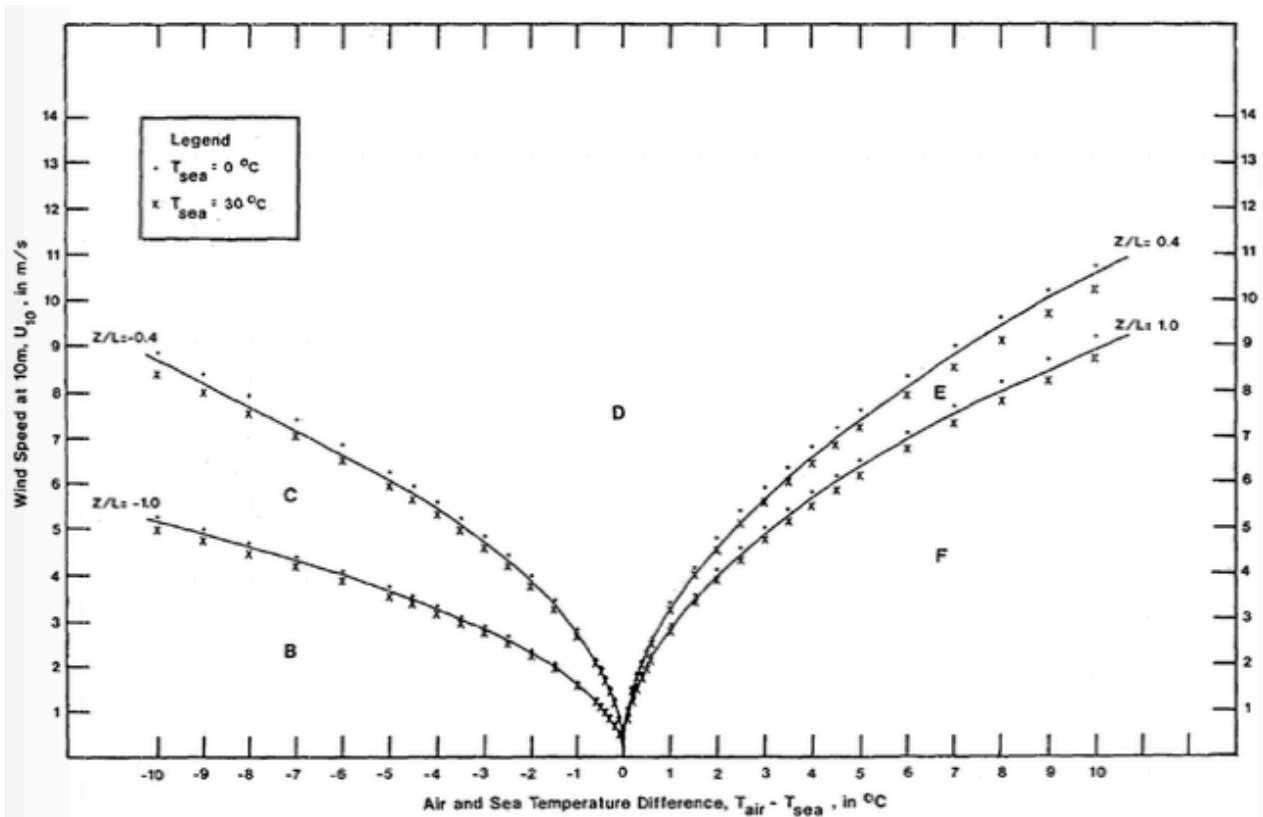
Figure 8: The stability classes as function of the wind speed and air-sea temperature differences. Source: Hsu (1992).

2.4 Methods for Extrapolating Wind Speeds

The power law is one of the most used methods for extrapolating the wind speeds between different altitudes because of its simplicity. The surface configuration and atmospheric conditions can be implemented in a single variable called the power law exponent, α. It has been found that the exponent varies with such parameters as elevation, time of day, season, nature of the terrain, wind speed, temperature and various thermal and mechanical mixing parameters (Manwell, 2009). The basic form of the power law equation is:

$$\frac{U(z)}{U(z_r)} = \left(\frac{z}{z_r}\right)^{\alpha} \; [\text{-}]$$

(2.5)

where,
U(z) : Wind speed at height z [m/s]
$U(z_r)$: Wind speed at reference height [m/s]
z : Height [m]
z_r : Reference height [m]
α : Power law exponent [-]

Since the exponent is strongly variable, specially offshore due to varying surface roughness caused by waves, the use of the power law method is not recommended in some literature (Heinemann, 2002). Especially at low wind speeds the surface roughness is an important consideration in determining power law exponent (Spera, 1979). Manwell (2009) presents different methods of calculating the exponent. One of them shows correlation for the power law exponent as a function of velocity and height as proposed by Justus (1978), another

shows correlation dependent on surface roughness given by Counihan (1975). An empirical formula where the exponent is varying according to surface roughness height, and simultaneously is a function of measured velocity and height, is given by Nfaoui (1998) and rewritten here according to Khalfa (2014):

$$\alpha = \frac{\mathcal{X} - 0.0881 \times \ln(U_r)}{1 - 0.0881 \times \ln\left(\frac{z_r}{10}\right)} \ [\text{-}] \tag{2.6}$$

Where $\mathcal{X}$ depends on roughness height according to:

$z_0 = 0 - 0.005$ m	$\mathcal{X} = 0.25$
$z_0 = 0.005 - 0.05$ m	$\mathcal{X} = 0.31$
$z_0 = 0.05 - 0.5$ m	$\mathcal{X} = 0.37$
$z_0 = 0.5 - 4$ m	$\mathcal{X} = 0.48$

Often a power law exponent value of 1/7 (≈ 0.143) is used for neutral atmosphere over land, and for stable (unstable) conditions higher (lower) values are used. The larger the power law exponent, the larger the vertical gradient in the mean horizontal wind speed. Offshore, a value of 0.11 is often considered as reasonable for neutral atmosphere. However, the value of the power law exponent can vary a lot between different cases of study.

The exponent varies between 0.050 and 0.169 in Hsu (1994), concluding with an exponent of 0.11 ±0.03 as standard deviation of 30 samples in the gulf of Mexico and the East coast of United States under near-neutral atmospheric stability conditions. Lower values of the power law exponents were found to be suitable for cases studied by Furevik (2012). This was a study based on data collected at Polarfront (66N, 2E) which was 400 km north-west of the site for this thesis. For unstable conditions an exponent value of 0.04 was established, 0.05 for neutral, and 0.09 for stable conditions. Based on temperature differences between air and sea, assumptions were that stable conditions occurred when $\Delta T > 0$, neutral when $-1 \leq \Delta T \leq 0$ and unstable when $\Delta T < -1$. In another study, Corrigan (2017) found the power law exponent to be at an average of 0.09 for lake Erie, 6 km from land in Cleveland, USA. When taking into account the atmospheric stability conditions, the average power law exponents of 0.02 and 0.14 were found for when unstable regimes and neutral/stable regimes was indicated, respectively.

Figure 9 and 10 shows how mean power law exponent change as a function of surface roughness height and of wind speed at 10 m, respectively. Results from several different methods for calculating power law exponent is implemented (Spera, 1979). Direct values of the power law exponent for each stability class can be found in literature, however, not for atmosphere over sea, e.g. EPA (2000). The result in Emeis (2005) show that the power law offers a good fit to the logarithmic profile for slightly stable conditions and very smooth surfaces only.
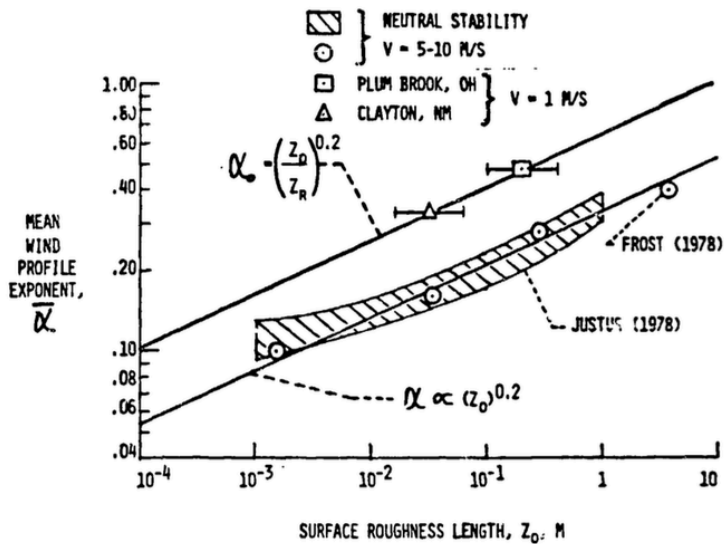
Figure 5 - Curve-fit of data relating wind profile exponent $\bar{\alpha}$ to surface roughness length.

Figure 9: Mean power law exponent as a function of surface roughness height. Source: Spera (1979).
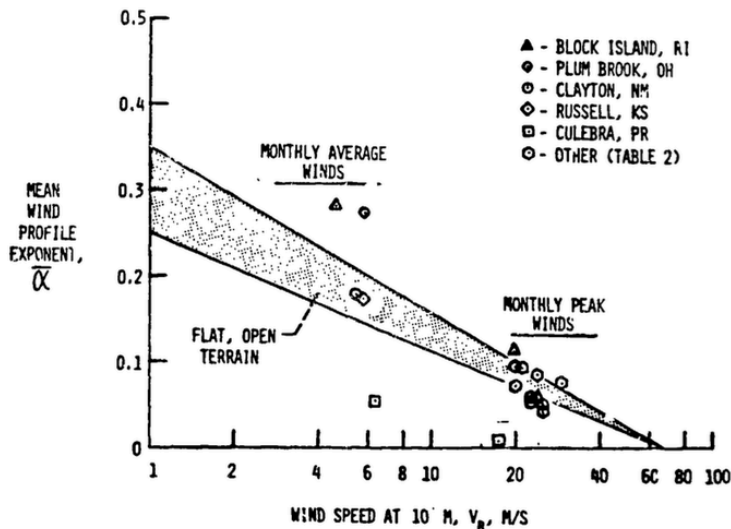
Figure 6 - Comparison of observed and calculated wind profile exponents for various sites.

Figure 10: Mean power law exponent as a function of wind speed at 10 m. Source: Spera (1979).

Another much used method for determining the vertical wind profile, is the logarithmic law (log law) that can be presented by

$$U(z) = \frac{u*}{k} ln \left(\frac{z}{z_0} \right) \ [m/s] \tag{2.7}$$

where,
u* : Friction velocity [m/s]
k : von Kármán constant ≈0.4 [-]

Friction velocity is defined by the relation:

$$u_* = \sqrt{\tau_0/\rho} \qquad [\text{m/s}] \tag{2.8}$$

Where,

τ_0 : Surface shear stress, or momentum flux at the surface [N/m^2]
ρ : Density [kg/m^3]

The log law can be rewritten for extrapolation of wind speeds between two known altitudes with the same roughness height:

$$\frac{U(z)}{U(z_r)} = \frac{\ln(z/z_0)}{\ln(z_r/z_0)} \qquad [\text{-}] \tag{2.9}$$

Variables are the same as those used for the power law in Equation 2.5. The log law as it is presented by Equations 2.7 and 2.9 is only valid if the thermal stratification of the atmosphere is neutral, and the surface roughness height is known. The atmospheric stability state can to be taken into account for by the boundary layer similarity theory, or Monin-Obukhov similarity theory (MOST). A stability correction function, ψ, is added to the logarithmic wind profile, and the log law can then be written as in Holtslag (2014):

$$\frac{\partial u}{\partial z} = \frac{u_*}{kz} - \psi\left(\frac{z}{L}\right) + \psi\left(\frac{z_0}{L}\right) \tag{2.10}$$

where,
L : Monin-Obukhov length [m]

The last term in Equation 2.10 is generally neglected since z >> z_0. The term z/L is defined as the stability parameter ζ, and is related to stability with z/L< 0 referring to unstable, z/L≈ 0 to neutral and z/L> 0 to stable conditions. According to Webb (1970), MOST is only valid in a range of -1 ≤ z/L ≤ 1. Newman (2014) states that the similarity theory methods only produce accurate wind speed estimates for unstable conditions. Also according to Optis (2016) there have been found limitations in the MOST for wind profile extrapolation under stable stratification conditions.

The Monin-Obukhov length is defined as

$$L = -\frac{\overline{\theta_v}\, u_*^3}{kg(\overline{w'\theta'})_s} \qquad [\text{m}] \tag{2.11}$$

Where,
$\overline{\theta_v}$: Mean virtual potential temperature [K]
g : Acceleration due to gravity [m/s^2]
$(\overline{w'\theta'})_s$: Surface virtual potential heat flux [m×K/s]

The Obukhov length calculation requires measurements of heat and momentum fluxes, as seen, typically from a sonic anemometer. Another commonly used stability parameter is the gradient Richardson number. The Richardson number, in contrast to the Obukhov length, depends on the vertical temperature gradient and the velocity gradient (Newman, 2014). Temperature measurements at two different levels are therefore required.

By examining the log law, a relation between wind speed and stability can be found, where

the Monin-Obukhov length is proportional to the friction velocity cubed in Equation 2.11, which in turn depends on the wind speed as seen in Equation 2.7. Large values of L, and hence $z/L \approx 0$, is therefore a result of high wind speed and also imply near-neutral conditions as stated (Motta, 2005).

When z/L is known, the wind profile for stable atmosphere is given by Emeis (2005):

$$u(z) = \frac{u_*}{k}\left(ln\frac{z}{z_0} + 4.7\frac{z}{L}\right) \qquad \text{[m/s]} \qquad (2.12)$$

For unstable atmosphere the stability correcting function can be approximated by (Emeis, 2005):

$$-\Psi\left(\frac{z}{L}\right) = ln\left(\frac{(1+x^2)}{2\left(\frac{(1+x)}{2}\right)^2}\right) - 2tan^{-1}(x) + \frac{\pi}{2} \qquad \text{[-]} \qquad (2.13)$$

Where

$$x = \left(1 - 15\frac{z}{L}\right)^{1/4} \qquad \text{[-]} \qquad (2.14)$$

The log law is a function of roughness height, and determining roughness height offshore is as seen, not straight forward. In combination with MOST, the Charnock model is often additionally used for describing the change in roughness height over the ocean as a function of the wind speeds. Because of the relation seen in Equation 2.8, friction velocity can be thought of as a proxy for the surface stress (WMO, 1998). The wind-stress acting at the air-sea interface is an important influence on the generation of surface waves, among other phenomena. The Charnock model is providing that the surface roughness is governed by gravity waves (Wu, 1969). The relation between roughness height and friction velocity is given by Charnock as follows:

$$z_0 = A_C\frac{u_*^2}{g} \text{ [m]} \qquad (2.15)$$

Here,
A_C : Charnock parameter [-]

The Charnock parameter was initially assumed to be a constant, however, it is found to be an empirical value that depends on how open the sea is and how old the waves are. For fully developed waves at open sea, Charnock parameter between 0.011 and 0.014 is recommended, and for near-coastal locations it is usually higher, with values of 0.018 or more (DNV, 2010). According to Manwell (2009), the Charnock parameter is normally set to 0.018 for coastal waters.

There have been many attempts to define the parameter, Kitaigorodskii (1965) proposed a wave-age based approach, expressed as either c_P/u_* or c_P/U_{10N}. Here, c_P is the wave phase speed at the peak of the spectrum and U_{10N} is the 10-meters neutral wind speed (Drennan,

2005). Hsu (1974) proposed instead that the Charnock parameter could be considered as a function of the wave steepness, thus considering the density of the wave field.

Taylor (2001) proposed an alternative to the classical wave-age scaling proposed by Kitaigorodskii (1965). It is similar to Hsu (1974) in which is based on wave steepness to predict roughness height, however, it is a simplified formula. The relation is rewritten as by Drennan (2005):

$$\frac{z_0}{H_S} = A \left(\frac{H_S}{L_P}\right)^B \ [\text{-}] \tag{2.16}$$

where,
H_S : Significant wave height [m]
L_P : Peak period wavelength [m]

The values of A and B are found empirically by Taylor (2001) to be 1200 and 4.5, respectively.

3. Methods applied for characterizing load and wind power production in the case study

In this chapter the methods used for handling the different sub-problems are presented. Firstly, the way the quantitative data were collected and processed is explained shortly, before the power consumption data are presented, followed by the most suitable extrapolation method of wind data at site.

3.1 Collecting and Processing the Data

Collecting the data on power consumption was done by contacting the industry, consultant companies and research centres with links to fish farming. The main aim when requesting data from a fish farm was that it was a relatively large facility and that there was good availability of data for a long period and with short intervals. Such data was given by the operational company SalMar Farming AS and their energy advisory company aPoint on a facility called Rataren in Sør-Trøndelag, Norway. At the location there is a SINTEF ACE owned Seawatch Midi 185 buoy as seen in Figure 11, that measures a number of weather parameters. Data from the buoy was given by SINTEF Ocean for the entire period of available power consumption data. The type of wind measure method at the buoy is sonic anemometer, where the velocity of ultrasonic sound waves between two pairs of transducers is measured to calculate the wind speed. The anemometer is a WindSonic by Gill Instruments Ltd, which measures direction and speed with 1 Hz, 10 minutes' average, 60 minutes' acquisition interval. An excerpt of the datasheet can be found in Appendix A.

Figure 11: Seawatch Midi 185 Buoy located at Rataren. Source: SINTEF Ocean.

Wind and air temperature is measured at 2.5 meters above sea level (masl), water temperature is measured at 1 meter below sea level (mbsl). Motta (2005) discuss how error can occur when the temperatures have been measured separately and the difference is calculated afterwards. Given that sea temperature varies slowly, it is claimed that using the difference may lead to many extreme (i.e. very stable, or very unstable) stratification conditions. Also, sea temperature should be measured at surface (skin temperature) with remote sensing ideally, not in the top layer which is more common and also is the case here (Motta, 2005). Nevertheless, this is the only possible and reasonable method in this case of study.

The hours of the wind and temperature data are in UTC and is therefore shifted one (two) hour(s) according to the power consumption data set, as the time for power demand is in CET (CEST). The buoy is placed 360 meters from the middle of the fish farm and 420 meters from the barge, forming an almost isosceles triangle. The data from the buoy is to be used for the extrapolation of wind speeds from the measured height to the turbine height, the last section of this chapter will explain the methods to do this.

Air temperature from the period was also collected from the Norwegian Meteorological Institutes climate database, at the web portal eKlima. The closest weather station to Rataren is

Sula lighthouse at 5 masl located 7.8 km north-west of Rataren. Official requirements give temperature measurement at 2 meter above ground level, resulting in temperature data at 7 masl at Sula lighthouse. It was decided not to use these data in the calculations as the measurements are not from a sufficient altitude when being this far apart from the measurements at the buoy.

The power curve for Hywind Demo 2.3 MW turbine is given by Statoil, it can be found in Appendix B. Also the GWP 750 kW turbines power curve can be found in Appendix C (GWP, 2002). The two turbines different power curves and hub heights are accounted for in the calculations. For comparison of different ratios of power production and power consumption, a wind farm of three 750 kW turbines is included in calculations and also the hourly consumption is multiplied by one, three and six times the original consumption at Rataren.

Excel was chosen as the computer software program used for all calculations. It is suitable for the simple, yet many calculations and to make graphs to present the results in a clear manner. There were not found any limitations with this program in this case compared to others.

3.1.1 Power Consumption at the Fish Farm

Rataren fish farm is located 100 km north-west of Trondheim, and about 50 km of the mainland, in between some smaller islands but less than 10 km from the open sea, see Figure 12. Rataren is one of the largest fish farms in Norway, and consists of system anchoring with the capacity to carry 16 cages. There are currently 14 cages, and each of them have a circumference of 160 meters. The barge has a feed capacity of 600 tonnes, in addition to eight bedrooms, seven bathrooms, two kitchens, TV-room, two meeting rooms, three offices and one control room (ACE, 2013). The location for the middle of the fish farm is 63°46'85.3"N, 8°31'04.3"E, and the barge is located 63°46'75.6"N, 8°31'36.7"E.
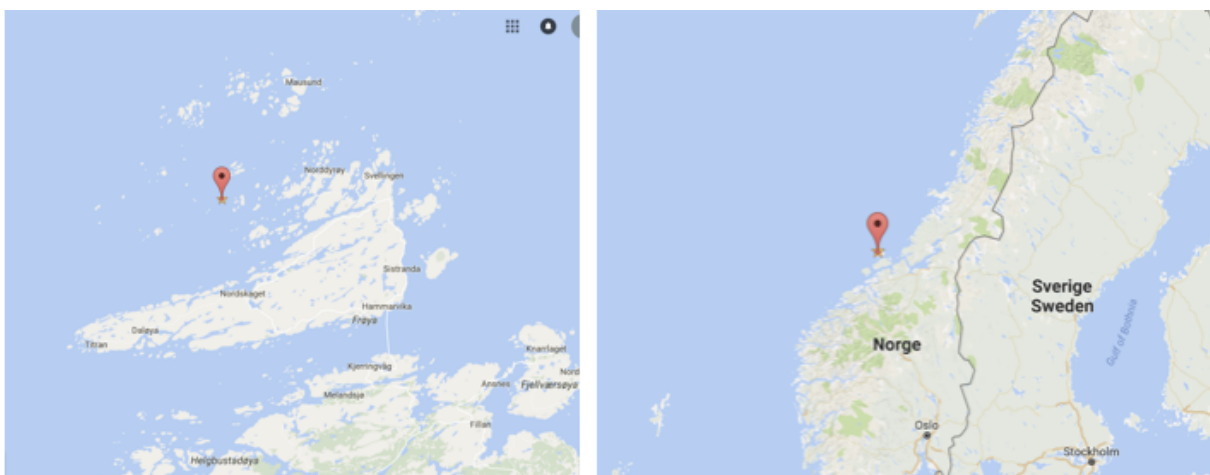
Figure 12: Location of the case of study, Rataren fish farm in Trøndelag, Norway.

Rataren is also a research facility and SalMar Farming AS is a partner in Exposed – a centre for research-based innovation on exposed aquaculture operations. One of Exposed's research partners and the centre host is SINTEF Ocean (Reed, 2013). As of June 2016 Rataren got connected to the onshore power grid, before that only diesel generators were used; two at 300 kW and one at 100 kW. There are now an 8 km long power transmission cable to shore and a transformer is placed on a skerry (Flathagen, 2016a). The power consumption has not been

registered before 1ˢᵗ of February 2016, and the received data set from SalMar on power consumption is from this date until 31ˢᵗ of August 2016. In general, fish farms use about 60 % of the energy consumption for feeding, so where the salmon is in the growth phase is important for power consumption. Rataren was empty from November 2014 before 2.5 million fish were set in 15 cages during March and April 2015 (Hammervik, 2015). The fish at Rataren were in the latest growing-phase when the power consumption was registered, according to SalMar and aPoint there are less fish after August.

The power measurements are hourly, which is not ideal regarding that power production from wind turbine can vary a lot within one hour. However, the data are regarded to be the best available. There are some periods, varying from a few hours to many days, where the main measure point is out of service and the consumption apparently drops to zero. These periods are filtered off, and is not contributing in any calculations. During the period with data from 1ˢᵗ of February 2016 till 31ˢᵗ of August 2016 there are in total 5100 hours. The periods with outages constitutes 430 hours, which results in 4670 hours for calculations. The data availability for the power consumption is then almost 92% during the whole seven months period, and the data are given in kW with one decimal, i.e. with an accuracy of 100 W. The remaining data are still considered very reliable and invaluable in this study.

3.1.2   Wind Resource Estimations

The methods for examining wind resource are emphasized because of the wind speeds' importance when calculating the wind power, as seen in Chapter 2. The data from the buoy is evidently the best source of information about the weather conditions at the site, but the wind speeds needs extrapolation from the buoy height to the hub height, which is 65 meters for the Hywind Demo 2.3 MW turbine and considered to be 55 meters for the GWP 750 kW turbine. Taking wind shear profile into account, the difference in wind speed over the area of the rotor of a turbine can be substantial, depending on the size of the turbine. It is therefore a problem that becomes more important for the Hywind turbine, however, it is not taken into account here; the wind is extrapolated to an altitude that is considered reasonable for the centre of the rotor for both turbines.

There are different methods around to extrapolate wind speed, the power law and the log law have been presented previously. The log law is more complex in its calculation and dependencies of variables. There has been done attempts in the thesis to find the most suitable variables based on literature research and trial and error. As mentioned in Chapter 2, the Monin-Obukhov length can be given by Richardsons number, which in turn depends on the temperature gradient and the velocity gradient. In this study these data are not available, but different example values for the parameter z/L per stability class is found (Hsu (1992), Cañadillas (2011)).

Roughness height was also varied in the calculations, causing changes in friction velocity due to Charnocks equation. As mentioned, there is interdependence between wave height and wave periods that could be used to calculate a varying roughness height for each hour (Manwell, 2009). From the buoy at Rataren, data on significant wave height were available, however, data on wave period was not. The MOST method for stable and unstable conditions are not directly depending on the wind speed measured at site, so friction velocity would either be constant for all wind speeds (also causing constant wind at hub height), or changing with the rule of thumb as stated in Ho (2015) that it is equal to one tenth of the wind speed, but holding $u_*<1$, which caused unreasonable jumps in the calculated wind speed. There was

also made attempts to find a reasonable estimate for friction velocity by the relation to wind speed given in WMO (1998), where $u* = v\sqrt{C_d}$ due to the drag law $\tau = \rho C_d v^2$, see Figure 13.
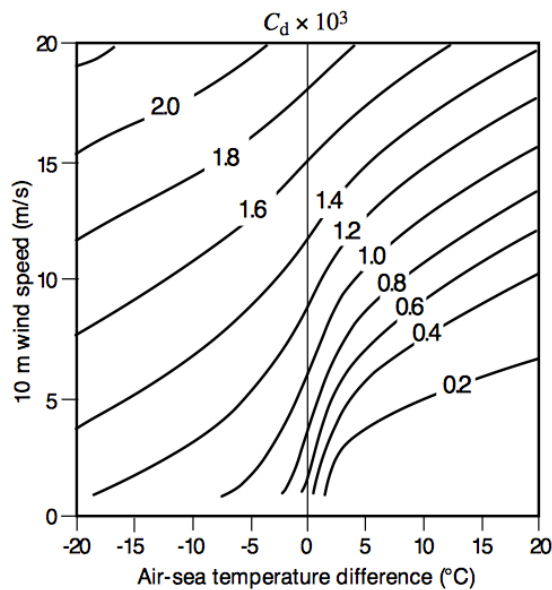
Figure 13: Drag coefficient as a function of stability and 10 meters wind speed. Source: WMO (1998).

However, calculations show inconsistencies in the wind speeds and the method is therefore not satisfying. A shorter period of the results for z/L= ±0.4 and u*= *v*/10 (u*=*v*/20) for *v* <10 (*v* >10) can be found in Appendix D.

The friction velocity has also been calculated using Charnocks equation assuming A_C=0.0185 (Wu, 1980). This was consequently not giving more reasonable results as the Charnock parameter is kept constant. Estimating more suitable Charnock constants for this particular case was not possible due to the unavailability of some parameters in the methods mentioned in Chapter 2.

As a result of this, the power law was decided to give the most reasonable values of wind speed calculation, even though the power law exponent also is uncertain and must be estimated best possible based on literature. A literature review revealed little in the way of atmospheric stability in general correlation with values of the power law exponent. Recommended power law exponents are found for urban and rural wind profiles, but not for offshore conditions, i.e. by EPA (2000). There are many studies done where different exponents are found to be valid for the particular site offshore, however, they are not directly transferrable to the site of interest in this thesis.

For most accurate results in this thesis, the power law exponent is set to be different for five stability classes. Power law exponents that are assumed to be reasonable are 0.07, 0.09, 0.11, 0.13 and 0.15, for respectively unstable, slightly unstable, near-neutral, slightly stable and stable conditions. In addition to temperature difference, wind speed in an indicator of atmospheric stability as previously seen. Therefore, sets of power law exponents was also calculated using the method by Nfaoui (1998) given in Equation 2.6. The results are as shown in Table 2, and compared to the chosen values of the power law exponent as listed above. The calculations can be found in Appendix E.

As seen in Chapter 2, $\mathcal{X} = 0.25$ for $z_0 = 0$-0.005 m., and $\mathcal{X} = 0.31$ for $z_0 = 0.005$-0.05 m. Roughness height below 0.01 meters is considered reasonable for all sea states in Table 1, and it is often accepted as approximately 0.002 meters for coastal areas. Both values of $\mathcal{X}$ are therefore used for calculating power law exponents, but $\mathcal{X} = 0.25$ is believed to result in the most reasonable values for power law exponent from this method, and in this case of study. The method was used to calculate power law exponents for each hour based on the wind speed at 2.5 meters height throughout the period, for both values of $\mathcal{X}$. The average exponents for each stability class as shown in Table 2 were found.

As seen are the chosen values for the power law exponents decreasing the more unstable the atmosphere is, as it should per definition. When $\mathcal{X}$ is set to be 0.25 the same pattern is found for slightly stable, near-neutral and slightly unstable conditions, with the exact same values of exponents as for the chosen values. However, for stable and unstable conditions the exponents are lower and higher than expected, respectively. This is not correct according to the theory on wind shear and atmospheric stability. The same pattern is found for when $\mathcal{X}$ is equal to 0.31, but the values are in general higher than the chosen values.

It is also evident that the maximum and minimum values with this method are quite extreme, as a power law exponent of 0.4 corresponds to city centres according to Table 1. These findings are also decreasing the credibility of the suitability of the method in this case of study. Partly based on these results, it is determined to use the chosen values of the power law exponents from 0.07 to 0.15, and not further use the method given by Nfaoui (1998).

Table 2: Power law exponents; chosen values and calculated values by taking into account the assumed roughness height and measured wind speed at 2.5 meters.

Atmospheric stability class	Chosen α based on stability class	Calculated average α when $\mathcal{X}$ =0.25 (z_0=0-0.005 m)	Calculated average α when $\mathcal{X}$ =0.31 (z_0=0.005-0.05 m)
Stable	0.15	0.12	0.17
Slightly stable	0.13	0.13	0.18
Near-neutral	0.11	0.11	0.17
Slightly unstable	0.09	0.09	0.15
Unstable	0.07	0.10	0.15
Minimum value of α found	0.07	0.02	0.07
Maximum value of α found	0.15	0.39	0.44

4. Results

In the first of the following subchapters the wind turbines power production is estimated. This is a result of the wind resource estimates at hub heights, which calculation is based on the determination of atmospheric stability for each hour. Following, the power consumption is presented and is compared to the power production using graphs and key numbers. Finally, the produced power is compared with the power demand for different fish farm sizes. The time periods with outage at the measure points at the fish farm are removed from all data where the total period is included in calculations. In several of the figures the data are only shown for two weeks, this is for illustration purposes and the first two weeks of the period are chosen by chance.

4.1 Estimation of the Power Production

Presented in the following sections are the chosen variables and the results of the calculations that provides the basis for the power productions. The atmospheric stability and wind distribution is therefore firstly determined.

4.1.1   Atmospheric Stability

Determining the atmospheric stability is critical for how to process the data on wind speed at the site. As mentioned, the difference in air and water temperature gives an indication of atmospheric stability. In this thesis, near-neutral atmospheric condition is assumed to be valid when the temperature difference is between 1°C and -1°C. If the air temperature is more than 3°C lower than the water temperature, the near surface atmosphere is considered to be unstable, and difference above 3°C gives assumed stable atmosphere. Slightly stable and slightly unstable conditions are assumed when temperature difference is between 1°C and 3°C, and -1°C and -3°C, respectively.

The stability class is determined for each hour throughout the period, and the conditions can therefore be characterized as shown in Figure 14. This is the total period between 1st of February till 31st of August 2016, including hours with outages in the measure points at Rataren. Out of the 4670 hours when excluding outage periods, there are found a vast majority of hours of near-neutral conditions throughout the period with 63%. Slightly unstable conditions found to occur 22 % of the time, while slightly stable, unstable and stable occurs 7%, 6% and 2 % of the time, respectively. Calculations for these results can be found in Appendix F.
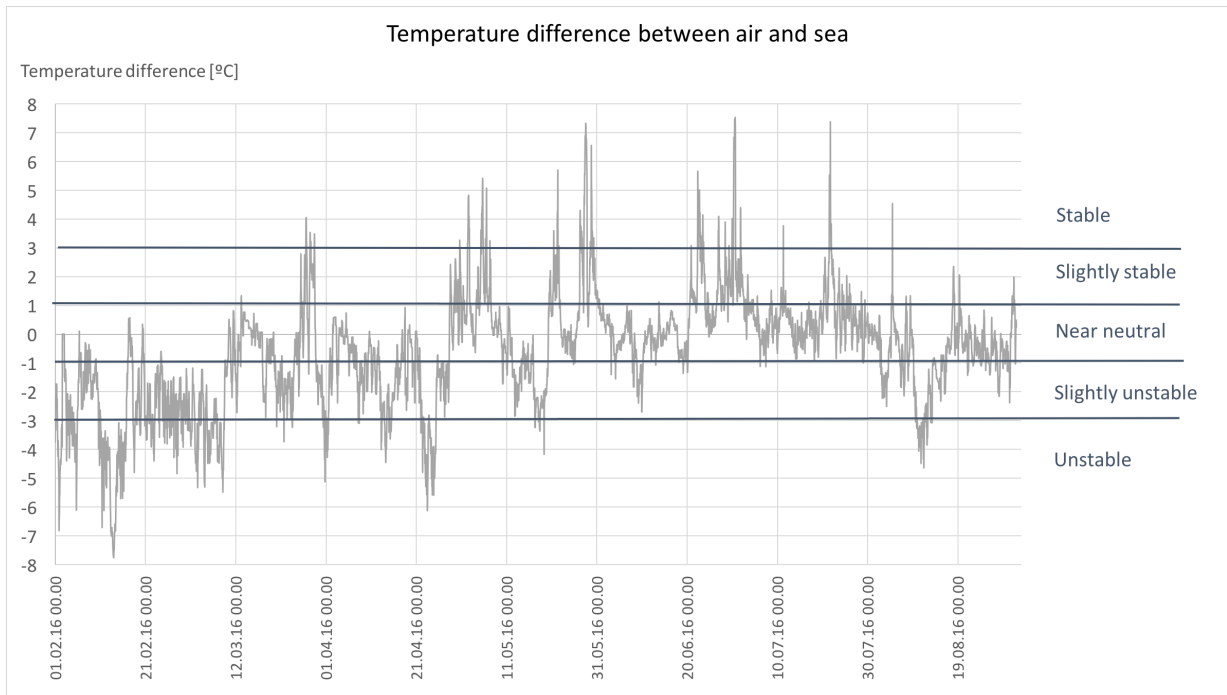
Figure 14: Temperature difference between air and sea (Ta-Ts), and corresponding stability classes.

Furthermore, the chosen power law exponent that is assumed reasonable for each atmospheric condition is given in Table 3, together with the corresponding temperature differences between air and sea. For wind speed extrapolation, the power law equation presented in Chapter 2 is applied to each hour using the power law exponent that is assumed correct for the applicable conditions.

Table 3: Stability classes and characteristics.

Pasquills stability categories	Atmospheric condition	ΔT ($T_{air} - T_{sea}$)	Power law exponent, α
B	Unstable	$\Delta T < -3$	0.07
C	Slightly Unstable	$-3 \leq \Delta T < -1$	0.09
D	Near-Neutral	$-1 \leq \Delta T \leq 1$	0.11
E	Slightly Stable	$1 < \Delta T \leq 3$	0.13
F	Stable	$3 < \Delta T$	0.15

4.1.2 Probability Distribution of the Wind Speed

The wind speeds are extrapolated to 65 meters altitude based on the specifications for the Hywind Demo turbine, and to 55 meters for the 750 kW turbine. Figure 15 shows a two weeks period of wind speed measured at 2.5 meters and extrapolated to 65 meters using the power law with the exponent changing according to establishments in the previous subchapter.
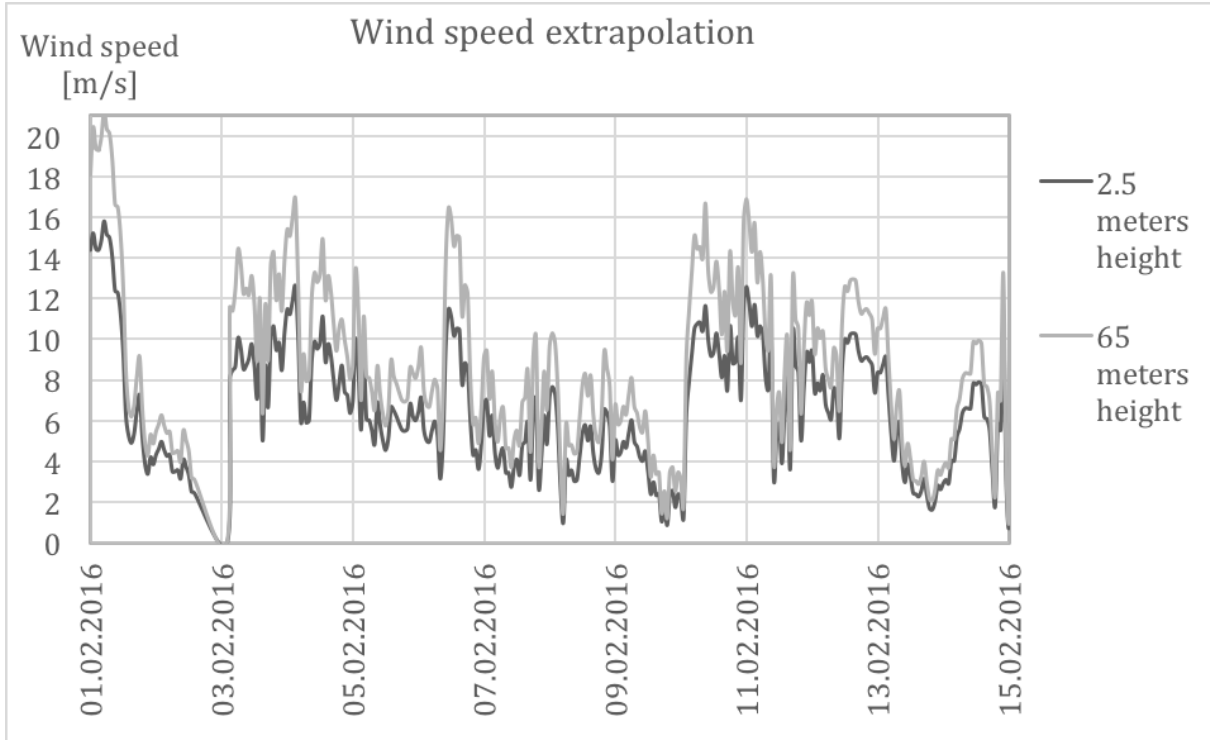
Figure 15: Wind speeds over two weeks period; measured at 2.5 meters and calculated for 65 meters altitude.

Taking into account the whole period of 4670 hours, Figure 16 shows how many hours the different wind speeds occurred in measurements at 2.5 meters and the results of calculated wind speed at 65 meters. It shows the same configuration as a typical histogram. For the whole period the average wind speed at 2.5 meters is 5.01 m/s, at 55 meters it is 6.92 m/s and at 65 meters it is 7.04 m/s. The most frequent wind speeds are however 4 m/s for 2.5 meters and 5 m/s for 65 meters altitude. The number of hours with zero wind speed is 28 at 2.5 meter, compared to 17 hours at 65 meter. The maximum mean wind speed during one hour is 21 m/s at 65 meters that occurs for one single hour, and at 2.5 meters the maximum mean wind speed is 14 m/s and occurs for 3 hours. At 55 meters altitude, the number of hours with no wind is 18 and maximum mean wind speed is 20 m/s, occurring for one single hour.
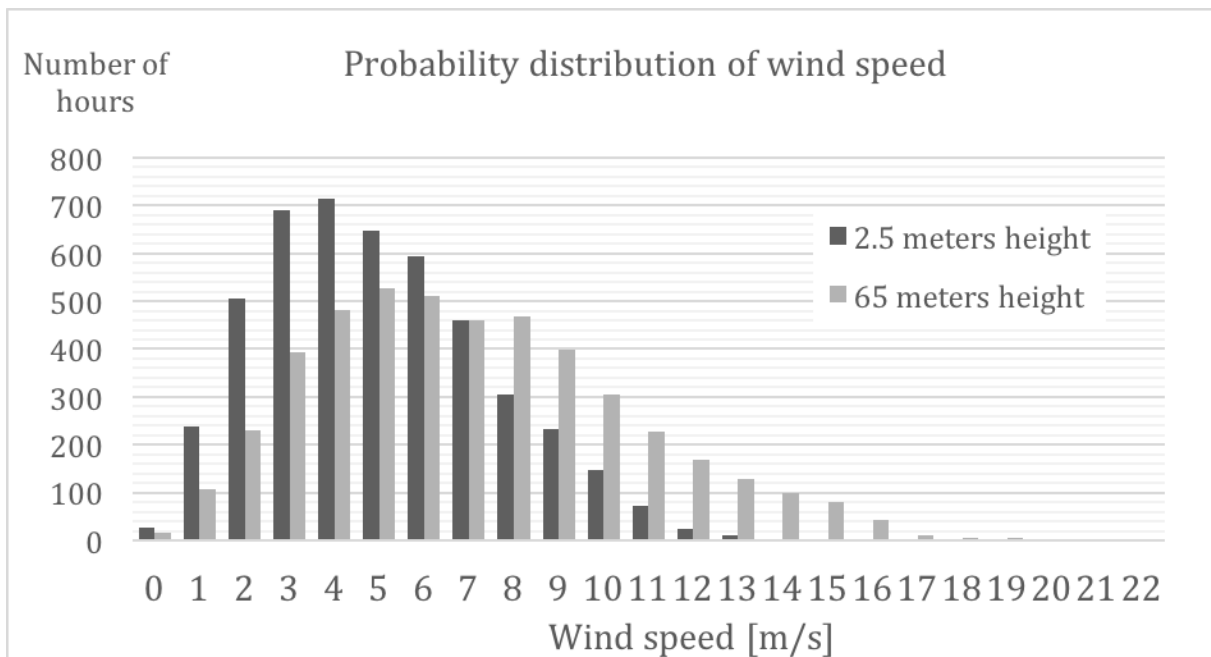
Figure 16: Probability distribution of wind speed in number of hours calculated for 65 meters height and measured at 2.5 meters height, each in total of 4670 hours.

Figure 17 shows the calculated mean wind profiles for each stability class, with corresponding horizontal error bars for confidence level 95% calculated for 65 meters' height. The legend shows the number of hours each of the atmospheric stability classes is found to occur. As seen, each of the mean wind profiles are results of many measurements that has various starting points for wind speed at 2.5 masl. Hence, there are large discrepancies between the measured values of wind speeds, with standard deviation at 2.5 meters between 2.3 and 2.5 m/s for all stability classes.
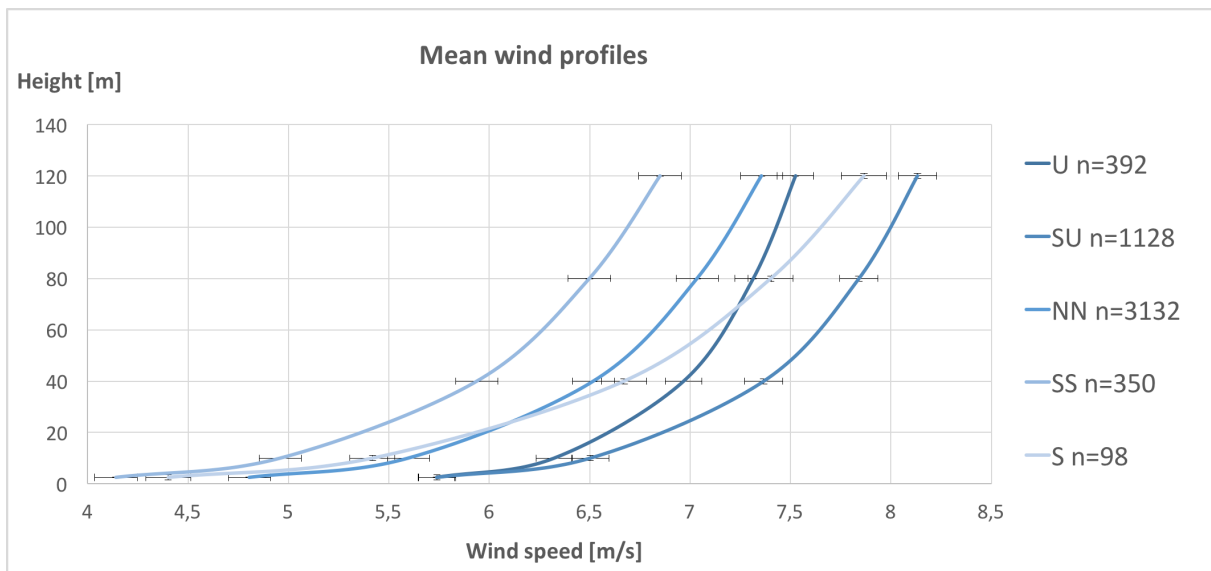
Figure 17: Average wind profiles calculated for each stability class.

In Figure 18 the frequency of occurrence of the different stability classes based on the calculated wind speeds at 65 meters altitude, can be seen. To fit into the categories of wind speed, they had to be rounded. The calculations can be found in Appendix G. It is prominent that all classes appear at almost the entire range of wind speeds, where it is expected to be clearer patterns. At higher wind speeds than 10 m/s at 10 masl, almost exclusively near-neutral conditions are expected. However, calculations based on 65 meters height show that all stability classes still occur during higher wind speeds, especially are there more hours than expected of slightly unstable conditions.
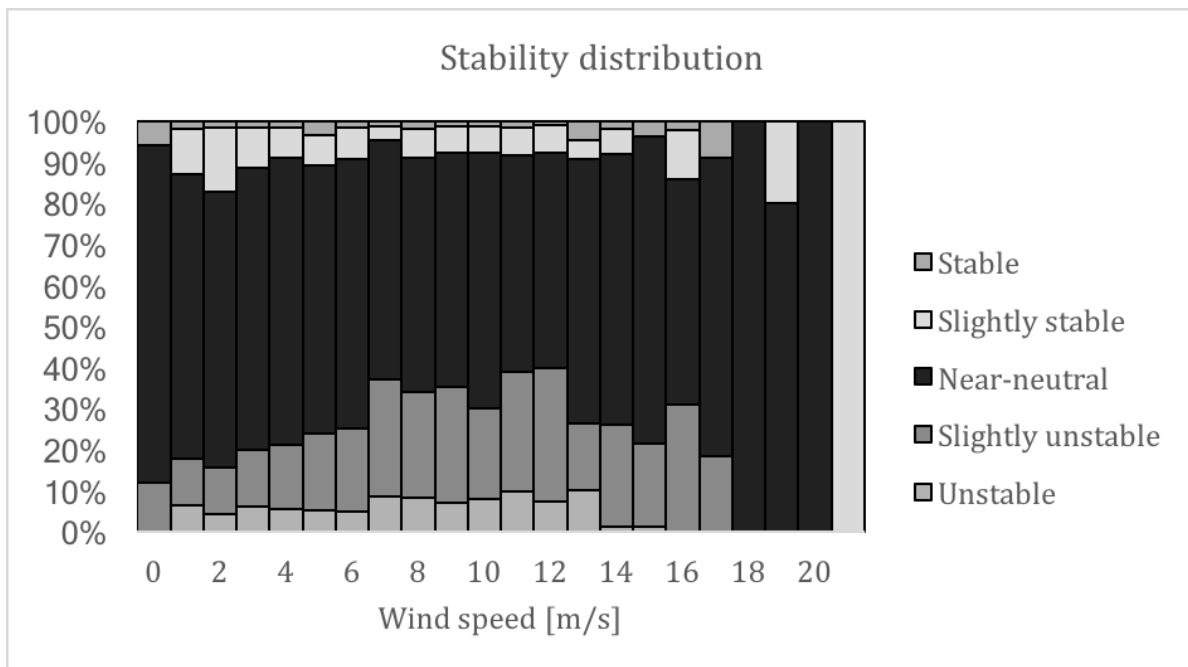
Figure 18: Frequency of occurrence of the different stability classes by calculated wind speeds at 65 meters height.

4.1.3   Power Production

In this subchapter the results from the calculated power production by both the 750 kW and the 2.3 MW turbine are presented. Figure 19 illustrates the power curves for both turbines, where the y-axis shows the power output over rated power. The shut-down wind speeds are the same for both turbines at 25 m/s, however, the cut-in wind speeds for the 750 kW turbine is 3 m/s - while for the 2.3 MW turbine it is 4 m/s.
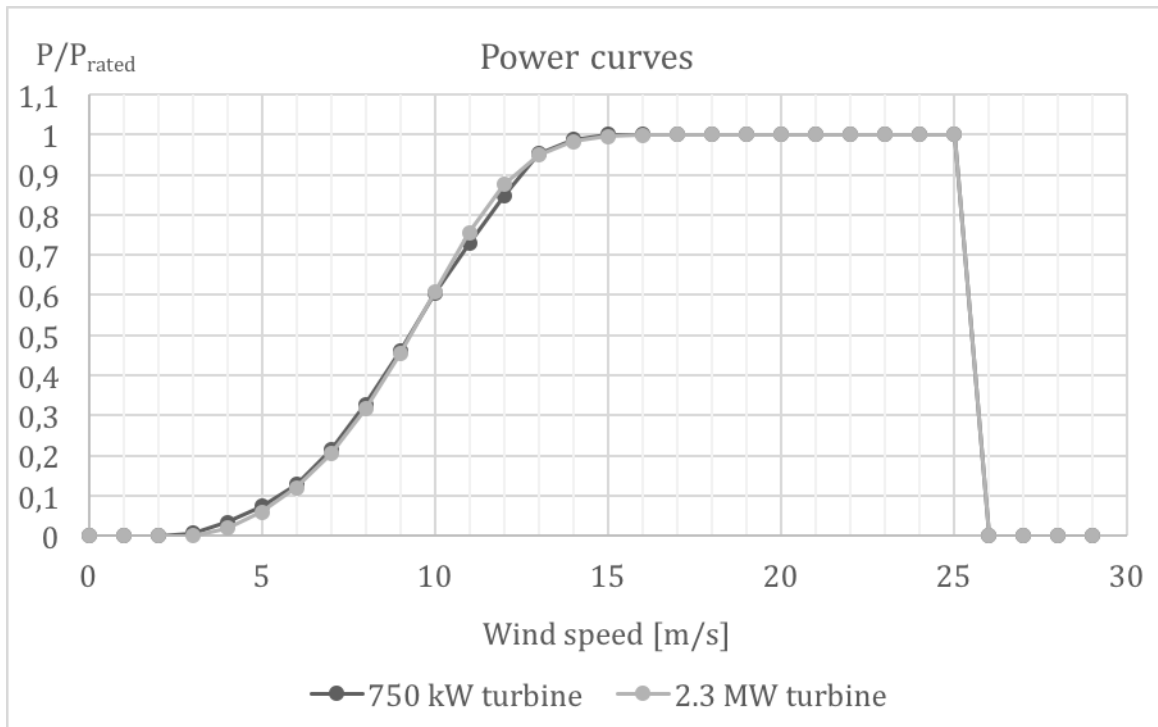
Figure 19: Power curves for both the GWP 750 kW turbine and the Hywind 2.3 MW turbine, where the power is shown at the y-axis as power production over rated power for each of the turbines.

Calculations of power production are done for each hour based on the wind speed extrapolated to hub height using the exponential profile according to the respective stability and using the power curve for both the Hywind 2.3 MW turbine and the GWP 750 kW turbine. In Table 4 some key numbers on the calculated energy production throughout the period can be seen.

For demonstrating the consequence of taking into account different atmospheric stability conditions, the energy production for 2.3 MW turbine for when only near-neutral conditions are assumed can be seen in the column to the far right. Here, the power law exponent is set to 0.11 for all hours regardless of temperature difference between air and sea. The result is an average wind speed of 7.17 m/s and a total energy production of 104.16 % compared to the production by 2.3 MW turbine when division of stability classes are made. Zero power production is the most common situation for both of these two cases, while maximum power production is the second least common production level for the case with five stability classes, and it is the least common situation when no consideration to classifications are made.

Table 4: Key numbers of energy production from the 750 kW turbine and the 2.3 MW turbine when division of the five stability classes are made. The production from the 2.3 MW turbine is also calculated when it is assumed exclusively near-neutral conditions throughout the period.

	GWP 750 kW turbine	Hywind 2.3 MW turbine	
	Calculated production when taking into account five different α according to stability	Calculated production when taking into account five different α according to stability	Calculated production if α=0.11 for all hours
Total energy production	1 027 305 kWh	3 205 195 kWh	3 338 634 kWh
Maximum possible energy production	3 502 500 kWh	10 741 000 kWh	10 741 000 kWh
Capacity factor, C_f	0.2933 (29.33 %)	0.2984 (29.84 %)	0.3108 (31.08 %)
Number of hours with zero power production	383 (8.20%)	748 (16.02 %)	740 (15.85 %)
Number of hours with maximum power production	119 (2.55%)	13 (0.28 %)	17 (0.36 %)

The energy production by Hywind has also been calculated by multiplying the probability of occurrence of each wind speed at hub height by the power production by the turbine at that same wind speed. The calculations can be found in Appendix F, and the results is seen in Figure 20. It is found that 10 m/s is the wind speed where highest power output is combined with most frequently occurring wind speed. In total, the energy produced by Hywind at 10 m/s is 426 564 kWh. At no other wind speed does the turbine produce more energy in total during the period. It is therefore at 10 m/s that the Hywind turbine should work best, i.e. have the highest power coefficient, if it were to be ideal for the wind conditions at site.

The GWP turbine also has its highest energy production of 138 818 kWh during hours with wind speed 10 m/s at 55 meters altitude. Calculations were done to estimate the power coefficients of both turbines for various wind speeds. The results show that maximum power coefficient for GWP is approximately 0.45 at 8 m/s, while Hywinds power coefficient at 9 m/s is 0.41 at its maximum. The calculations that these results are based on can be found in Appendix H.
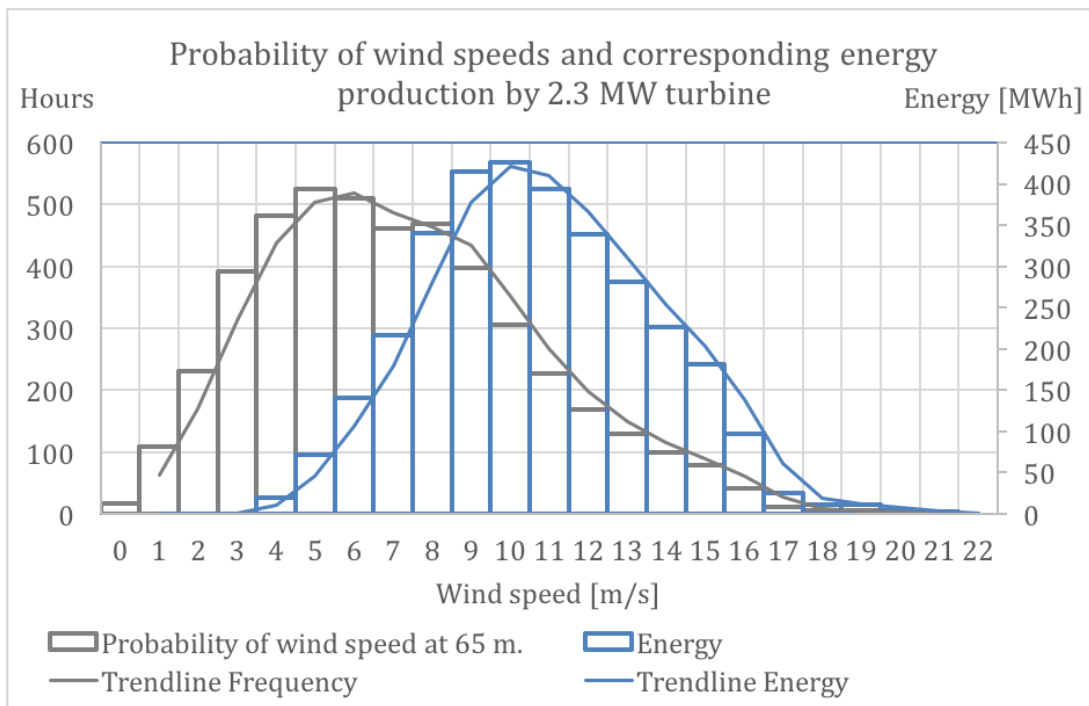
Figure 20: Frequency of wind speeds at 65 meters altitude and energy produced by Hywind 2.3 MW turbine.

The results from calculated power production for both the 750 kW turbine and the 2.3 MW turbine the throughout the period can be seen in Figure 21 below, where it is clear that the power production varies greatly and also becomes zero at times. The production is somewhat higher during the winter months and early spring, which is consistent with the normally higher wind speeds during this season and is slightly predictable from the result for calculated wind speed at 65 meters in this case.
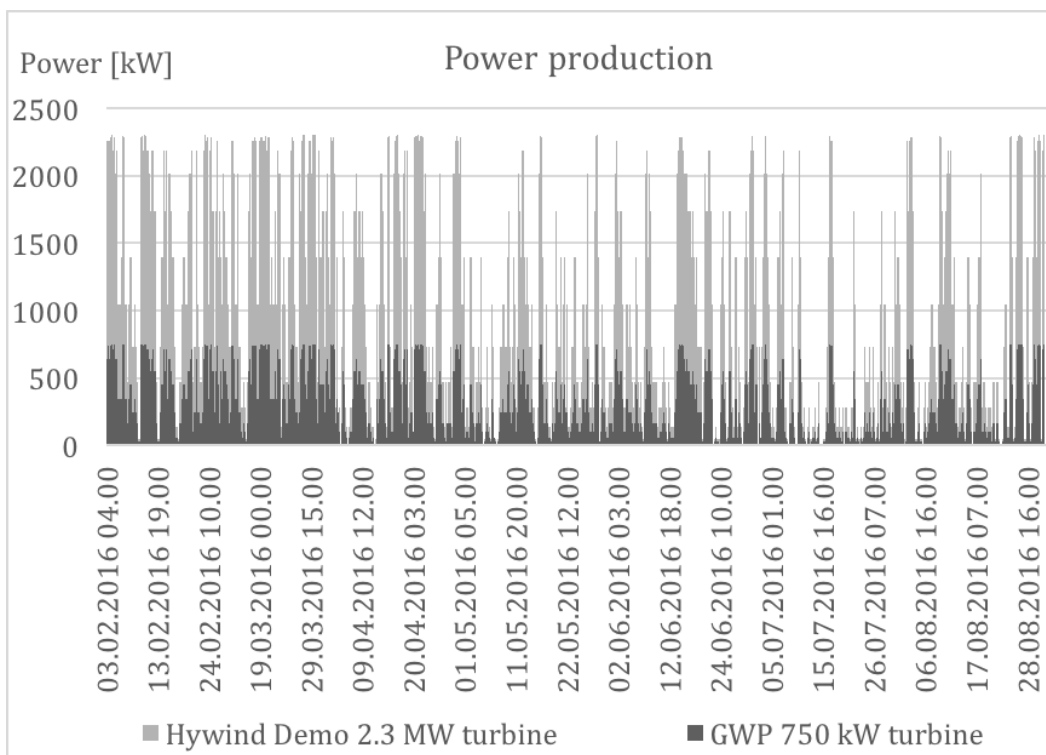
Figure 21: Power production by 750 kW and 2.3 MW turbine based on calculated wind speeds at 55 meters and 65 meters altitude, respectively.

Further, the average wind speeds and average power production for the Hywind 2.3 MW turbine for each stability class is calculated, as seen in Table 5. The average power production was found by taking the sum of energy produced during each stability class and divide it by number of hours of that stability class. The average wind speeds at both 2.5 and 65 meters are increasing for slightly stable, near-neutral and slightly unstable conditions, however, both for stable and unstable conditions this pattern is not valid. Following, the average power production must show the same pattern.

When average wind speeds at 2.5 meters are compared to average wind speeds at 65 meters for each stability class, the difference increase by almost 10 % for each classification, starting from least stable. Average capacity factor is found for each stability class, they are inevitable showing the same pattern as average wind speed and power production. The highest capacity factor is found for slightly unstable conditions and lowest value is found for slightly stable conditions. There is no evident dependence of stability class and capacity factor.

Table 5: Stability dependent values of average wind speeds and average power production (energy per hour) by the Hywind Demo 2.3 MW turbine.

Stability classes	Number of hours in total	Average wind speed at 2.5 m	Average wind speed at 65 m	Average power production	Average capacity factor, C_f
Unstable	296 (6%)	5.74 m/s	7.21 m/s	728 kW	31.63 %
Slightly unstable	1001 (22%)	5.74 m/s	7.70 m/s	804 kW	34.98 %
Near-neutral	2940 (63%)	4.81 m/s	6.88 m/s	654 kW	28.44 %
Slightly stable	342 (7%)	4.14 m/s	6.33 m/s	572 kW	24.87 %
Stable	91 (2%)	4.40 m/s	7.17 m/s	720 kW	31.29 %
Total	4670 (100%)	5.01 m/s	7.04 m/s	686 kW	29.84 %

4.2 Power Consumption

The complete power consumption data set from Rataren between 1st of February and 31st of August 2016 can be seen in Figure 22. Figure 23 shows the power consumption when periods with outages on the main measure point are excluded, which is the data used for further calculations. Maximum consumption is found at 195 kW on the 11th of May between 08.00 and 09.00. During spring and summer the power consumption is reduced because the base load is lighting. There is also less fish after August. The periods that are removed from the data sets are:

- 1st - 3rd of February
- 2nd - 15th of March
- 8th of April
- 20th -21st of April
- 12th of May
- 13th of June
- 22nd - 23rd of June
- 3rd - 4th of August
- 22nd - 23rd of August
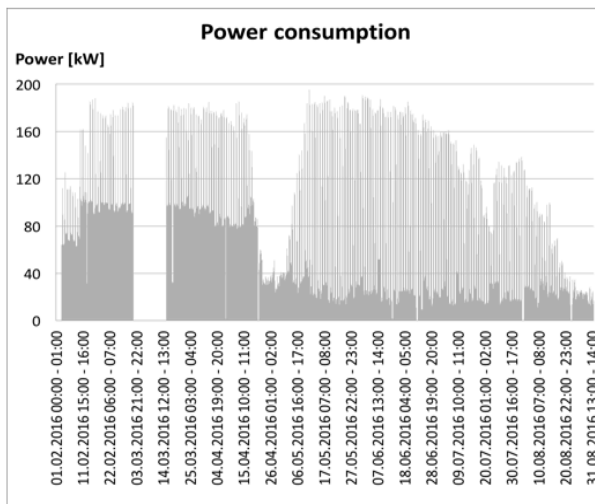
Figure 22: Power consumption as raw data. Source: SalMar ASA.
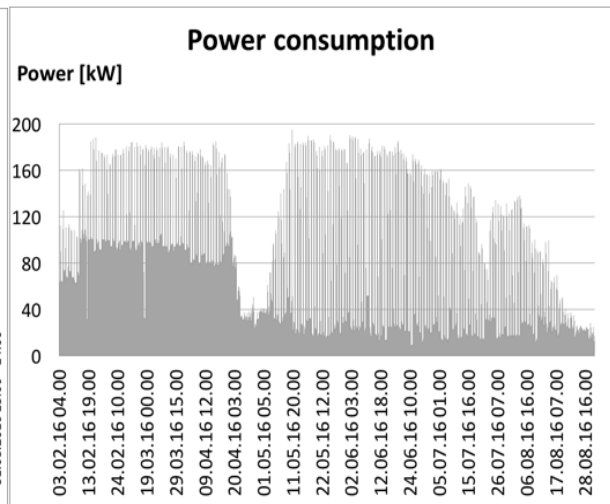
Figure 23: Power consumption when outage periods are excluded.

Figure 24 below is implemented to show the difference in energy demanding operations through the day for a period of two weeks. There are five measure point at Rataren, where the operation of feeding is shown to draw 38 % of the total energy consumption over the period of two weeks. The feeding is very regularly happening during daytime and this is by far the highest power load. There are two courses of light in the cages, which are used when there is no feeding.
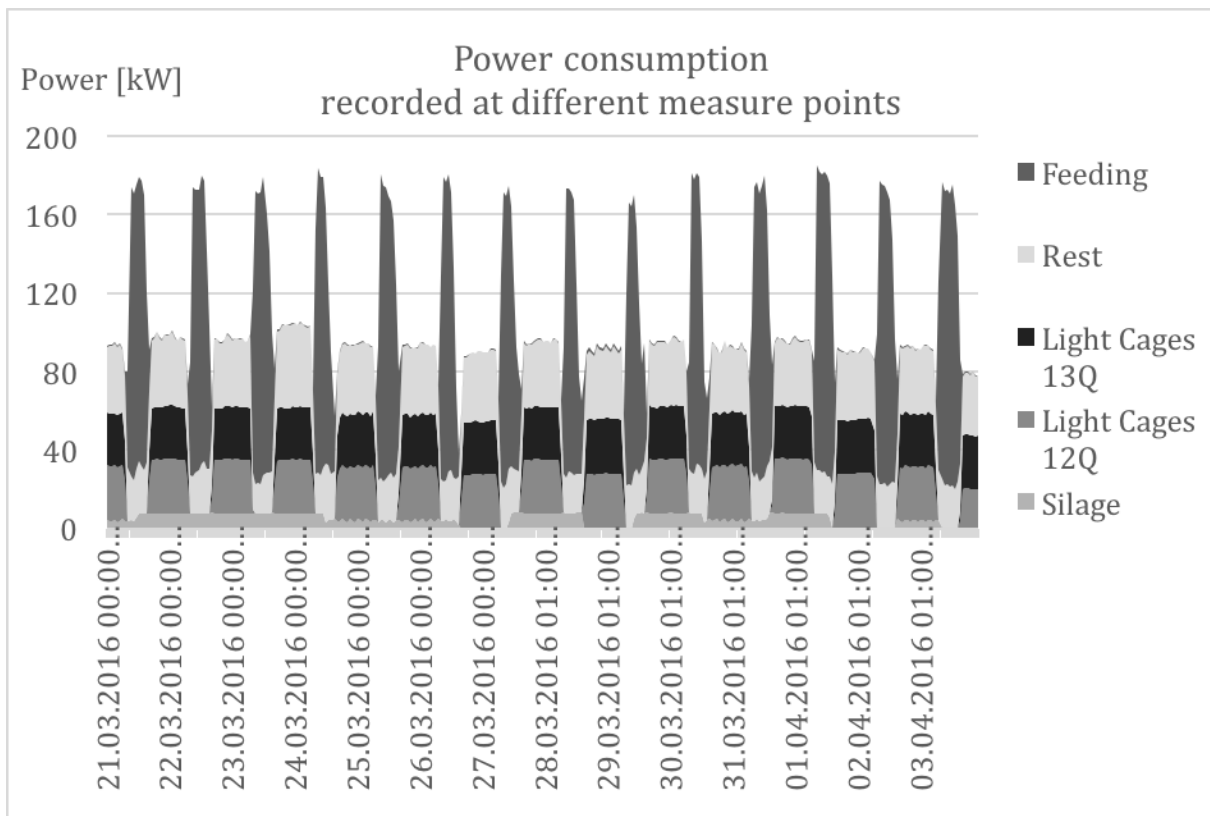
Figure 24: Power consumption as recorded at different measure points at Rataren fish farm. Source: SalMar ASA.

4.3 Comparing Production and Consumption

Over the seven months with available power consumption data, the load and estimated power production can be compared on hourly basis. For an illustration of the differences, Figure 25 shows the values for the first two weeks of that period. It is evident that the production in general is much higher than the consumption, especially for the Hywind turbine, but sometimes the production drops below what is adequate supply for the consumption at that time. For Hywind this happens a whole 1027 hours during the period, which corresponds to 22.00 % of the time. However, the lacking in power are not more than 187 kW as the fish farm does not consume much more than this. Nevertheless, these periods are very critical and makes the facility strongly dependent on a second energy source or an energy storage.
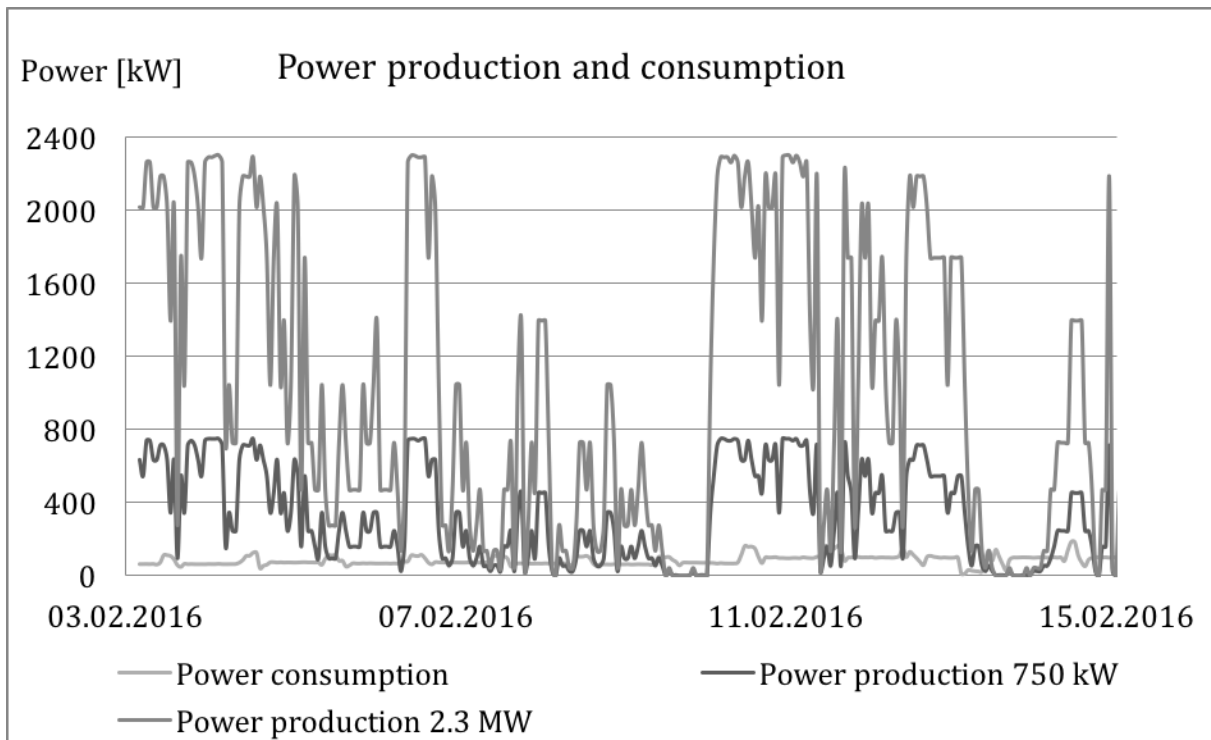
Figure 25: Comparison between power production by the 2.3 MW turbine, power production by the 750 kW turbine, and power consumption at the fish farm over two weeks.

By subtracting the power consumption from the power production for each hour, the continuous balance in power is found. This is shown in Figure 26 where the great surplus most of the time is evident for both turbines. The surplus and deficit represents the power that necessarily would be transferred between the onshore grid and the offshore facility without a large capacity energy storage at site. For Hywind 2.3 MW turbine, the total amount of turbine power utilized is only 8.43 %, which means that 91.57 % of all turbine power produced during the period is not utilized at the facility without energy storage. The summary results from the two turbines and the power consumption can be seen in Table 6 below.
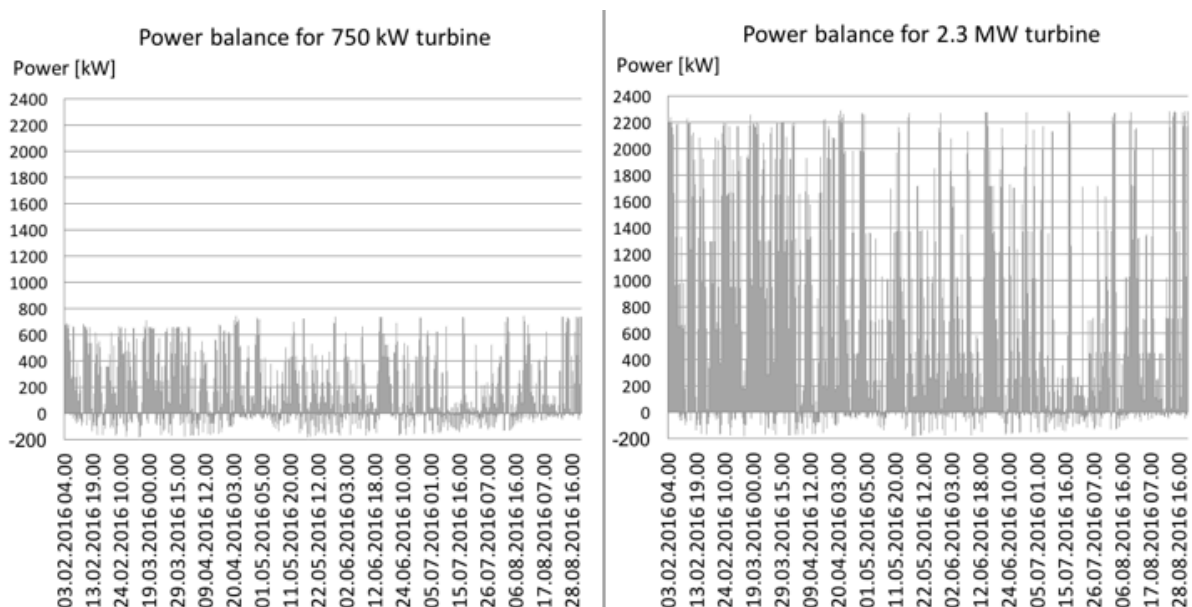
Figure 26: Power production minus power consumption is illustrated for the two cases.

A turbine farm consisting of three 750 kW turbines have a capacity of 2250 kW, i.e. almost the same capacity as one Hywind Demo 2.3 MW turbine. Table 5 shows a comparison between one 750 kW turbine, three 750 kW turbines and one 2.3 MW turbine, when serving the same consumption as previously shown. Differences between the scenarios with three 750 kW turbines and one 2.3 MW turbine are then almost exclusively due to differences in the power curves between the two turbines.

Table 6: Results from one 750 kW turbine, three 750 kW turbines, and one 2.3 MW turbine when serving the consumption at Rataren.

	1x 750 kW turbine	3x 750 kW turbines	1x 2.3 MW turbine
Total energy production	1 027 305 kWh	3 081 915 kWh	3 205 195 kWh
Total energy consumption	328 723 kWh	328 723 kWh	328 723 kWh
Total lacking in energy	82 949 kWh	48 136 kWh	58 654 kWh
Total surplus in energy	781 531 kWh	2 801 328 kWh	2 935 126 kWh
Total consumption covered by turbine production	245 774 kWh	280 587 kWh	270 069 kWh
Capacity factor, C_f	29.33 %	29.33 %	29.84 %
Percent covered by turbine production	74.77 %	85.36 %	82.16 %
Percent used of all turbine production	23.92 %	9.10 %	8.43 %
Percent of time with inadequate production	32.98 %	21.18 %	22.00 %

4.4 Scaling the Consumption

Further, the power consumption was scaled up to compare the difference in key numbers relative to an unchanged turbine capacity for the Hywind Demo 2.3 MW turbine. For this purpose, the original power consumption is multiplied by three and by six in two different cases, while the power production remains the same. The results from multiplying the consumption each hour by three, are shown in Figure 27. Likewise, the consumption is multiplied by six for the results in Figure 28. In theory, the two cases represent the consumption of 42 fish cages and three barges, and 84 fish cages and six barges, respectively. In Table 7 some key numbers for the two cases are listed.
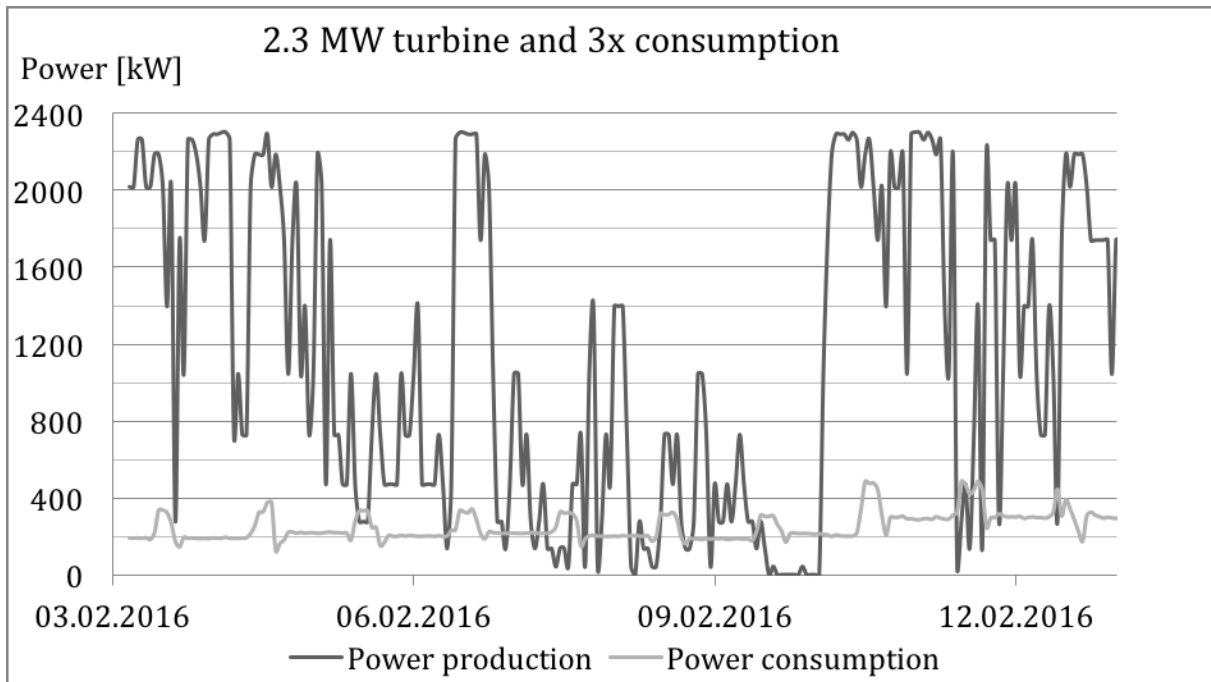
Figure 27: Two weeks of power production from 2.3 MW turbine and three times Ratarens power consumption.
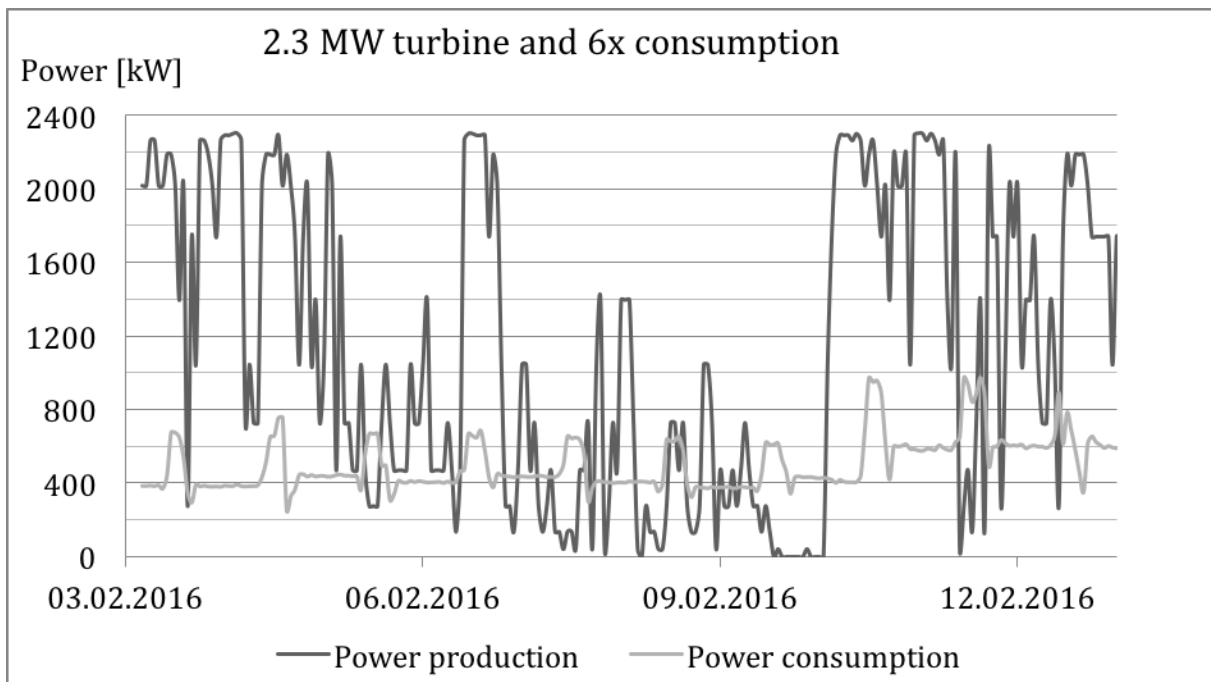
Figure 28: Two weeks of power production from 2.3 MW turbine and six times Ratarens power consumption.

Table 7: Results for upscaled fish farm power consumption while maintaining the 2.3 MW turbines power production.

	2.3 MW turbine and 3x consumption	2.3 MW turbine and 6x consumption
Total energy production	3 205 195 kWh	3 205 195 kWh
Total energy consumption	986 169 kWh	1 972 338 kWh
Total consumption covered by turbine	718 271 kWh	1 234 259 kWh
Total surplus of produced energy	2 486 924 kWh	1 970 936 kWh
Total inadequacy (lacking in production compared to consumption)	267 898 kWh	738 079 kWh

Figure 29 shows the comparison of key characteristics by the three different power consumption cases studied. The y-axis is set in percentage; for inadequate power production it gives the percentage of the time when this happens, i.e. the sum of hours when the power production does not cover the consumption, divided by all 4670 hours.

To calculate the percent of the consumption that is covered by the production, the amount of consumed power that is covered by the turbine production is summed and divided by the total energy consumption. To calculate the percent of the total energy that is utilized by the fish farm of all the energy that is produced, the amount of consumed power that is covered by the turbine for each hour is summed and divided by the total energy production. These values are also shown as percentage by the y-axis.

The lines are almost linear as the difference in the cases are simply the multiplication. The case with three times the consumption results in inadequate power production 35.74 % of the time, where six times the consumption gives a total of inadequate production 48.18 % of the time. Simultaneously, not more than 62.58 % of the fish farms consumption is covered. However, the surplus is still great, and only 38.51 % of the energy produced is utilized. 22.41 % of the produced energy is utilized for the case with three times the consumption, while 72.83 % of the time the consumption is covered.
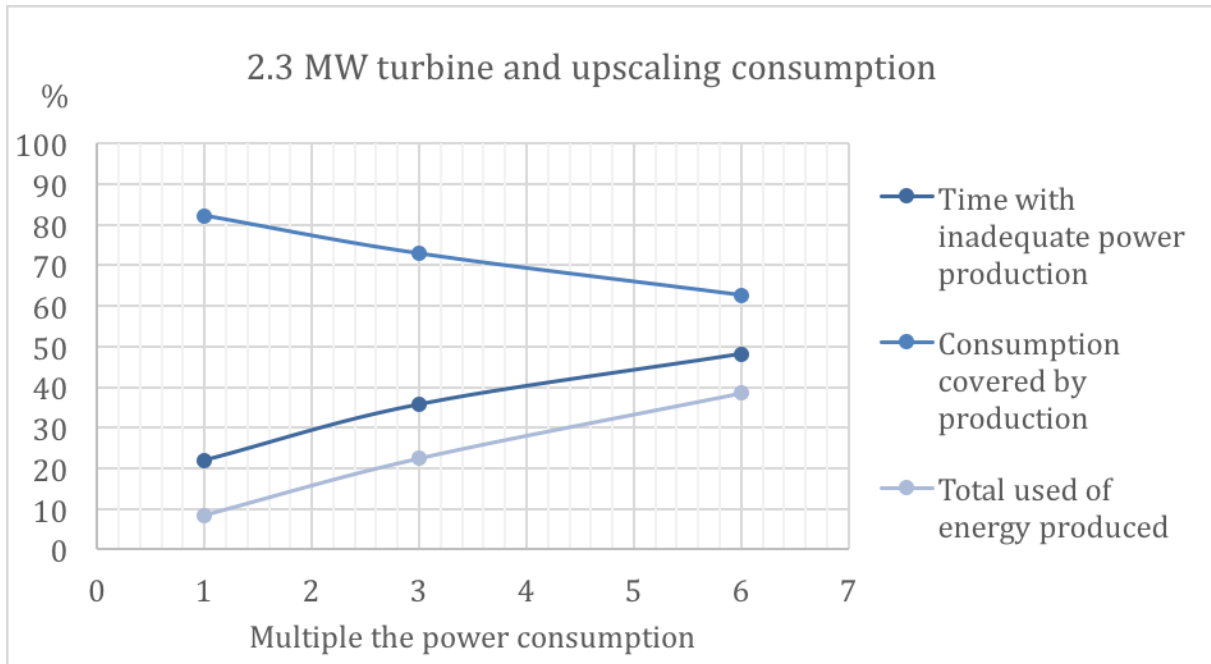
Figure 29: Relationship between change in power consumption and key characteristics. The percent of time with inadequate power production point to the sum of hours when the power production does not cover the consumption - divided by the total 4670 hours.

To sum up and for better to estimate the most preferred sizing, the energy necessary to transfer between Rataren and the mainland for the different cases mentioned, is presented in Table 8. The energy needed from the onshore grid in the case of three times the consumption is 4.6 times the energy needed in the case of original power consumption, both with the power production by the Hywind turbine. For six times the consumption this is 12.6 times the energy. On the other hand, the energy transferred to the onshore grid for three times the consumption is above 0.8 times compared to the case of original consumption. For six times the consumption the energy transferred to the onshore grid is almost 0.7 times the case with original consumption.

When comparing the results from the wind farm consisting of three 750 kW turbines with the one 2.3 MW turbine, both with the original power consumption at Rataren, it is found that the ratio of energy import to export to the onshore power grid would be lower for the case with 750 kW turbines. The amount of energy needed by the fish farm and not covered by the turbine is lower in the case with the three 750 kW turbines, however, also the total surplus of energy is lower for the 750 kW turbines than for one 2.3 MW turbine.

Table 8: Necessary energy transfer between fish farm and onshore grid when no energy storage is implemented. Ratio of energy import to export equals total energy transferred from the onshore power grid divided by total energy transferred to the grid.

Power production	GWP 750 kW		Hywind 2.3 MW		
	1 turbine	3 turbines	1 turbine	1 turbine	1 turbine
Power consumption compared to Rataren	1x consumption	1x consumption	1x consumption	3x consumption	6x consumption
Total energy transferred from grid	82 949 kWh	48 136 kWh	58 654 kWh	267 898 kWh	738 079 kWh
Total energy transferred to grid	781 531 kWh	2 801 328 kWh	2 935 126 kWh	2 486 924 kWh	1 970 936 kWh
Ratio of energy import to export	10.61 %	1.72 %	2.00 %	10.77 %	37.45 %

5. Discussion

The results presented in the previous chapter will be discussed here, and important aspects will be emphasized. The results are based on actual data measured at site, and even though there had to be some simplifications and assumptions, the results are expected to be as good as they could be in this case of study. Power law was chosen as the method used for extrapolating the wind speeds between altitudes, due to its simplicity and suitability when certain variables are unavailable. Assumptions had to be made both considering the chosen values of the power law exponents and the limits of temperature difference between air and sea, determining the stability classes and therefore when to apply the different exponents. This had the strongest impact on the result of power production as it is dependent on wind speed to the power of three, which can make a small error significant.

Firstly, the results from the determination of atmospheric stability classes were presented. Because of the method used for this, where temperature of air and sea is measured separately and the difference is calculated afterwards, there was a chance that the results would falsely show extreme stratification conditions most of the time, as mentioned in Chapter 3. This was however not the case as near-neutral conditions were found to occur 63 % of the time. As seen in Chapter 2, warm sea below colder air will heat up the air and this mass will rise, hence causing unstable conditions, and vice versa. Therefore, unstable conditions typically occur more often during winter months; tendencies that are also found in temperature distribution over the current period. When studying the temperature difference, it seems as July is the month more typical for the tendencies expected in the summer season, where in August the temperature differences causes some shorter unstable periods. The wind speeds during this period in August is not very high, which could have explained the labelling of "unstable" if it really was near-neutral conditions. This increase the credibility of the assumptions of stability classifications, but nevertheless, the uncompromising limits of temperature differences are known as simplifications.

From February till May there are only one shorter period of a few days when the atmosphere is found not to be near-neutral, slightly unstable or unstable. For example, 27th of March, which is during this stable period, wind speeds of 8 m/s are measured while the air temperature is 4°C higher than the sea temperature. According to Hsu (1994), at 4°C difference, wind speeds over 7 m/s at 10 meters height corresponds to neutral conditions.

Unless the stable conditions are actually causing an inverse wind profile, this is an occasion where the chosen simplification result in the wrong conclusion regarding stability. By simplification in this case it is meant that only the temperature differences between air and sea was considered when determining the applicable stability classes, and the wind speeds are not included as a factor in this. Inverse wind profile is assumed to be unlikely in this situation because it requires a relatively large decrease in wind speed between 2.5 meters and 10 meters height. The temperature data are the base for further results, and can therefore indicate slight disturbances to the stability and wind speed, and hence, the power production. However, this is considered almost impossible to avoid with the simplifications that had to be made.

In Chapter 3 the method given by Nfaoui (1998) was evaluated, which is including wind speed in estimations of power law exponent. During the discussed hours the 27th of March, the power law exponents were found to be 0.06 for $\mathcal{X} = 0.25$ and 0.11 for $\mathcal{X} = 0.31$ with this method. These are regarded as more reasonable for wind speed of 8 m/s while temperature difference is 4°C. However, there was found extreme values when using this method as

mentioned in Chapter 3; e.g. for $\mathcal{X} = 0.21$ the exponent drops to 0.02 right after the hours discussed 27th of March, and $\mathcal{X} = 0.31$ gives $\alpha = 0.25$ just hours before. It is therefore still considered reasonable to not use the method by Nfaoui (1998), however, there is also clear disadvantages with choosing the power law exponent values of 0.07-0.15 as well. Calculations from 27th of March can be found in Appendix E. In all, the limits set for temperature differences and the exponents for each stability class are assumed to be reasonable for the available data.

The wind distribution at 65 meters appears as a slightly understated extrapolation from 2.5 meters, with an average increase of 2.03 m/s. This can be due to the many low velocities found at 65 meters. At low velocities, there are very small differences in wind speed between the altitudes, which is also the nature of the logarithmic mean wind speed profile. When the wind speeds are higher, the difference in wind speed between the altitudes are also much higher, as expected.

The results for stability classes with wind speed show a slightly unexpected distribution. High wind speeds are expected to cause near-neutral conditions, while stable and unstable conditions are expected to dominate at wind speeds lower than 10 m/s at 10 meters' height, according to Hsu (1992), among others. This is not the tendency here, where a simple relation of stability to actual wind speed can not be identified, and near-neutral conditions occur at all wind speeds. The other stability classes are also distributed over the majority of the wind speeds. This can be a consequence of the varying temperature differences found throughout the period and is not necessarily an indication that the determinations of stability classes are inaccurate.

The power curves show similar characteristics for both types of turbine; the shut-down wind speeds are the same at 25 m/s, however, the cut-in wind speeds for the 750 kW turbine is 3 m/s - while for the 2.3 MW turbine it is 4 m/s. As the wind velocities at site are shown to be quite low, it is expected that the lower cut-in wind speed gives some benefits to the production by the 750 kW turbine. However, according to calculations the available energy in the wind during 3 m/s is only 11 305 kWh over the 394 hours at 55 m height, for the rotor area of the chosen 750 kW turbine. This is the energy that the 750 kW turbine can extract a small fraction of, while the 2.3 MW turbine can not extract anything at this speed.

For Hywind the energy available at 3 m/s is 36 786 kWh because of the much bigger rotor area, and the number of hours with this wind speed is only shorten by 2 hours at 65 meters compared to 55 meters height. The actual energy that the 750 kW turbine extract during these hours at 3 m/s is 1 576 kWh, which is just above 0.15 % of its total energy production of approximately 1.027 GWh throughout the period. The lower cut-in wind speed is much less important than what was first expected; because of the wind powers dependence on wind speed cubed, the lower wind speeds have much less impact on the power production than the higher velocities.

The assumption of near-neutral conditions for all hours was implemented for the Hywind 2.3 MW turbine in Table 4 to be able to evaluate the effect of changing power law exponent for different stability assumptions. The energy production became 104.16 % higher and hence, the capacity factor increased by 1.24 % for the Hywind turbine. The purpose of implementing stability classes is to effect the wind speed, and thereby the power production, to be more accurate. However, if the wrong stability class is implemented, i.e. by errors in the limits of temperature difference, it can enhance the error compared to if all hours were considered

near-neutral. In this case of study, it is expected that implementing five stability classes with corresponding power law exponents enhanced the accuracy of the energy production results, however, this could not be validated.

For the 750 kW turbine the capacity factor is shown to be only slightly lower than for the 2.3 MW turbine, however the number of hours with zero production is halved for the GWP turbine. This is due to the lower cut-in wind speed for the 750 kW turbine, and also the effect on wind speed by difference in hub heights. The number of hours with maximum power production is much higher for GWP than for Hywind. The 750 kW turbine reaches rated power at 15 m/s, however, the 2.3 MW turbine does not fully reach the rated power before wind speed is 18 m/s. Nevertheless, the power produced for the 2.3 MW turbine at for example 15 m/s is 2288 kW, i.e. very close to maximum. This causes the large difference in number of hours at maximum power production with 119 and 13 hours.

For best possible energy production, a turbine needs to work most efficient during the wind speed where the combination of high power output and high probability is at its maximum. In total, the most energy was produced by Hywind during the hours with a wind speed of 10 m/s. According to calculations on Hywinds power coefficient, it operates at its best at 9 m/s. At 10 m/s the turbine has a power coefficient at 0.401, which is very close to optimum at approximately 0.412. The GWP turbine was found to have the optimum power production at 8 m/s with a power coefficient of 0.452. The most energy was produced by GWP while the wind speed also was 10 m/s, at which the turbine has a power coefficient slightly above 0.426. These results indicate that the characteristics of the GWP turbine is more suitable for the conditions at site, and is expected to have a much larger impact on the total energy production than the lower cut-in wind speed of the GWP turbine. Further, the turbines capacity factors are relatively high; both the Hywind and the GWP turbine has a capacity factor close to 30 % for the period in total.

The comparison between the continuous power production by the turbines and the power consumption at Rataren shows large differences. The total production by the Hywind turbine was almost 9.8 times the energy consumed at the fish farm during the whole period, for the GWP turbine the ratio was just above 3.1. However, the turbines production does not cover the power demand at all times, which is the main challenge with wind power as discussed previously. A whole 22 % of the time the Hywind turbine does not produce the power needed by the fish farm, which is significant but not unreasonable, as it is typical that the power production varies greatly. Unaffected by the turbine capacity, such periods will exist because of calm winds or windless conditions. These periods are critical for the operation of the fish farm and would in this case without other additional energy source or energy storage, be strongly dependent on bi-directional transport of power from the onshore grid or other energy sources.

In addition to one single 750 kW turbine, a wind farm of three 750 kW turbines were compared to one 2.3 MW turbine. The wind farm consisting of three 750 kW turbines have almost the same capacity as one 2.3 MW turbine, however, the benefits with the 750 kW turbines are shown to be many. Even though the production by three 750 kW turbines is lower in total, the percent of the fish farms consumption that is covered by the production is higher, following is also the percent utilized of all energy produced by the turbines slightly higher. In addition, there is also a few more hours when the production is high enough to cover the power demand at that time. The benefits of utilizing three 750 kW turbines instead of one 2.3 MW turbine can be mainly due to the differences in the power coefficients at the wind speeds

around 10 m/s, as previously discussed. The main disadvantages of utilizing three turbines instead of one are considered to be the costs in conjunction with three foundations and installations, and also the wake that they would produce that can affect the power production. However, this is not taken into account here as economic aspects and placing of turbines are beyond the scope of the thesis.

The fish farm had diesel generators with a total of 700 kW capacity before becoming connected to the onshore grid in June 2016. If comparing the capacity of the diesel generators, it shows that one 750 kW turbine would be more than enough capacity if it was operating at maximum power production at all times. The capacity factor is just under 30 % in this case of study, which gives that the wind farm with three 750 kW turbines should supply almost enough energy – if production occurred whenever power was needed for the fish farm. However, during the period studied, the maximum power needed was 195 kW. Following, the diesel generator capacity would have been much higher than needed at this time and one 750 kW turbine is shown to supply over three times the amount of energy consumed during the seven months period.

Finally, the fish farm consumption was upscaled to compare different scenarios of production versus demand. It was decided to multiply the consumption by three and by six, and have the power production from the 2.3 MW turbine compared to both cases. Results show that the produced energy is 3.3 and 1.6 times the consumed energy during the whole period for three and six times the consumption, respectively. Even though the production is in total still higher than the consumption, the case where the consumption is multiplied by three resulted an inadequate production 35.74 % of the time. Six times the consumption shows inadequate production a whole 48.18 % of the time. These numbers show high frequencies of very critical periods as previously discussed, because additional solutions are needed for the power to be supplied to the fish farm. However, the facility would in any case be dependent on either energy storage or additional power sources.

Some key numbers for all different cases are presented for how much energy that must be transferred between the fish farm and the onshore grid as needed in the case of Rataren. It is evident that the total mismatch for the 2.3 MW turbine, i.e. the sum of lacking energy and surplus energy, is getting smaller as the consumption increase. Because of the scaling, it is reasonable to compare the wind farm with three 750 kW turbines to the one 2.3 MW turbine supplying normal power consumption, and the one 750 kW turbine to the 2.3 MW turbine supplying three times the consumption. In both cases the 750 kW turbine seems to be favourable, based on the results in this thesis. For the first comparison mentioned, the results can be summed up as follows.

From Table 6 it was clear that the three 750 kW turbines compared to the one 2.3 MW turbine has these advantages; higher percent of the consumption is covered by the turbine production, higher percent utilized of all turbine energy produced, and lower percent of time where the production is not high enough to cover the consumption at the time. In addition, results in Table 8 shows that it would be necessary to transfer much less energy to the fish farm for the three 750 kW turbines than for the one 2.3 MW turbine, and simultaneously is the unused energy available to be transferred to the onshore power grid only slightly lower. The difference between the three 750 kW turbines and the one 2.3 MW turbine for the original consumption at Rataren, is exclusively due to the difference in wind speed at hub height and power curve characteristics. As seen from the power coefficients, the GWP turbine has a higher value than Hywind at the speed where probability times the wind speed to the power of

three (i.e. proportional to the power in the wind) is highest, namely at 10 m/s. This is believed to be the main cause of the discovered advantages by the 750 kW turbine.

Finding the optimum combination of turbine size and fish farm size is not straight forward and unambiguous. Nevertheless, in this case there are reasons as mentioned to expect that the wind farm with three 750 kW turbines is most suitable for the energy consumption at Rataren fish farm. This is based on the assumptions regarding transferring power by transmission lines to and from shore, where it is most favourable with large transport from the wind turbines, and as small transport as possible to the fish farm from the onshore grid.

In general, for improving the balance in power supply and demand sufficiently, a control system for when the power is supplied is required. Power transferred from the onshore grid, or diesel generator if necessary, can be utilized, but more preferred is the solution of energy storage for utilizing more of the free wind power at site. In the case of fish farms with already installed cables to the onshore grid, which is the case at Rataren, an uneven supply and demand can be regularized by transferring the power quantities as seen. In that case, the system should be suitable for bi-directional transmission, if not, the surplus power produced by the wind turbines is wasted. The unpredictability regarding whether the power will be needed by the onshore grid when it is supplied can cause uncertainties in the potential income from selling the power, and vice versa; if the turbines does not produce enough power for a predicted surplus to the grid, it can have economic consequences because of the strict balance of the power market.

Whether the prediction of power transferred to and from the onshore grid can be estimated good enough, depends mostly on the accuracy of the wind resource estimations because the consumption at the fish farms is quite predictable. Wind estimations with very high accuracy are, as seen, nearly impossible to achieve. Power from the grid would be a great benefit to take advantage of if already installed, because of the costs of energy storage in the needed size. However, such a system would also be costly due to additional investments, and energy storage would make the facility power independent while also the power is free and guarantied renewable.

6. Conclusion and Future Work

The growth of the fish farming industry is dependent on the ability to be more sustainable and take into use technology development in the food production. There is currently a shift in use of energy source at the Norwegian offshore facilities from diesel generators to connections to the onshore power grid. Because available coastal areas are becoming fewer, the trend is to install facilities further offshore at exposed locations. This is making the power connection to shore more difficult, and simultaneously the autonomous operations increase, further enhancing the importance of reliable power supply.

Offshore wind power industry is developing rapidly and with the floating turbines entering the market, new areas of applications increase drastically. There are several benefits with the synergy of the two industries mentioned, hereby is the most important considered to be no continuous expenses for fuel, fuel transportation and storage, environmental advantages, i.e. no emissions, less noise and no risks regarding spill. In addition, and perhaps the most important for the future of fish farming industry; the facility's power independence is a significant advantage that enables fish farming further offshore regardless of the possibilities of cable connection to shore. Limitations on coastal areas can also be a factor that makes it necessary to share area, and can especially be beneficial for MUPs where the surplus power is to be transferred to the onshore grid.

The objective of this thesis has been to study the possibility of wind turbine as power supply for an offshore fish farm, by examine a specific facility's power consumption for a period and calculate the possible power production from wind turbines at site during the same period. In this thesis a fish farming facility outside Trøndelag in Norway have been studied regarding their power consumption from 1st of February to 31st of August 2016, the data has been given by curtesy from SalMar ASA through aPoint. The estimated power production from a Hywind Demo 2.3 MW turbine at the same location has been estimated with regards to the wind resource during the same period, the power curve is given from Statoil ASA. Also a GWP 750 kW turbine has been used for estimation on power production.

Data on wind speeds, air and sea temperature at site has been collected as data series from a SINTEF Ocean owned Seawatch Midi 185 Buoy. Measurements are done at 2.5 masl and at 1 mbsl. The wind speeds have further been extrapolated to hub heights at 55 and 65 meters by taking into account wind shear and atmospheric stability, using the power law. There are five stability classes included, where they are estimated based on the difference in air and sea temperature for each hour. The temperature differences where the atmosphere is assumed to change in stability are set to -3°C, -1°C, 1°C and 3°C. The power law exponent was determined for each stability class at values of 0.07, 0.09, 0.11, 0.13 and 0.15 for unstable, slightly unstable, near-neutral, slightly stable and stable, respectively. The validity of these strict limits for temperature and power law exponents has been discussed, however, simplifications had to be made and the values chosen are considered to be reasonable. As these assumptions are the base for wind resource estimations, smaller errors may have a large impact on calculated power production. The data on power consumption and weather conditions are at one-hour frequency, with weather data being the average of the last 15 minutes of the hour. For optimum results the data would have even higher frequency, as the conditions may change rapidly.

Results have shown as expected that the power production varies greatly while the power consumption at the fish farm is relatively stable and predictable. A high number of hours are

found for both turbines for when the power production is not high enough to cover the power consumption at that time. The capacity factors are close to 30 %, which is relatively high considering that these turbines are not designed for the wind conditions at site, and typical capacity factors for turbines offshore are 0.35-0.45 as mentioned.

For further evaluation of the suitability of the 2.3 MW turbine, the power consumption for each hour is multiplied by three and by six. The cases correspond to the total energy consumption for 42 cages and three barges, and 84 cages and six barges, given that this simplification in scaling is valid. This inevitably increase the percent of the time when the power production is inadequate to supply the power consumption, which is also associated with relatively low power utilization of the production. Based on this, the case with six times the consumption seems to be too high for the production by the Hywind Demo 2.3 MW turbine. Still, the amount of energy produced is 1.6 times as great as the energy consumed during the period, so it is possible that with sufficient energy storage this ratio of turbine capacity by power consumption is feasible.

In all, the results show that wind turbine is not suitable without energy storage or additional power sources. Hence, it is not possible to make a firm conclusion of which turbine is most suitable without further investigations. The 750 kW turbine had the highest power coefficient of the two at the wind speed occurring most frequent while also holding the most energy, which is also reflected when comparing the energy production of the two turbines. The case with three 750 kW turbines are supplying the consumption at Rataren show the lowest ratio of energy import to export from the onshore grid. These results indicate that the GWP 750 kW turbine is slightly more suitable than the Hywind Demo 2.3 MW turbine, however, this can not be validated in this case.

In general, a shortage in research on the power law exponent for different stability classes offshore was discovered, in addition to very few studies on wind turbine as power supply for offshore fish farms. Optimum solutions can be found by more research, and stimulate the development of demo projects. If the synergy of the two industries mentioned evolve, it could possibly be an example for the sustainable development of other industries in the future. The subject of renewable energy production from wind turbines for aquaculture use urges a lot of subjects for studying. The following lists a few of them.

- Storage systems can be evaluated, as this is an essential part for utilizing the intermittent wind power. This is a very important subject of study for RES in general, but essential to off-grid power systems.
- Optimization in the ratio of capacity between fish farm, turbine and energy storage size through simulation.
- Control and demand side management (DSM).
- Evaluate more exposed locations for multiuse and possibly closed or semi-closed cages that are particularly relevant further offshore.
- For the estimation of wind resources offshore, there were found some shortages in literature regarding the atmospheric stability and its impact on the power law exponent. The results from this thesis and power law exponents chosen could have been compared to other findings for indications of their validity. Also to compare the results with other methods (log law) if more data are available. Future work could therefor study a general correlation between the two methods offshore that would likely to be of great advantage of other wind resource studies.

7. References

ACE. (2013). Rataren - fasiliteter og bruk. Retrieved from
http://www.sintef.no/globalassets/sintef-fiskeri-og-havbruk/aquanor2015/flate-fasiliteter-rataren.pdf

Ahrens, C. D. (2015). *Essentials of Meteorology: An Invitation to the Atmosphere* (7th ed.): Cengage Learning.

Aquafarm. (2017). Aquafarm Equipment: Closed Cage. Retrieved from
http://aquafarm.no/

Bjelland, H. V., Føre, M., Lader, P. et.al. (2015). *Exposed Aquaculture In Norway: Technologies For Robust Operations In Rough Conditions*. Paper presented at the OCEANS'15 MTS/IEEE Washington, Washington, DC, USA.
http://ieeexplore.ieee.org/stamp/stamp.jsp?arnumber=7404486&tag=1

Bosma, T., Bunschoten, J. et.al. (2014). *DNV GL: Electrifying The Future*. Retrieved from
http://production.presstogo.com/fileroot6/gallery/dnvgl/files/original/f7a2169b6b9c4763e04385ee5e4dbd8c_hi.pdf

Boyle, G. (2012). *Renewable Energy: Power For a Sustainable Future* (3rd ed.): Oxford University Press.

Cañadillas, B., Neumann, T., Muñoz-Esparza, D. (2011). *First insight in offshore wind profiles up to 250 m under free and wind turbine wake flows*. Paper presented at the EWEA Offshore 2011, Amsterdam, The Netherlands.

Christensen, E. D. (2016). *MERMAID Report Summary*. Retrieved from
http://cordis.europa.eu/result/rcn/183781_en.html

Corrigan, D., Matthiesen, D. H. (2017). Analysis of the power law exponent applied to Lake Erie wind shear. *Wind Engineering, 41*(2), 103-113.

Counihan, J. (1975). Adiabatic atmospheric boundary layers: a review and analysis of data from the period 1880-1972. *Atmospheric Environment, 9*(10), 871-905. doi:10.1016/0004-6981(75)90088-8

DNV. (2010). *Recommended Practice DNV-RP-C205: Environmental conditions and environmental loads* Retrieved from
https://rules.dnvgl.com/docs/pdf/DNV/codes/docs/2010-10/RP-C205.pdf

Drennan, W. M., Taylor, P.K, Yelland, M.J. (2005). Parameterizing the Sea Surface Roughness. *Journal of Physical Oceanography, 35*, 835-848.

Dyrbye, C., Hansen, S.O. (1997). *Wind Loads on Structures*. Chichester, England: John Wiley and Sons.

ECF. (2010). *Roadmap 2050: A practical guide to a prosperous, low-carbon Europe*. Retrieved from
http://www.roadmap2050.eu/attachments/files/Volume1_fullreport_PressPack.pdf

Emeis, S. (2005). How Well Does a Power Law Fit to a Diabatic Boundary-Layer Wind Profile? *DEWI Magazin, 26*.

EPA. (2000). *Meteorological Monitoring Guidance for Regulatory Modeling Applications*: U.S. Environmental Protection Agency

Flakne, E., Gärdeman, O. (2015). Havets gull får strøm fra land [Press release]. Retrieved from http://presse.enova.no/news/havets-gull-faar-stroem-fra-land-103514

Flathagen, D. M. (2016a). En stille revolusjon til havs. Retrieved from
https://www.fornybar.no/bedrift/transport/transporthistorier/en-stille-revolusjon-til-havs/

Flathagen, D. M. (2016b). Næringen må bygge ut landstrøm på alle anlegg. Retrieved from http://presse.enova.no/news/6-kjappe-om-fiskeri-og-havbruk-naeringen-maa-bygge-ut-landstroem-paa-alle-anlegg-199453

Furevik, B. R., Haakenstad, H. (2012). Near-surface marine wind profiles from rawinsonde and NORA10 hindcast. *Journal of Geophysical Research, 117*(D23).

GWP. (2002). GWP47-750kW. Retrieved from http://www.gwpl.co.in/wind_turbines/pdf/GWP47-750kW.pdf

H2OCEAN. (2014). H2OCEAN development of a wind-wave power open-sea platform equipped for hydrogen generation with support for multiple users of energy. Retrieved from http://www.h2ocean-project.eu/

H2OCEAN. (2016). *Final Report Summary - H2OCEAN*. Retrieved from http://cordis.europa.eu/result/rcn/177009_en.html

Haakull, A. W., Askeland, J. V., Frugaard, L.T. (2016). *Fornybare energikilder til oppdrettsanlegg.* (Bachelor), Haugesund University College. Retrieved from https://brage.bibsys.no/xmlui/bitstream/id/436185/ING3039BacheloroppgaveHaakull AskelandFrugaard.pdf

Hammervik, T. (2015). Fyller opp forsøksanlegget med 2,5 millioner fisk. *Hitra-Frøya*. Retrieved from http://www.hitra-froya.no/naeringsliv/article10721439.ece

HaugeAqua. (2017). Technology for sustainable growth in aquaculture. Retrieved from http://www.haugeaqua.com/Technology/

He, W., Weissenberger, J., et. al. (2011). Integration of a wind farm with a wave- and an aquaculture farm. Retrieved from https://brage.bibsys.no/xmlui/bitstream/id/48544/EWEAOffshoreWind2011_Poster33 9_Final.pdf

He, W., Yttervik, R., et. al. (2013). A case study of multi-use offshore platforms. Retrieved from http://www.vliz.be/projects/mermaidproject/images/PDFs/EWEA2013Poster.pdf

Heinemann, D. (2002). *Energy Meteorology*. Carl Von Ossietzky Universitat, Oldenburg. Lecture notes. Retrieved from https://www.uni-oldenburg.de/fileadmin/user_upload/physik/ag/ehf/enmet/download/lectures/Energy_ Meteorology_Script.pdf

Ho, D., Sansone, F. (2015). *Air-Sea Gas Exchange*. OCN 623 – Chemical Oceanography. SOEST, University of Hawaii. Retrieved from https://www.soest.hawaii.edu/oceanography/courses/OCN623/Spring 2015/Gas_Exchange_2015_one-lecture1.pdf

Holtslag, M. C., Bierbooms, W. A. A. M., van Bussel, G. J. W. . (2014). Estimating atmospheric stability from observations and correcting wind shear models accordingly. *Journal of Physics: Conference Series (JPCS), 555*. doi:10.1088/1742-6596/555/1/012052

Hsu, S. A. (1974). A dynamic roughness equation and its application to wind stress determination at the air-sea interface. *Journal of Physical Oceanography, 4*(1), 116-120.

Hsu, S. A. (1992). An overwater stability criterion for the offshore and coastal dispersion model. *Boundary-Layer Meteorology, 60*(4), 397-402.

Hsu, S. A. (1994). Determining the Power-Law Wind-Profile Exponent under Near-Neutral Stability Conditions at Sea. *Journal of Applied Meteorology, 33*, 757-765.

JCSS. (2001). *(Joint Committee on Structural Safety); Probabilistic Model Code, Part 2: Loads*. Retrieved from

Justus, C. G. (1978). *Winds and wind system performance*. Philadelphia, USA: Franklin Institute Press.

Khalfa, D., Benretem, A., Herous, L., Meghlaoui I. (2014). Evaluation of the adequacy of the wind speed extrapolation laws for two different roughness meteorological sites. *American Journal of Applied Sciences, 11*(4), 570-583.

Kitaigorodskii, S. A., Volkov, Y.A. (1965). On the roughness parameter of the sea surface and the calculation of momentum flux in the near-water layer of the atmosphere. *Izv. Atmos. Oceanic Phys., 1*, 973-988.

Knain, M. (2017). [Enova Financial Support, e-mail].

Lagerveld, S., Röckmann, C., Scholl, M. (Eds.). (2014). Combining Offshore Wind Energy and Large-scale Mussel Farming: Background & Technical, Ecological and Economic Considerations.

Manwell, J. F., McGowan, J. G., Rogers, A. L. . (2009). *Wind Energy Explained: Theory, Design and Application* (2nd ed.). UK: John Wiley & Sons Ltd.

Mathew, S., Philip, G. S., et.al. (2011). *Advances in Wind Energy Conversion Technology*. Berlin, Germany: Springer.

Mermaid. (2016). *Go offshore - Combining food and energy production*: DTU Mechanical Engineering,Technical University of Denmark.

Michalis, M., Vassos, V., Loucas, P., et. al. (2013). *A feeding management system: The integration of a renewable energy sources system with aquaculture*. Retrieved from Research Gate: http://www.wseas.us/e-library/conferences/2013/Lemesos/ENVIR/ENVIR-43.pdf

Mohan, N. (2012). *Power Electronics: A First Course*. USA: John Wiley & Sons, Inc.

Motta, M., and Barthelmie, R. J. (2005). The Influence of Non-logarithmic Wind Speed Profiles on Potential Power Output at Danish Offshore Sites. *Wind Energy, 8*, 219-236. doi:10.1002/we.146

Moxnes, S. (2017). *Hva er utsiktene for flytende vindturbiner til havs?* Paper presented at the Klimafrokost, Klimastiftelsen, Bergen.

Myrseth, G. J. (2016). The Green Fish Farm Concept. Retrieved from http://prototech.no/news/2016/11/07/the-green-fish-farm-concept/

Næss, A. (2017). [Typical power demand at fish farms].

Newman, J. F., Klein, P. M. (2014). The Impacts of Atmospheric Stability on the Accuracy of Wind Speed Extrapolation Methods. *Resources, 3*, 81-105. doi:10.3390/resources3010081

Nfaoui, H., Buret J., Sayigh A.A.M. . (1998). Wind characteristics and wind energy potential in Morocco. *Solar Energy, 63*, 51-60. doi:10.1016/S0038-092X(98)00040-1

Nielsen, F. G. (2016a). *Wind Energy: Extracting Power*. University of Bergen. Lecture ENERGI200.

Nielsen, F. G. (2016b). *Wind Energy: Technical issues*. University of Bergen. Lecture ENERGI200.

Optis, M., Monahan, A., Bosveld, F.C. (2016). Limitations and breakdown of Monin–Obukhov similarity theory for wind profile extrapolation under stable stratification. *Wind Energy, 19*(6), 1053-1072.

Panofsky, H. A., Dutton, J.A. (1984). *Atmospheric Turbulence, Models and Methods for Engineering Applications*. New York, USA: John Wiley and Sons.

Pasquill, F. (1961). The estimation of the dispersion of windborne material. *Meteor. Mag, 90*, 33-49.

Reed, J. L. (2013). *Lokalitetsrapport Rataren I*. Retrieved from http://aceaqua.no/wp-content/uploads/2013/03/Rataren-I-Lokalitetsrapport-0213-siste.pdf

Simiu, E., Scanlan, R.U. (1978). *Wind Effects on Structures; An Introduction to Wind Engineering*. New York, USA: John Wiley and Sons.

SINTEF. (2011). Matproduksjon fra miljøvennlig akvakultur - drøm eller realitet? Retrieved from http://www.sintef.no/siste-nytt/matproduksjon-fra-miljovennlig-akvakultur-drom-ell/

SINTEFOcean. (2015). Lukkede system for oppdrett og transport. Retrieved from http://www.sintef.no/prosjekter/lukkede-system-for-oppdrett-og-transport/

SjømatNorge. (2017). Norwegian Seafood Federation. Retrieved from http://sjomatnorge.no/norwegian-seafood-federation/

Spera, D. A., Richards, T.R. (1979). *Modified power law equations for vertical wind profiles*. Paper presented at the Wind Characteristics and Wind Energy Siting Conference, Portland, Oregon.

Stull, R. B. (1988). *An introduction to boundary layer meteorology*: Springer Netherlands.

Subasinghe, P. R. (2003). An outlook for aquaculture development: major issues, opportunities and challenges. *Review of the state of world aquaculture, 886*(FAO Fisheries Department).

Taylor, P. K., Yelland, M.J. (2001). The dependence of sea surface roughness on the height and steepness of the waves. *Journal of Physical Oceanography, 31*(2), 572–590.

Toner, D., Mathies, M. (2002). *The Potential for Renewable Energy Usage in Aquaculture*. Retrieved from http://www.aquacultureinitiative.eu/Renewable Energy Report.pdf

van der Tempel, J. (2006). *Design of Support Structures for Offshore Wind Turbines.* (PhD), Technische Universiteit Delft, Delft, Nederland. Retrieved from http://www.tudelft.nl/fileadmin/UD/MenC/Support/Internet/TU_Website/TU_Delft_portal/Onderzoek/Kenniscentra/Kenniscentra/DUWIND/Dissertations/doc/JvdT_final.pdf

Webb. (1970). Profile relationships; the log linear range, and extension to strong stability. *Quarterly Journal of the Royal Meteorological society, 96*, 67-90.

Wever, L., Krause, G. Buck, B. H. (2015). Lessons from stakeholder dialogues on marine aquaculture in offshore wind farms: Perceived potentials, constraints and research gaps. *Marine Policy, 51*, 251–259.

WindEurope. (2017a). *The European offshore wind industry - Key trends and statistics 2016*. Retrieved from https://windeurope.org/wp-content/uploads/files/about-wind/statistics/WindEurope-Annual-Offshore-Statistics-2016.pdf

WindEurope. (2017b). *Wind in power - 2016 European statistics*. Retrieved from https://windeurope.org/wp-content/uploads/files/about-wind/statistics/WindEurope-Annual-Statistics-2016.pdf

WMO. (1998). *Guide to Wave Analysis and Forecasting* (2nd ed.). Geneva, Switzerland: Secretariat of the World Meteorological Organization.

Wu, J. (1969). Wind Stress and Surface Roughness at Air-Sea Interface. *Journal of Geophysical Research, 74*(2), 417–733. doi:10.1029/JB074i002p00444

Wu, J. (1980). Wind stress coefficients over sea surface near neautral conditions - A revisit. *Journal of Physical Oceanography, 10*, 727-740.

Zanuttigha, B., Angelellia, E., Kortenhausb, A., Kocac, K., Krontirad, Y., Koundourie, P. (2016). A methodology for multi-criteria design of multi-use offshore platforms for marine renewable energy harvesting. *Renewable Energy, 85*(January 2016), 18.

Appendices

In addition to received datasheet and power curves, essential calculations for the thesis are shown with the first few hours of the period as examples.

Appendix A: Datasheet for Gill Instrument

On the buoy there is a Gill instrument measuring the wind speed. The following shows an excerpt from the datasheet supplied by SINTEF Ocean.

GILL INSTRUMENTS

WindSonic

User Manual

Doc No. 1405-PS-0019
Issue 18

22/10/2009
APPLIES TO UNITS SUPPLIED FROM OCTOBER 2009
WITH SERIAL NUMBERS 09430000 ONWARDS

Gill Instruments Limited
Saltmarsh Park,
67 Gosport Street,
Lymington,
Hampshire.
SO41 9EG
UK

Tel: +44 (0) 1590 613500
Fax: +44 (0) 1590 613501
E-mail: anem@gill.co.uk
Website: www.gill.co.uk

4   PRINCIPLE OF OPERATION

The WindSonic measures the times taken for an ultrasonic pulse of sound to travel from the North transducer to the South transducer, and compares it with the time for a pulse to travel from S to N transducer. Likewise times are compared between West and East, and E and W transducer.

If, for example, a North wind is blowing, then the time taken for the pulse to travel from N to S will be faster than from S to N, whereas the W to E, and E to W times will be the same. The wind speed and direction can then be calculated from the differences in the times of flight on each axis. This calculation is independent of factors such as temperature.

TIME OF FLIGHT THEORY

$$T_2 = \frac{L}{C - V} \quad \text{And} \quad T_1 = \frac{L}{C + V}$$

Therefore

$$V = \frac{L}{2}\left\{\frac{1}{T_1} - \frac{1}{T_2}\right\} \qquad C = \frac{L}{2}\left\{\frac{1}{T_1} + \frac{1}{T_2}\right\}$$

KEY

L = Distance between transducer faces
C = Speed of sound
V = Velocity of gas flow
T1 = Transit time of ultrasound
T2 = Transit time of ultrasound
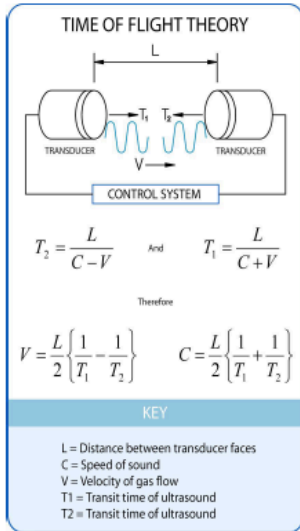
Figure 1 Time of Flight details

NORTH MARKER ARROWS
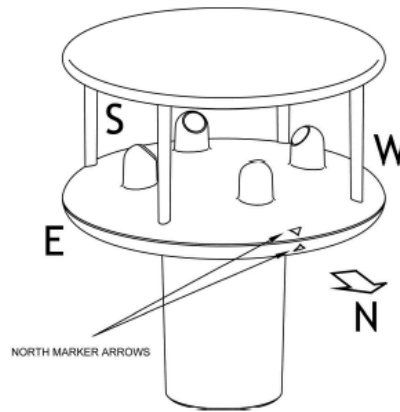
Figure 2 Compass Points

5   SPECIFICATION

This Specification relates only to Option 1, 2 and 3 WindSonic Sensors fitted with a Red Tab adjacent to the North Marker arrow and Serial Numbers 08100001 onwards.

Output		
Units of measure	Metres/second (m/s), Knots, Miles per hour (mph), Kilometres per hour (kph), Feet per minute (fpm)	
Output frequency	0.25, 0.5, 1, 2, or 4 outputs per second	
	Digital	**Analogue**
Parameters	Polar - Speed and Direction UV - 2 axis, signed Speed NMEA Speed and Direction Tunnel - U speed & U Polarity	Polar - Speed and Direction UV - U Speed and U Polarity NMEA – Speed and Direction Tunnel - U Speed & U Polarity
Wind Speed		0 – 5m/s, 0 – 10m/s, 0 – 20m/s,
Range	0 – 60m/s,	0 – 30m/s, 0-40m/s, 0 – 50m/s, 0 – 60m/s
Accuracy	± 2% (at 12m/s)	± 2% (at 12m/s)
Resolution	0.01 m/s	10 bits
Wind Direction		
Range	0 - 359°	0 - 359° Or 0 - 539° (Wraparound mode)
Accuracy	± 3° (at 12m/s)	±3° (at 12m/s)
Resolution	1°	1°
Analogue output formats		
0-5V	± 1% of full scale N.B. Analogue output impedance = 1KΩ (V out) Load resistance between the Analogue outputs (Pins 8 & 9) and Signal Ground (Pin 1) must be <= 300 ohms, including cable resistance.	
4-20mA		
0-20mA		
Digital output formats		
Gill	Continuous or Polled (output on request by host system) Polar (Speed and Direction) or UV (2 axis, signed Speed)	
Marine – NMEA	NMEA 0183 version 3	
Communication formats		
WindSonic Option 1	RS232	
WindSonic Option 2	RS232, RS422, RS485	
WindSonic Option 3	RS232, RS422, RS485, and Analogue	
Baud Rate	2400, 4800, 9600, 19200, 38400 Baud	
Anemometer status	Status OK and Error codes included in output message	

Environmental	
Moisture protection	IP65
Temperature	Operating -35°C to +70°C Storage -40°C to +80°C
Humidity	Operating <5% to 100%
EMC	EN 61326
Standards	Manufactured within ISO9001: 2000 quality system

Power requirement	5 – 30 V DC Option 1 and 2 units. 7 – 30 V DC. Option 3 unit. Current drain depends on variant i.e. RS232 approximately 9mA rising to 44mA for Analogue variant. Lowest power consumption is obtained with the following configuration:- M2, P20, B3, S9 (approximately 5.5mA at 12v).
Mechanical	
Size / weight	142mm diameter x 160mm 0.5kg
Mounting	Pipe mounting 1.75 inches (44.45mm) diameter
Material	External - Acrylate Styrene Acrylonitrile, Polycarbonate blend.

The Specification for the Option 4 SDI-12 unit is detailed in Section 14.

Appendix B: Power Curve for Hywind Demo 2.3 MW Turbine
By courtesy from Statoil.

Wind speed [m/s]	Power output [kW]
0	0
1	0
2	0
3	0
4	42
5	136
6	276
7	470
8	727
9	1043
10	1394
11	1738
12	2015
13	2183
14	2260
15	2288
16	2297
17	2299
18	2300
19	2300
20	2300
21	2300
22	2300
23	2300
24	2300
25	2300
26	0
27	0
28	0
29	0
30	0
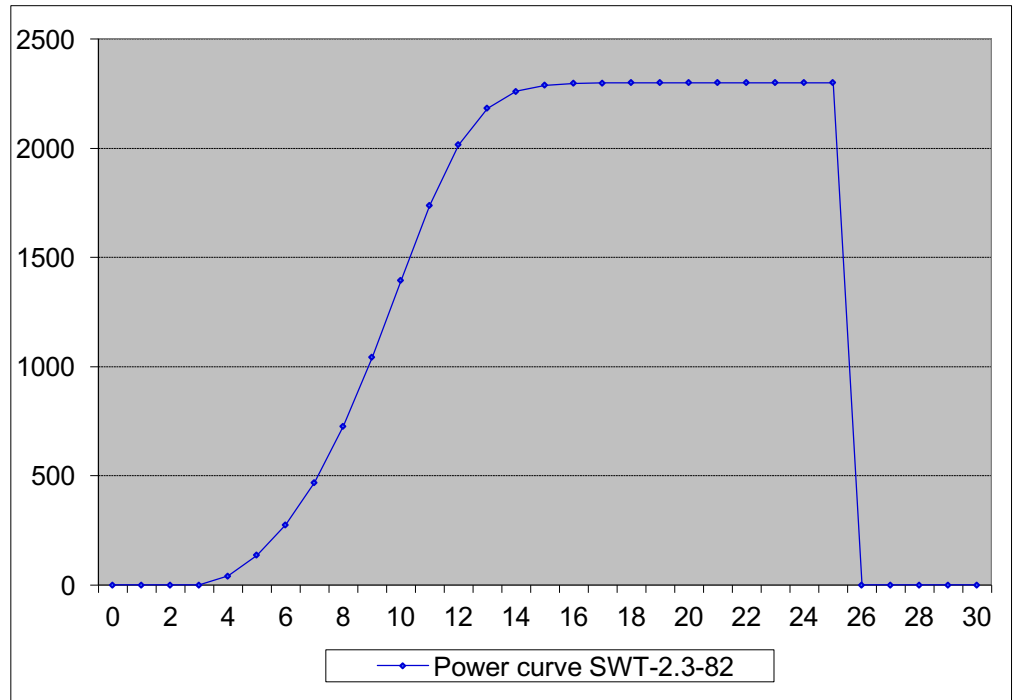
Appendix C: Power Curve for GWP 750 kW Turbine
This is a turbine randomly chosen and used for all calculations involving a 750 kW turbine in the thesis (GWP, 2002).

Wind speed [m/s]	Electrical power [kW]
1	0
2	0
3	4
4	25
5	55
6	96
7	160
8	246
9	345
10	453
11	546
12	635
13	714
14	740
15	750
16	750
17	750
18	750
19	750
20	750
21	750
22	750
23	750
24	750
25	750

Power curve GWP47-750kW
Wind speed [m/s]
Calculated power curve for air density 1,225kg/m^3
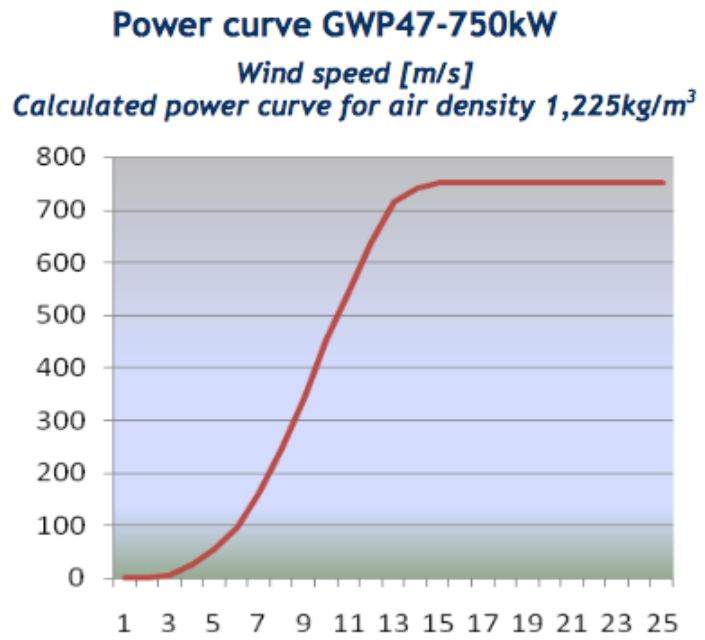
Appendix D: Log Law Calculations

Following is a small excerpt of the attempts to apply the logarithmic wind profile that resulted in inconsistencies and are rejected from the results in the thesis. The data are only divided into three stability classes and the hub height is set to 80 meters, as seen. From row 14 and 15, an example of the unreasonable jumps is shown; the difference in wind speed at 2.5 m. is 2 m/s but at 80 m. the difference become 10 m/s in mean wind speed from one hour to the next. This is due to the friction velocity, which value is kept under 1 according to (Ho, 2015). As seen, it has also been calculated using Charnocks equation assuming A$_C$=0.0185, consequently not giving more reasonable results as the Charnock parameter is kept constant.

Results:

	A	B	C	D	E
1					u*
2	TimeStamp UTC	Wind Speed 2.5m	Tair - Twater	Stability classification	If wind<10; u*=wind/10, If wind>10; u*=wind/20
3	01/02/16 0:00	14,414	-3,750	Stable	0,7207
4	01/02/16 1:00	15,234	-2,481	Stable	0,7617
5	01/02/16 2:00	14,473	-2,255	Stable	0,72365
6	01/02/16 3:00	14,414	-2,529	Stable	0,7207
7	01/02/16 4:00	14,883	-2,280	Stable	0,74415
8	01/02/16 5:00	15,820	-1,734	Stable	0,791
9	01/02/16 6:00	15,176	-1,734	Stable	0,7588
10	01/02/16 7:00	15,000	-1,758	Stable	0,75
11	01/02/16 8:00	14,063	-1,758	Stable	0,70315
12	01/02/16 9:00	12,422	-1,734	Stable	0,6211
13	01/02/16 10:00	12,305	-3,325	Stable	0,61525
14	01/02/16 11:00	11,309	-2,255	Stable	0,56545
15	01/02/16 12:00	9,375	-2,851	Stable	0,9375

	F	G	H	I
1				
2	Wind speed 80 m, by log law:	If unstable, wind speed at 80m:	If near neutral, wind speed at 80m:	If stable, wind speed at 80 m:
3	20,54	20,14	20,80	20,54
4	21,71	21,28	21,98	21,71
5	20,63	20,22	20,88	20,63
6	20,54	20,14	20,80	20,54
7	21,21	20,79	21,48	21,21
8	22,55	22,10	22,83	22,55
9	21,63	21,20	21,90	21,63
10	21,38	20,95	21,64	21,38
11	20,04	19,65	20,29	20,04
12	17,70	17,35	17,92	17,70
13	17,54	17,19	17,76	17,54
14	16,12	15,80	16,32	16,12
15	26,72	26,19	13,53	26,72

	J	K
1		
2	z/L for Stable:	0,04
3	z/L for Unstable:	-0,04
4	x calc.:	1,12468265
5	-Ψ(z/L) calc.:	-0,113793685
6	k:	0,4
7	z0:	0,001
8	z2:	80
9	z1:	2,5
10	u*	0,16491278
11	Charnock: z0=0,0185*(u*)^2/g :	
12	u* calc.:	0,728196588
13	Bulk transfer relation: τ=rho*Cd*u^2 (WMO 1998):	
14	τ calc.:	0,033315376
15	Cd	0,001

Formulas:

	A	B	C	D
1				
2	TimeStamp UTC	Wind Speed 2.5m	Tair - Twater	Stability classification
3	01/02/16 0:00	14,414	-3,750	=IF(AND(C3<=1;C3>=-1);"Near Neutral";IF(C3>=1;"Unstable";"Stable"))
4	01/02/16 1:00	15,234	-2,481	=IF(AND(C4<=1;C4>=-1);"Near Neutral";IF(C4>=1;"Unstable";"Stable"))
5	01/02/16 2:00	14,473	-2,255	=IF(AND(C5<=1;C5>=-1);"Near Neutral";IF(C5>=1;"Unstable";"Stable"))
6	01/02/16 3:00	14,414	-2,529	=IF(AND(C6<=1;C6>=-1);"Near Neutral";IF(C6>=1;"Unstable";"Stable"))
7	01/02/16 4:00	14,883	-2,280	=IF(AND(C7<=1;C7>=-1);"Near Neutral";IF(C7>=1;"Unstable";"Stable"))
8	01/02/16 5:00	15,820	-1,734	=IF(AND(C8<=1;C8>=-1);"Near Neutral";IF(C8>=1;"Unstable";"Stable"))
9	01/02/16 6:00	15,176	-1,734	=IF(AND(C9<=1;C9>=-1);"Near Neutral";IF(C9>=1;"Unstable";"Stable"))
10	01/02/16 7:00	15,000	-1,758	=IF(AND(C10<=1;C10>=-1);"Near Neutral";IF(C10>=1;"Unstable";"Stable"))
11	01/02/16 8:00	14,063	-1,758	=IF(AND(C11<=1;C11>=-1);"Near Neutral";IF(C11>=1;"Unstable";"Stable"))
12	01/02/16 9:00	12,422	-1,734	=IF(AND(C12<=1;C12>=-1);"Near Neutral";IF(C12>=1;"Unstable";"Stable"))
13	01/02/16 10:00	12,305	-3,325	=IF(AND(C13<=1;C13>=-1);"Near Neutral";IF(C13>=1;"Unstable";"Stable"))
14	01/02/16 11:00	11,309	-2,255	=IF(AND(C14<=1;C14>=-1);"Near Neutral";IF(C14>=1;"Unstable";"Stable"))
15	01/02/16 12:00	9,375	-2,851	=IF(AND(C15<=1;C15>=-1);"Near Neutral";IF(C15>=1;"Unstable";"Stable"))

	E	F
1	u*	
2	If wind<10; u*=wind/10, If wind>10; u*=wind/20	Wind speed 80 m, by log law:
3	=IF(B3<10;B3/10;B3/20)	=IF(D3="Unstable";G3;IF(D3="Near Neutral";H3;IF(D3="Stable";I3)))
4	=IF(B4<10;B4/10;B4/20)	=IF(D4="Unstable";G4;IF(D4="Near Neutral";H4;IF(D4="Stable";I4)))
5	=IF(B5<10;B5/10;B5/20)	=IF(D5="Unstable";G5;IF(D5="Near Neutral";H5;IF(D5="Stable";I5)))
6	=IF(B6<10;B6/10;B6/20)	=IF(D6="Unstable";G6;IF(D6="Near Neutral";H6;IF(D6="Stable";I6)))
7	=IF(B7<10;B7/10;B7/20)	=IF(D7="Unstable";G7;IF(D7="Near Neutral";H7;IF(D7="Stable";I7)))
8	=IF(B8<10;B8/10;B8/20)	=IF(D8="Unstable";G8;IF(D8="Near Neutral";H8;IF(D8="Stable";I8)))
9	=IF(B9<10;B9/10;B9/20)	=IF(D9="Unstable";G9;IF(D9="Near Neutral";H9;IF(D9="Stable";I9)))
10	=IF(B10<10;B10/10;B10/20)	=IF(D10="Unstable";G10;IF(D10="Near Neutral";H10;IF(D10="Stable";I10)))
11	=IF(B11<10;B11/10;B11/20)	=IF(D11="Unstable";G11;IF(D11="Near Neutral";H11;IF(D11="Stable";I11)))
12	=IF(B12<10;B12/10;B12/20)	=IF(D12="Unstable";G12;IF(D12="Near Neutral";H12;IF(D12="Stable";I12)))
13	=IF(B13<10;B13/10;B13/20)	=IF(D13="Unstable";G13;IF(D13="Near Neutral";H13;IF(D13="Stable";I13)))
14	=IF(B14<10;B14/10;B14/20)	=IF(D14="Unstable";G14;IF(D14="Near Neutral";H14;IF(D14="Stable";I14)))
15	=IF(B15<10;B15/10;B15/20)	=IF(D15="Unstable";G15;IF(D15="Near Neutral";H15;IF(D15="Stable";I15)))

	G	H
1		
2	If unstable, wind speed at 80m:	If near neutral, wind speed at 80m:
3	=E3/$K$6*(LN($K$8/$K$7)+$K$5)	=B3*((LN($K$8/$K$7))/(LN($K$9/$K$7)))
4	=E4/$K$6*(LN($K$8/$K$7)+$K$5)	=B4*((LN($K$8/$K$7))/(LN($K$9/$K$7)))
5	=E5/$K$6*(LN($K$8/$K$7)+$K$5)	=B5*((LN($K$8/$K$7))/(LN($K$9/$K$7)))
6	=E6/$K$6*(LN($K$8/$K$7)+$K$5)	=B6*((LN($K$8/$K$7))/(LN($K$9/$K$7)))
7	=E7/$K$6*(LN($K$8/$K$7)+$K$5)	=B7*((LN($K$8/$K$7))/(LN($K$9/$K$7)))
8	=E8/$K$6*(LN($K$8/$K$7)+$K$5)	=B8*((LN($K$8/$K$7))/(LN($K$9/$K$7)))
9	=E9/$K$6*(LN($K$8/$K$7)+$K$5)	=B9*((LN($K$8/$K$7))/(LN($K$9/$K$7)))
10	=E10/$K$6*(LN($K$8/$K$7)+$K$5)	=B10*((LN($K$8/$K$7))/(LN($K$9/$K$7)))
11	=E11/$K$6*(LN($K$8/$K$7)+$K$5)	=B11*((LN($K$8/$K$7))/(LN($K$9/$K$7)))
12	=E12/$K$6*(LN($K$8/$K$7)+$K$5)	=B12*((LN($K$8/$K$7))/(LN($K$9/$K$7)))
13	=E13/$K$6*(LN($K$8/$K$7)+$K$5)	=B13*((LN($K$8/$K$7))/(LN($K$9/$K$7)))
14	=E14/$K$6*(LN($K$8/$K$7)+$K$5)	=B14*((LN($K$8/$K$7))/(LN($K$9/$K$7)))
15	=E15/$K$6*(LN($K$8/$K$7)+$K$5)	=B15*((LN($K$8/$K$7))/(LN($K$9/$K$7)))

Column I

	I
1	
2	If stable, wind speed at 80 m:
3	=(E3/$K$6)*LN(($K$8/$K$7)+4,7*($K$8/$K$2))
4	=(E4/$K$6)*LN(($K$8/$K$7)+4,7*($K$8/$K$2))
5	=(E5/$K$6)*LN(($K$8/$K$7)+4,7*($K$8/$K$2))
6	=(E6/$K$6)*LN(($K$8/$K$7)+4,7*($K$8/$K$2))
7	=(E7/$K$6)*LN(($K$8/$K$7)+4,7*($K$8/$K$2))
8	=(E8/$K$6)*LN(($K$8/$K$7)+4,7*($K$8/$K$2))
9	=(E9/$K$6)*LN(($K$8/$K$7)+4,7*($K$8/$K$2))
10	=(E10/$K$6)*LN(($K$8/$K$7)+4,7*($K$8/$K$2))
11	=(E11/$K$6)*LN(($K$8/$K$7)+4,7*($K$8/$K$2))
12	=(E12/$K$6)*LN(($K$8/$K$7)+4,7*($K$8/$K$2))
13	=(E13/$K$6)*LN(($K$8/$K$7)+4,7*($K$8/$K$2))
14	=(E14/$K$6)*LN(($K$8/$K$7)+4,7*($K$8/$K$2))
15	=(E15/$K$6)*LN(($K$8/$K$7)+4,7*($K$8/$K$2))

Columns J and K

	J	K
1		
2	z/L for Stable:	0,04
3	z/L for Unstable:	-0,04
4	x calc.:	=(1-15*K3)^0,25
5	-Ψ(z/L) calc.:	=LN((1+K4^2)/(2*((1+K4)/2)^2))-2*ATAN(K4)+PI()/2
6	k:	0,4
7	z0:	0,001
8	z2:	80
9	z1:	2,5
10	u*	=(K14/1,225)^0,5
11	Charnock: z0=0,0185*(u*)^2/g :	
12	u* calc.:	=($K$7*9,81/0,0185)^0,5
13	Bulk transfer relation: τ=rho*Cd*u^2 (WMO 1998):	
14	τ calc.:	=1,225*K15*B22^2
15	Cd	0,001

Appendix E: Calculations of Alternative Power Law Exponents

Power law exponents were calculated according to the method given by Nfaoui (1998). They are compared to the chosen values of 0.07-0.15. $\mathcal{X} = 0.25$ refers to $z_0 = 0$-0.005 m. and $\mathcal{X} = 0.31$ refers to $z_0 = 0.005$-0.05 m. The following shows excerpts of the period, including the calculations for the hours during 27th of March that is discussed in Chapter 5. The average values take into account the whole period of seven months (4670 hours).

Results:

	A	B	C	D	E	F
1	TimeStamp UTC	Wind speed @2.5m	Stability class (Tdiff)	α chosen	α when x=0.25	α when x=0.31
2	03/02/2016 04:00	8,496	Near-neutral	0,11	0,05	0,11
3	03/02/2016 05:00	8,672	Slightly unstable	0,09	0,05	0,11
4	03/02/2016 06:00	10,078	Near-neutral	0,11	0,04	0,09
5	03/02/2016 07:00	9,609	Near-neutral	0,11	0,05	0,10
6	03/02/2016 08:00	8,555	Near-neutral	0,11	0,05	0,11
7	03/02/2016 09:00	8,73	Near-neutral	0,11	0,05	0,11
8	03/02/2016 10:00	9,082	Near-neutral	0,11	0,05	0,10
9	03/02/2016 11:00	9,785	Slightly unstable	0,09	0,04	0,10
10	03/02/2016 12:00	8,73	Slightly unstable	0,09	0,05	0,11
11	03/02/2016 13:00	7,09	Slightly unstable	0,09	0,07	0,12
12	03/02/2016 14:00	9,551	Unstable	0,07	0,05	0,10
13	03/02/2016 15:00	5,039	Unstable	0,07	0,10	0,15
14	03/02/2016 16:00	8,73	Unstable	0,07	0,05	0,11
15	03/02/2016 17:00	6,68	Slightly unstable	0,09	0,07	0,13
16	03/02/2016 18:00	10,195	Slightly unstable	0,09	0,04	0,09
17	03/02/2016 19:00	10,664	Slightly unstable	0,09	0,04	0,09
18	03/02/2016 20:00	9,492	Slightly unstable	0,09	0,05	0,10
19	03/02/2016 21:00	9,844	Unstable	0,07	0,04	0,10
20	03/02/2016 22:00	8,496	Slightly unstable	0,09	0,05	0,11

	A	B	C	D	E	F
1	TimeStamp UTC	Wind speed @2.5m	Stability class (Tdiff)	α chosen	α when x=0.25	α when x=0.31
968	27/03/2016 09:00	1,406	slightly stable	0,13	0,20	0,25
969	27/03/2016 10:00	2,051	Near-neutral	0,11	0,17	0,22
970	27/03/2016 11:00	2,637	slightly stable	0,13	0,15	0,20
971	27/03/2016 12:00	3,281	slightly stable	0,13	0,13	0,18
972	27/03/2016 13:00	4,746	slightly stable	0,13	0,10	0,15
973	27/03/2016 14:00	5,098	slightly stable	0,13	0,09	0,15
974	27/03/2016 15:00	8,145	stable	0,15	0,06	0,11
975	27/03/2016 16:00	8,32	stable	0,15	0,06	0,11
976	27/03/2016 17:00	7,852	stable	0,15	0,06	0,11
977	27/03/2016 18:00	9,492	slightly stable	0,13	0,05	0,10
978	27/03/2016 19:00	8,496	slightly stable	0,13	0,05	0,11
979	27/03/2016 20:00	12,598	slightly stable	0,13	0,02	0,08
980	27/03/2016 21:00	13,594	slightly stable	0,13	0,02	0,07
981	27/03/2016 22:00	12,832	Near-neutral	0,11	0,02	0,08

	G	H	I	J
1	**Stability class**	**α chosen**	**Avg. α when x=0.25**	**Avg. α when x=0.31**
2	**Stable**	0,15	0,12	0,17
3	**Slightly stable**	0,13	0,13	0,18
4	**Near-neutral**	0,11	0,11	0,17
5	**Slightly unstable**	0,09	0,09	0,15
6	**Unstable**	0,07	0,10	0,15
7	**MIN VALUES**	0,07	0,02	0,07
8	**MAX VALUES**	0,15	0,39	0,44

Formulas:

	E	F
1	α when x=0.25	α when x=0.31
2	=(0,25-0,0881*LN(B2))/(1-0,0881*LN(2,5/10))	=(0,31-0,0881*LN(B2))/(1-0,0881*LN(2,5/10))
3	=(0,25-0,0881*LN(B3))/(1-0,0881*LN(2,5/10))	=(0,31-0,0881*LN(B3))/(1-0,0881*LN(2,5/10))
4	=(0,25-0,0881*LN(B4))/(1-0,0881*LN(2,5/10))	=(0,31-0,0881*LN(B4))/(1-0,0881*LN(2,5/10))
5	=(0,25-0,0881*LN(B5))/(1-0,0881*LN(2,5/10))	=(0,31-0,0881*LN(B5))/(1-0,0881*LN(2,5/10))
6	=(0,25-0,0881*LN(B6))/(1-0,0881*LN(2,5/10))	=(0,31-0,0881*LN(B6))/(1-0,0881*LN(2,5/10))
7	=(0,25-0,0881*LN(B7))/(1-0,0881*LN(2,5/10))	=(0,31-0,0881*LN(B7))/(1-0,0881*LN(2,5/10))
8	=(0,25-0,0881*LN(B8))/(1-0,0881*LN(2,5/10))	=(0,31-0,0881*LN(B8))/(1-0,0881*LN(2,5/10))
9	=(0,25-0,0881*LN(B9))/(1-0,0881*LN(2,5/10))	=(0,31-0,0881*LN(B9))/(1-0,0881*LN(2,5/10))
10	=(0,25-0,0881*LN(B10))/(1-0,0881*LN(2,5/10))	=(0,31-0,0881*LN(B10))/(1-0,0881*LN(2,5/10))
11	=(0,25-0,0881*LN(B11))/(1-0,0881*LN(2,5/10))	=(0,31-0,0881*LN(B11))/(1-0,0881*LN(2,5/10))
12	=(0,25-0,0881*LN(B12))/(1-0,0881*LN(2,5/10))	=(0,31-0,0881*LN(B12))/(1-0,0881*LN(2,5/10))
13	=(0,25-0,0881*LN(B13))/(1-0,0881*LN(2,5/10))	=(0,31-0,0881*LN(B13))/(1-0,0881*LN(2,5/10))
14	=(0,25-0,0881*LN(B14))/(1-0,0881*LN(2,5/10))	=(0,31-0,0881*LN(B14))/(1-0,0881*LN(2,5/10))
15	=(0,25-0,0881*LN(B15))/(1-0,0881*LN(2,5/10))	=(0,31-0,0881*LN(B15))/(1-0,0881*LN(2,5/10))
16	=(0,25-0,0881*LN(B16))/(1-0,0881*LN(2,5/10))	=(0,31-0,0881*LN(B16))/(1-0,0881*LN(2,5/10))
17	=(0,25-0,0881*LN(B17))/(1-0,0881*LN(2,5/10))	=(0,31-0,0881*LN(B17))/(1-0,0881*LN(2,5/10))
18	=(0,25-0,0881*LN(B18))/(1-0,0881*LN(2,5/10))	=(0,31-0,0881*LN(B18))/(1-0,0881*LN(2,5/10))
19	=(0,25-0,0881*LN(B19))/(1-0,0881*LN(2,5/10))	=(0,31-0,0881*LN(B19))/(1-0,0881*LN(2,5/10))
20	=(0,25-0,0881*LN(B20))/(1-0,0881*LN(2,5/10))	=(0,31-0,0881*LN(B20))/(1-0,0881*LN(2,5/10))

	E	F
1	**α when x=0.25**	**α when x=0.31**
968	=(0,25-0,0881*LN(B968))/(1-0,0881*LN(2,5/10))	=(0,31-0,0881*LN(B968))/(1-0,0881*LN(2,5/10))
969	=(0,25-0,0881*LN(B969))/(1-0,0881*LN(2,5/10))	=(0,31-0,0881*LN(B969))/(1-0,0881*LN(2,5/10))
970	=(0,25-0,0881*LN(B970))/(1-0,0881*LN(2,5/10))	=(0,31-0,0881*LN(B970))/(1-0,0881*LN(2,5/10))
971	=(0,25-0,0881*LN(B971))/(1-0,0881*LN(2,5/10))	=(0,31-0,0881*LN(B971))/(1-0,0881*LN(2,5/10))
972	=(0,25-0,0881*LN(B972))/(1-0,0881*LN(2,5/10))	=(0,31-0,0881*LN(B972))/(1-0,0881*LN(2,5/10))
973	=(0,25-0,0881*LN(B973))/(1-0,0881*LN(2,5/10))	=(0,31-0,0881*LN(B973))/(1-0,0881*LN(2,5/10))
974	=(0,25-0,0881*LN(B974))/(1-0,0881*LN(2,5/10))	=(0,31-0,0881*LN(B974))/(1-0,0881*LN(2,5/10))
975	=(0,25-0,0881*LN(B975))/(1-0,0881*LN(2,5/10))	=(0,31-0,0881*LN(B975))/(1-0,0881*LN(2,5/10))
976	=(0,25-0,0881*LN(B976))/(1-0,0881*LN(2,5/10))	=(0,31-0,0881*LN(B976))/(1-0,0881*LN(2,5/10))
977	=(0,25-0,0881*LN(B977))/(1-0,0881*LN(2,5/10))	=(0,31-0,0881*LN(B977))/(1-0,0881*LN(2,5/10))
978	=(0,25-0,0881*LN(B978))/(1-0,0881*LN(2,5/10))	=(0,31-0,0881*LN(B978))/(1-0,0881*LN(2,5/10))
979	=(0,25-0,0881*LN(B979))/(1-0,0881*LN(2,5/10))	=(0,31-0,0881*LN(B979))/(1-0,0881*LN(2,5/10))
980	=(0,25-0,0881*LN(B980))/(1-0,0881*LN(2,5/10))	=(0,31-0,0881*LN(B980))/(1-0,0881*LN(2,5/10))
981	=(0,25-0,0881*LN(B981))/(1-0,0881*LN(2,5/10))	=(0,31-0,0881*LN(B981))/(1-0,0881*LN(2,5/10))

	G	H	I	J
1	**Stability class**	**α chosen**	**Avg. α when x=0.25**	**Avg. α when x=0.31**
2	Stable	0,15	=AVERAGEIFS($E$2:$E$4671;$C$2:$C$4671;G2)	=AVERAGEIFS($F$2:$F$4671;$C$2:$C$4671;G2)
3	Slightly stable	0,13	=AVERAGEIFS($E$2:$E$4671;$C$2:$C$4671;G3)	=AVERAGEIFS($F$2:$F$4671;$C$2:$C$4671;G3)
4	Near-neutral	0,11	=AVERAGEIFS($E$2:$E$4671;$C$2:$C$4671;G4)	=AVERAGEIFS($F$2:$F$4671;$C$2:$C$4671;G4)
5	Slightly unstable	0,09	=AVERAGEIFS($E$2:$E$4671;$C$2:$C$4671;G5)	=AVERAGEIFS($F$2:$F$4671;$C$2:$C$4671;G5)
6	Unstable	0,07	=AVERAGEIFS($E$2:$E$4671;$C$2:$C$4671;G6)	=AVERAGEIFS($F$2:$F$4671;$C$2:$C$4671;G6)
7	MIN VALUES	0,07	=MIN(E2:E4671)	=MIN(F2:F4671)
8	MAX VALUES	0,15	=MAX(E2:E4671)	=MAX(F2:F4671)

Appendix F: Production Calculations Using Power Law

As an example of calculated power production based on the power law, the following shows the Hywind production at 65 meters altitude for a few hours of the period. It also includes the stability determination, mean wind profiles and probability of wind speeds and corresponding energy production for the complete period. The same method is used for calculation of the GWP 750 kW turbines production.

Results:

	E Rounded	F Stability class	G α	H Wind speed @65m	I Rounded	J Power prod
1	Rounded	Stability class	α	Wind speed @65m	Rounded	Power prod
2	-1	Near-neutral	0,11	12,15798413	12	2015
3	-2	Slightly unstable	0,09	11,62697853	12	2015
4	-1	Near-neutral	0,11	14,42186488	14	2260
5	-1	Near-neutral	0,11	13,75071439	14	2260
6	-1	Near-neutral	0,11	12,24241457	12	2015
7	-1	Near-neutral	0,11	12,49284386	12	2015
8	-1	Near-neutral	0,11	12,99656448	13	2183
9	-2	Slightly unstable	0,09	13,11923258	13	2183
10	-3	Slightly unstable	0,09	11,70474199	12	2015
11	-3	Slightly unstable	0,09	9,505913028	10	1394
12	-4	Unstable	0,07	11,99767185	12	2015
13	-4	Unstable	0,07	6,329836506	6	276
14	-4	Unstable	0,07	10,96635695	11	1738
15	-2	Slightly unstable	0,09	8,956205786	9	1043
16	-3	Slightly unstable	0,09	13,66893982	14	2260
17	-2	Slightly unstable	0,09	14,29775127	14	2260
18	-2	Slightly unstable	0,09	12,72639301	13	2183
19	-4	Unstable	0,07	12,36572942	12	2015
20	-3	Slightly unstable	0,09	11,39100664	11	1738

	O	P Hours	Q Avg. wind speed@2.5 m	R Std.dev: @2.5m	S Confidence 95%	T Avg. wind speed@65m	U Std.dev: @65m	V Confidence 95%
26				Average wind speed, Standard deviation and Confidence level				
27		Hours	Avg. wind speed@2.5 m	Std.dev: @2.5m	Confidence 95%	Avg. wind speed@65m	Std.dev: @65m	Confidence 95%
28	Unstable	296	5,74	2,467083188	0,070757657	7,21	3,099073869	0,088883588
29	Slightly unstable	1001	5,74	2,415889997	0,069289401	7,70	3,499418417	0,100365748
30	Near-neutral	2940	4,81	2,495508951	0,071572928	6,88	3,571134441	0,102422613
31	Slightly stable	342	4,14	2,348748803	0,067363745	6,33	3,587427286	0,102889903
32	Stable	91	4,40	2,320944963	0,066566311	7,17	3,783649027	0,108517679
33	Total	4670	5,01	2,509593479		7,04	3,499418417	0,100365748

	N z	O	P	Q	R	S
35				Mean wind profiles		
36			0,07	0,09	0,11	0,13	0,15
37	z	U n=392	SU n=1128	NN n=3132	SS n=350	S n=98
38	2,5	5,74	5,74	4,81	4,14	4,40
39	10	6,323021922	6,50213896	5,596714047	4,95916898	5,418225976
40	40	6,967370203	7,366168448	6,518680824	5,938499246	6,670618641
41	80	7,313764744	7,840330055	7,03514441	6,498462319	7,401514803
42	120	7,524322035	8,131722673	7,356022604	6,850187655	7,865644265

Formulas:

	A	B	C	D
1	TimeStamp UTC	Wind speed @2.5m	Rounded	Tair@2.5 - Tsea
2	03/02/2016 04:00	8,496	8	-0,996
3	03/02/2016 05:00	8,672	9	-1,641
4	03/02/2016 06:00	10,078	10	-1,216
5	03/02/2016 07:00	9,609	10	-1,289
6	03/02/2016 08:00	8,555	9	-1,24
7	03/02/2016 09:00	8,73	9	-1,216
8	03/02/2016 10:00	9,082	9	-1,392
9	03/02/2016 11:00	9,785	10	-1,641
10	03/02/2016 12:00	8,73	9	-2,735
11	03/02/2016 13:00	7,09	7	-3,008
12	03/02/2016 14:00	9,551	10	-4,375
13	03/02/2016 15:00	5,039	5	-4,15
14	03/02/2016 16:00	8,73	9	-3,677
15	03/02/2016 17:00	6,68	7	-2,285

	E	F	G
1	Rounded T	Stability class	α
2	=ROUND(D2;0)	=VLOOKUP(E2;$P$2:$Q$18;2;FALSE)	=VLOOKUP(F2;$Q$2:$R$18;2;FALSE)
3	=ROUND(D3;0)	=VLOOKUP(E3;$P$2:$Q$18;2;FALSE)	=VLOOKUP(F3;$Q$2:$R$18;2;FALSE)
4	=ROUND(D4;0)	=VLOOKUP(E4;$P$2:$Q$18;2;FALSE)	=VLOOKUP(F4;$Q$2:$R$18;2;FALSE)
5	=ROUND(D5;0)	=VLOOKUP(E5;$P$2:$Q$18;2;FALSE)	=VLOOKUP(F5;$Q$2:$R$18;2;FALSE)
6	=ROUND(D6;0)	=VLOOKUP(E6;$P$2:$Q$18;2;FALSE)	=VLOOKUP(F6;$Q$2:$R$18;2;FALSE)
7	=ROUND(D7;0)	=VLOOKUP(E7;$P$2:$Q$18;2;FALSE)	=VLOOKUP(F7;$Q$2:$R$18;2;FALSE)
8	=ROUND(D8;0)	=VLOOKUP(E8;$P$2:$Q$18;2;FALSE)	=VLOOKUP(F8;$Q$2:$R$18;2;FALSE)
9	=ROUND(D9;0)	=VLOOKUP(E9;$P$2:$Q$18;2;FALSE)	=VLOOKUP(F9;$Q$2:$R$18;2;FALSE)
10	=ROUND(D10;0)	=VLOOKUP(E10;$P$2:$Q$18;2;FALSE)	=VLOOKUP(F10;$Q$2:$R$18;2;FALSE)
11	=ROUND(D11;0)	=VLOOKUP(E11;$P$2:$Q$18;2;FALSE)	=VLOOKUP(F11;$Q$2:$R$18;2;FALSE)
12	=ROUND(D12;0)	=VLOOKUP(E12;$P$2:$Q$18;2;FALSE)	=VLOOKUP(F12;$Q$2:$R$18;2;FALSE)
13	=ROUND(D13;0)	=VLOOKUP(E13;$P$2:$Q$18;2;FALSE)	=VLOOKUP(F13;$Q$2:$R$18;2;FALSE)
14	=ROUND(D14;0)	=VLOOKUP(E14;$P$2:$Q$18;2;FALSE)	=VLOOKUP(F14;$Q$2:$R$18;2;FALSE)
15	=ROUND(D15;0)	=VLOOKUP(E15;$P$2:$Q$18;2;FALSE)	=VLOOKUP(F15;$Q$2:$R$18;2;FALSE)

	H	I	J
1	Wind speed @65m	Rounded	Power prod
2	=B2*(65/2,5)^G2	=ROUND(H2;0)	=VLOOKUP(I2;$M$2:$N$29;2;FALSE)
3	=B3*(65/2,5)^G3	=ROUND(H3;0)	=VLOOKUP(I3;$M$2:$N$29;2;FALSE)
4	=B4*(65/2,5)^G4	=ROUND(H4;0)	=VLOOKUP(I4;$M$2:$N$29;2;FALSE)
5	=B5*(65/2,5)^G5	=ROUND(H5;0)	=VLOOKUP(I5;$M$2:$N$29;2;FALSE)
6	=B6*(65/2,5)^G6	=ROUND(H6;0)	=VLOOKUP(I6;$M$2:$N$29;2;FALSE)
7	=B7*(65/2,5)^G7	=ROUND(H7;0)	=VLOOKUP(I7;$M$2:$N$29;2;FALSE)
8	=B8*(65/2,5)^G8	=ROUND(H8;0)	=VLOOKUP(I8;$M$2:$N$29;2;FALSE)
9	=B9*(65/2,5)^G9	=ROUND(H9;0)	=VLOOKUP(I9;$M$2:$N$29;2;FALSE)
10	=B10*(65/2,5)^G10	=ROUND(H10;0)	=VLOOKUP(I10;$M$2:$N$29;2;FALSE)
11	=B11*(65/2,5)^G11	=ROUND(H11;0)	=VLOOKUP(I11;$M$2:$N$29;2;FALSE)
12	=B12*(65/2,5)^G12	=ROUND(H12;0)	=VLOOKUP(I12;$M$2:$N$29;2;FALSE)
13	=B13*(65/2,5)^G13	=ROUND(H13;0)	=VLOOKUP(I13;$M$2:$N$29;2;FALSE)
14	=B14*(65/2,5)^G14	=ROUND(H14;0)	=VLOOKUP(I14;$M$2:$N$29;2;FALSE)
15	=B15*(65/2,5)^G15	=ROUND(H15;0)	=VLOOKUP(I15;$M$2:$N$29;2;FALSE)

Table M/N

	M	N
1	Hywind Demo 2.3 MW turbine	
2	Wind speed	Power production
3	0	0
4	1	0
5	2	0
6	3	0
7	4	42
8	5	136
9	6	276
10	7	470
11	8	727
12	9	1043
13	10	1394
14	11	1738
15	12	2015
16	13	2183
17	14	2260
18	15	2288
19	16	2297
20	17	2299
21	18	2300
22	19	2300
23	20	2300
24	21	2300
25	22	2300
26	23	2300
27	24	2300
28	25	2300
29	26	0

Table P/Q/R

	P	Q	R
1	temp differece	stability class	α
2	-8	Unstable	0,07
3	-7	Unstable	0,07
4	-6	Unstable	0,07
5	-5	Unstable	0,07
6	-4	Unstable	0,07
7	-3	Slightly unstable	0,09
8	-2	Slightly unstable	0,09
9	-1	neutral	0,11
10	0	neutral	0,11
11	1	neutral	0,11
12	2	slightly stable	0,13
13	3	slightly stable	0,13
14	4	stable	0,15
15	5	stable	0,15
16	6	stable	0,15
17	7	stable	0,15
18	8	stable	0,15

Table O/P/Q/R (rows 26-33)

	O	P	Q	R
26	Average wind speed, Standard deviation and Confidence level			
27		Hours	Avg. wind speed@2.5 m	Std.dev: @2.5m
28	Unstable	=COUNTIF($F$2:F4671;"Unstable")	=AVERAGEIF($F$2:$F$4671;"Unstable";$B$2:$B$4671)	=STDEV.S(IF($F$2:$F$4671=O28;$B$2:$B$4671))
29	Slightly unstable	=COUNTIF(F2:F4671;"Slightly unstable")	=AVERAGEIF($F$2:$F$4671;"Slightly unstable";$B$2:$B$4671)	=STDEV.S(IF($F$2:$F$4671=O29;$B$2:$B$4671))
30	Near-neutral	=COUNTIF(F2:F4671;"Near-Neutral")	=AVERAGEIF($F$2:$F$4671;"near-neutral";$B$2:$B$4671)	=STDEV.S(IF($F$2:$F$4671=O30;$B$2:$B$4671))
31	Slightly stable	=COUNTIF(F2:F4671;"Slightly stable")	=AVERAGEIF($F$2:$F$4671;"Slightly stable";$B$2:$B$4671)	=STDEV.S(IF($F$2:$F$4671=O31;$B$2:$B$4671))
32	Stable	=COUNTIF(F2:F4671;"Stable")	=AVERAGEIF($F$2:$F$4671;"Stable";$B$2:$B$4671)	=STDEV.S(IF($F$2:$F$4671=O32;$B$2:$B$4671))
33	Total	=SUM(P28:P32)	=AVERAGE(B2:B4671)	=STDEV.S($B$2:$B$4671)

Table S/T/U/V (rows 26-33)

	S	T	U	V
26	Average wind speed, Standard deviation and Confidence level			
27	Confidence 95%	Avg. wind speed@65m	Std.dev: @65m	Confidence 95%
28	=CONFIDENCE(0,05;R28;4670)	=AVERAGEIF($F$2:$F$4671;"Unstable";$H$2:$H$4671)	=STDEV.S(IF($F$2:$F$4671=O28;$H$2:$H$4671))	=CONFIDENCE(0,05;U28;4670)
29	=CONFIDENCE(0,05;R29;4670)	=AVERAGEIF($F$2:$F$4671;"Slightly unstable";$H$2:$H$4671)	=STDEV.S(IF($F$2:$F$4671=O29;$H$2:$H$4671))	=CONFIDENCE(0,05;U29;4670)
30	=CONFIDENCE(0,05;R30;4670)	=AVERAGEIF($F$2:$F$4671;"Near-neutral";$H$2:$H$4671)	=STDEV.S(IF($F$2:$F$4671=O30;$H$2:$H$4671))	=CONFIDENCE(0,05;U30;4670)
31	=CONFIDENCE(0,05;R31;4670)	=AVERAGEIF($F$2:$F$4671;"Slightly stable";$H$2:$H$4671)	=STDEV.S(IF($F$2:$F$4671=O31;$H$2:$H$4671))	=CONFIDENCE(0,05;U31;4670)
32	=CONFIDENCE(0,05;R32;4670)	=AVERAGEIF($F$2:$F$4671;"Stable";$H$2:$H$4671)	=STDEV.S(IF($F$2:$F$4671=O32;$H$2:$H$4671))	=CONFIDENCE(0,05;U32;4670)
33		=AVERAGE(H2:H4671)	=STDEV.S($H$2:$H$4671)	=CONFIDENCE(0,05;U33;4670)

Table N/O/P/Q/R/S (rows 35-42)

	N	O	P	Q	R	S
35	Mean wind profiles					
36		0,07	0,09	0,11	0,13	0,15
37	z	U n=392	SU n=1128	NN n=3132	SS n=350	S n=98
38	2,5	=Q28	=Q29	=Q30	=Q31	=Q32
39	10	=$O$38*(N39/$N$38)^$R$2	=$P$38*(N39/$N$38)^$R$7	=$Q$38*(N39/$N$38)^$R$9	=$R$38*(N39/$N$38)^$R$12	=$S$38*(N39/$N$38)^$R$14
40	40	=$O$38*(N40/$N$38)^$R$2	=$P$38*(N40/$N$38)^$R$7	=$Q$38*(N40/$N$38)^$R$9	=$R$38*(N40/$N$38)^$R$12	=$S$38*(N40/$N$38)^$R$14
41	80	=$O$38*(N41/$N$38)^$R$2	=$P$38*(N41/$N$38)^$R$7	=$Q$38*(N41/$N$38)^$R$9	=$R$38*(N41/$N$38)^$R$12	=$S$38*(N41/$N$38)^$R$14
42	120	=$O$38*(N42/$N$38)^$R$2	=$P$38*(N42/$N$38)^$R$7	=$Q$38*(N42/$N$38)^$R$9	=$R$38*(N42/$N$38)^$R$12	=$S$38*(N42/$N$38)^$R$14

Results:

	W	X	Y	Z	AA
1	Wind speed [m/s]	Power produced [kW]	Hours at 2.5 m [-]	Hours at 65 m [-]	E (h*P) 65m [kWh]
2	0	0	28	17	0
3	1	0	238	108	0
4	2	0	505	231	0
5	3	0	689	392	0
6	4	42	713	482	20244
7	5	136	648	526	71536
8	6	276	595	511	141036
9	7	470	461	461	216670
10	8	727	304	469	340963
11	9	1043	234	398	415114
12	10	1394	147	306	426564
13	11	1738	71	227	394526
14	12	2015	24	168	338520
15	13	2183	10	129	281607
16	14	2260	3	100	226000
17	15	2288	0	79	180752
18	16	2297	0	42	96474
19	17	2299	0	11	25289
20	18	2300	0	5	11500
21	19	2300	0	5	11500
22	20	2300	0	2	4600
23	21	2300	0	1	2300
24	22	2300	0	0	0
25			SUM: 4670	4670	3205195

Formulas:

	W	X	Y	Z	AA
1	Wind speed [m/s]	Power produced [kW]	Hours at 2.5 m [-]	Hours at 65 m [-]	E (h*P) 65m [kWh]
2	0	0	=COUNTIF($C$2:$C$4671;W2)	=COUNTIF($I$2:$I$4671;W2)	=Z2*X2
3	1	0	=COUNTIF($C$2:$C$4671;W3)	=COUNTIF($I$2:$I$4671;W3)	=Z3*X3
4	2	0	=COUNTIF($C$2:$C$4671;W4)	=COUNTIF($I$2:$I$4671;W4)	=Z4*X4
5	3	0	=COUNTIF($C$2:$C$4671;W5)	=COUNTIF($I$2:$I$4671;W5)	=Z5*X5
6	4	42	=COUNTIF($C$2:$C$4671;W6)	=COUNTIF($I$2:$I$4671;W6)	=Z6*X6
7	5	136	=COUNTIF($C$2:$C$4671;W7)	=COUNTIF($I$2:$I$4671;W7)	=Z7*X7
8	6	276	=COUNTIF($C$2:$C$4671;W8)	=COUNTIF($I$2:$I$4671;W8)	=Z8*X8
9	7	470	=COUNTIF($C$2:$C$4671;W9)	=COUNTIF($I$2:$I$4671;W9)	=Z9*X9
10	8	727	=COUNTIF($C$2:$C$4671;W10)	=COUNTIF($I$2:$I$4671;W10)	=Z10*X10
11	9	1043	=COUNTIF($C$2:$C$4671;W11)	=COUNTIF($I$2:$I$4671;W11)	=Z11*X11
12	10	1394	=COUNTIF($C$2:$C$4671;W12)	=COUNTIF($I$2:$I$4671;W12)	=Z12*X12
13	11	1738	=COUNTIF($C$2:$C$4671;W13)	=COUNTIF($I$2:$I$4671;W13)	=Z13*X13
14	12	2015	=COUNTIF($C$2:$C$4671;W14)	=COUNTIF($I$2:$I$4671;W14)	=Z14*X14
15	13	2183	=COUNTIF($C$2:$C$4671;W15)	=COUNTIF($I$2:$I$4671;W15)	=Z15*X15
16	14	2260	=COUNTIF($C$2:$C$4671;W16)	=COUNTIF($I$2:$I$4671;W16)	=Z16*X16
17	15	2288	=COUNTIF($C$2:$C$4671;W17)	=COUNTIF($I$2:$I$4671;W17)	=Z17*X17
18	16	2297	=COUNTIF($C$2:$C$4671;W18)	=COUNTIF($I$2:$I$4671;W18)	=Z18*X18
19	17	2299	=COUNTIF($C$2:$C$4671;W19)	=COUNTIF($I$2:$I$4671;W19)	=Z19*X19
20	18	2300	=COUNTIF($C$2:$C$4671;W20)	=COUNTIF($I$2:$I$4671;W20)	=Z20*X20
21	19	2300	=COUNTIF($C$2:$C$4671;W21)	=COUNTIF($I$2:$I$4671;W21)	=Z21*X21
22	20	2300	=COUNTIF($C$2:$C$4671;W22)	=COUNTIF($I$2:$I$4671;W22)	=Z22*X22
23	21	2300	=COUNTIF($C$2:$C$4671;W23)	=COUNTIF($I$2:$I$4671;W23)	=Z23*X23
24	22	2300	=COUNTIF($C$2:$C$4671;W24)	=COUNTIF($I$2:$I$4671;W24)	=Z24*X24
25			SUM: =SUM(Y2:Y24)	=SUM(Z2:Z24)	=SUM(AA3:AA24)

Appendix G: Stability Distribution by Wind Speed at 65 Meters Height

A small excerpt is shown from the wind speeds, where the data are sorted from smallest to largest value. The hourly wind speeds are also rounded to fit into the categories as shown. Formulas used are shown for two of the stability classes.

	AJ	AK	AL
	Stability class	**Wind speed @65m**	**rounded**
1			
2	Near-neutral	0,167429866	0
3	Slightly unstable	0,235971889	0
4	Near-neutral	0,251860311	0
5	Near-neutral	0,251860311	0
6	Near-neutral	0,251860311	0
7	Near-neutral	0,251860311	0
8	Near-neutral	0,251860311	0
9	Slightly unstable	0,313735352	0
10	Near-neutral	0,334859732	0
11	Near-neutral	0,334859732	0
12	Near-neutral	0,334859732	0
13	Near-neutral	0,334859732	0
14	Near-neutral	0,419290178	0
15	Near-neutral	0,419290178	0
16	Near-neutral	0,419290178	0
17	Near-neutral	0,419290178	0
18	stable	0,477654224	0
19	Near-neutral	0,503720623	1
20	Unstable	0,515029364	1
21	slightly stable	0,537637061	1
22	Near-neutral	0,586720044	1
23	Near-neutral	0,586720044	1
24	Near-neutral	0,586720044	1
25	Near-neutral	0,586720044	1
26	Unstable	0,589143346	1
27	slightly stable	0,626224986	1
28	Slightly unstable	0,706574918	1
29	Slightly unstable	0,706574918	1

Results:

	65 meters height						
1							
2	**Wind speed**	**Unstable**	**Slightly unstable**	**Near-neutral**	**Slightly stable**	**Stable**	
3	0	0	2	14	0	1	
4	1	7	12	75	12	2	
5	2	10	26	155	36	4	
6	3	24	54	269	39	6	
7	4	26	75	337	36	8	
8	5	27	98	343	40	18	
9	6	24	104	336	38	9	
10	7	39	131	269	16	6	
11	8	38	121	267	34	9	
12	9	28	112	227	26	5	
13	10	24	68	190	20	4	
14	11	22	66	120	15	4	
15	12	12	55	88	11	2	
16	13	13	21	83	6	6	
17	14	1	25	66	6	2	
18	15	1	16	59	0	3	
19	16	0	13	23	5	1	
20	17	0	2	8	0	1	
21	18	0	0	5	0	0	
22	19	0	0	4	1	0	
23	20	0	0	2	0	0	
24	21	0	0	0	1	0	
25	**SUM**	296	1001	2940	342	91	4670

Formulas:

	AM	AN	AO
1	65 meters height		
2	Wind speed	Unstable	Slightly unstable
3	0	=COUNTIFS($AL$2:$AL$4671;AM3;$AJ$2:$AJ$4671;$AN$2)	=COUNTIFS($AL$2:$AL$4671;AM3;$AJ$2:$AJ$4671;$AO$2)
4	1	=COUNTIFS($AL$2:$AL$4671;AM4;$AJ$2:$AJ$4671;$AN$2)	=COUNTIFS($AL$2:$AL$4671;AM4;$AJ$2:$AJ$4671;$AO$2)
5	2	=COUNTIFS($AL$2:$AL$4671;AM5;$AJ$2:$AJ$4671;$AN$2)	=COUNTIFS($AL$2:$AL$4671;AM5;$AJ$2:$AJ$4671;$AO$2)
6	3	=COUNTIFS($AL$2:$AL$4671;AM6;$AJ$2:$AJ$4671;$AN$2)	=COUNTIFS($AL$2:$AL$4671;AM6;$AJ$2:$AJ$4671;$AO$2)
7	4	=COUNTIFS($AL$2:$AL$4671;AM7;$AJ$2:$AJ$4671;$AN$2)	=COUNTIFS($AL$2:$AL$4671;AM7;$AJ$2:$AJ$4671;$AO$2)
8	5	=COUNTIFS($AL$2:$AL$4671;AM8;$AJ$2:$AJ$4671;$AN$2)	=COUNTIFS($AL$2:$AL$4671;AM8;$AJ$2:$AJ$4671;$AO$2)
9	6	=COUNTIFS($AL$2:$AL$4671;AM9;$AJ$2:$AJ$4671;$AN$2)	=COUNTIFS($AL$2:$AL$4671;AM9;$AJ$2:$AJ$4671;$AO$2)
10	7	=COUNTIFS($AL$2:$AL$4671;AM10;$AJ$2:$AJ$4671;$AN$2)	=COUNTIFS($AL$2:$AL$4671;AM10;$AJ$2:$AJ$4671;$AO$2)
11	8	=COUNTIFS($AL$2:$AL$4671;AM11;$AJ$2:$AJ$4671;$AN$2)	=COUNTIFS($AL$2:$AL$4671;AM11;$AJ$2:$AJ$4671;$AO$2)
12	9	=COUNTIFS($AL$2:$AL$4671;AM12;$AJ$2:$AJ$4671;$AN$2)	=COUNTIFS($AL$2:$AL$4671;AM12;$AJ$2:$AJ$4671;$AO$2)
13	10	=COUNTIFS($AL$2:$AL$4671;AM13;$AJ$2:$AJ$4671;$AN$2)	=COUNTIFS($AL$2:$AL$4671;AM13;$AJ$2:$AJ$4671;$AO$2)
14	11	=COUNTIFS($AL$2:$AL$4671;AM14;$AJ$2:$AJ$4671;$AN$2)	=COUNTIFS($AL$2:$AL$4671;AM14;$AJ$2:$AJ$4671;$AO$2)
15	12	=COUNTIFS($AL$2:$AL$4671;AM15;$AJ$2:$AJ$4671;$AN$2)	=COUNTIFS($AL$2:$AL$4671;AM15;$AJ$2:$AJ$4671;$AO$2)
16	13	=COUNTIFS($AL$2:$AL$4671;AM16;$AJ$2:$AJ$4671;$AN$2)	=COUNTIFS($AL$2:$AL$4671;AM16;$AJ$2:$AJ$4671;$AO$2)
17	14	=COUNTIFS($AL$2:$AL$4671;AM17;$AJ$2:$AJ$4671;$AN$2)	=COUNTIFS($AL$2:$AL$4671;AM17;$AJ$2:$AJ$4671;$AO$2)
18	15	=COUNTIFS($AL$2:$AL$4671;AM18;$AJ$2:$AJ$4671;$AN$2)	=COUNTIFS($AL$2:$AL$4671;AM18;$AJ$2:$AJ$4671;$AO$2)
19	16	=COUNTIFS($AL$2:$AL$4671;AM19;$AJ$2:$AJ$4671;$AN$2)	=COUNTIFS($AL$2:$AL$4671;AM19;$AJ$2:$AJ$4671;$AO$2)
20	17	=COUNTIFS($AL$2:$AL$4671;AM20;$AJ$2:$AJ$4671;$AN$2)	=COUNTIFS($AL$2:$AL$4671;AM20;$AJ$2:$AJ$4671;$AO$2)
21	18	=COUNTIFS($AL$2:$AL$4671;AM21;$AJ$2:$AJ$4671;$AN$2)	=COUNTIFS($AL$2:$AL$4671;AM21;$AJ$2:$AJ$4671;$AO$2)
22	19	=COUNTIFS($AL$2:$AL$4671;AM22;$AJ$2:$AJ$4671;$AN$2)	=COUNTIFS($AL$2:$AL$4671;AM22;$AJ$2:$AJ$4671;$AO$2)
23	20	=COUNTIFS($AL$2:$AL$4671;AM23;$AJ$2:$AJ$4671;$AN$2)	=COUNTIFS($AL$2:$AL$4671;AM23;$AJ$2:$AJ$4671;$AO$2)
24	21	=COUNTIFS($AL$2:$AL$4671;AM24;$AJ$2:$AJ$4671;$AN$2)	=COUNTIFS($AL$2:$AL$4671;AM24;$AJ$2:$AJ$4671;$AO$2)
25	SUM	=SUM(AN3:AN24)	=SUM(AO3:AO24)

Appendix H: Calculating the Power Coefficients for the GWP and Hywind Turbines

The power coefficients are calculated for Hywind Demo 2.3 MW turbine and for GWP 750 kW turbine. The results are shown first, followed by the formulas. The difference in power curve and in swept area is taken into account. The rotor diameters are 85 meters and 47 meters.

Results:

	A	B	C	D
1	Swept area [m2]:	5674,50	Hywind 2.3 MW turbine	
2	Wind speed [m/s]	Power in the wind [kW]	Pturbine [kW]	Cp [-]
3	1	3	0	0
4	2	28	0	0
5	3	94	0	0
6	4	222	42	0,188814564
7	5	434	136	0,313036565
8	6	751	276	0,36763894
9	7	1192	470	0,394248375
10	8	1780	727	0,408536274
11	9	2534	1043	0,411645104
12	10	3476	1394	0,401078099
13	11	4626	1738	0,375697142
14	12	6006	2015	0,335503833
15	13	7636	2183	0,285884002
16	14	9537	2260	0,236968438
17	15	11730	2288	0,195051106
18	16	14236	2297	0,16134935
19	17	17076	2299	0,134635126
20	18	20270	2300	0,113468809
21	19	23839	2300	0,096479092
22	20	27805	2300	0,082718761
23	21	32188	2300	0,071455576
24	22	37009	2300	0,06214783
25	23	42288	2300	0,054388928
26	24	48047	2300	0,047869654
27	25	54307	2300	0,042352006
28	26	61088	0	0

	A	E	F	G
1	**Swept area [m2]:**	**1734,94**	**GWP 750 kW turbine**	
2	**Wind speed [m/s]**	**Power in the wind [kW]**	**Pturbine [kW]**	**Cp [-]**
3	1	1	0	0
4	2	9	0	0
5	3	29	4	0,139413406
6	4	68	25	0,367593941
7	5	133	55	0,414057815
8	6	230	96	0,418240217
9	7	364	160	0,438969324
10	8	544	246	0,452140547
11	9	775	345	0,44534838
12	10	1063	453	0,426291342
13	11	1414	546	0,386031636
14	12	1836	635	0,345810596
15	13	2335	714	0,305827451
16	14	2916	740	0,253779141
17	15	3586	750	0,209120109
18	16	4353	750	0,17230966
19	17	5221	750	0,143655682
20	18	6197	750	0,121018581
21	19	7289	750	0,102898435
22	20	8501	750	0,088222546
23	21	9841	750	0,076209952
24	22	11315	750	0,066282904
25	23	12929	750	0,058007756
26	24	14690	750	0,051054714
27	25	16604	750	0,045169943
28	26	18677	0	0

Formulas:

	A	B	C	D
1	**Swept area [m2]:**	=PI()*(42,5^2)	**Hywind 2.3 MW turbine**	
2	Wind speed [m/s]	Power in the wind [kW]	Pturbine [kW]	Cp [-]
3	1	=0,5*$B$1*1,225*(A3^3)/1000	0	=C3/B3
4	2	=0,5*$B$1*1,225*(A4^3)/1000	0	=C4/B4
5	3	=0,5*$B$1*1,225*(A5^3)/1000	0	=C5/B5
6	4	=0,5*$B$1*1,225*(A6^3)/1000	42	=C6/B6
7	5	=0,5*$B$1*1,225*(A7^3)/1000	136	=C7/B7
8	6	=0,5*$B$1*1,225*(A8^3)/1000	276	=C8/B8
9	7	=0,5*$B$1*1,225*(A9^3)/1000	470	=C9/B9
10	8	=0,5*$B$1*1,225*(A10^3)/1000	727	=C10/B10
11	9	=0,5*$B$1*1,225*(A11^3)/1000	1043	=C11/B11
12	10	=0,5*$B$1*1,225*(A12^3)/1000	1394	=C12/B12
13	11	=0,5*$B$1*1,225*(A13^3)/1000	1738	=C13/B13
14	12	=0,5*$B$1*1,225*(A14^3)/1000	2015	=C14/B14
15	13	=0,5*$B$1*1,225*(A15^3)/1000	2183	=C15/B15
16	14	=0,5*$B$1*1,225*(A16^3)/1000	2260	=C16/B16
17	15	=0,5*$B$1*1,225*(A17^3)/1000	2288	=C17/B17
18	16	=0,5*$B$1*1,225*(A18^3)/1000	2297	=C18/B18
19	17	=0,5*$B$1*1,225*(A19^3)/1000	2299	=C19/B19
20	18	=0,5*$B$1*1,225*(A20^3)/1000	2300	=C20/B20
21	19	=0,5*$B$1*1,225*(A21^3)/1000	2300	=C21/B21
22	20	=0,5*$B$1*1,225*(A22^3)/1000	2300	=C22/B22
23	21	=0,5*$B$1*1,225*(A23^3)/1000	2300	=C23/B23
24	22	=0,5*$B$1*1,225*(A24^3)/1000	2300	=C24/B24
25	23	=0,5*$B$1*1,225*(A25^3)/1000	2300	=C25/B25
26	24	=0,5*$B$1*1,225*(A26^3)/1000	2300	=C26/B26
27	25	=0,5*$B$1*1,225*(A27^3)/1000	2300	=C27/B27
28	26	=0,5*$B$1*1,225*(A28^3)/1000	0	=C28/B28

	A	E	F	G
1	**Swept area [m2]:**	=PI()*(23,5^2)	**GWP 750 kW turbine**	
2	Wind speed [m/s]	Power in the wind [kW]	Pturbine [kW]	Cp [-]
3	1	=0,5*1,225*$E$1*A3^3/1000	0	=F3/E3
4	2	=0,5*1,225*$E$1*A4^3/1000	0	=F4/E4
5	3	=0,5*1,225*$E$1*A5^3/1000	4	=F5/E5
6	4	=0,5*1,225*$E$1*A6^3/1000	25	=F6/E6
7	5	=0,5*1,225*$E$1*A7^3/1000	55	=F7/E7
8	6	=0,5*1,225*$E$1*A8^3/1000	96	=F8/E8
9	7	=0,5*1,225*$E$1*A9^3/1000	160	=F9/E9
10	8	=0,5*1,225*$E$1*A10^3/1000	246	=F10/E10
11	9	=0,5*1,225*$E$1*A11^3/1000	345	=F11/E11
12	10	=0,5*1,225*$E$1*A12^3/1000	453	=F12/E12
13	11	=0,5*1,225*$E$1*A13^3/1000	546	=F13/E13
14	12	=0,5*1,225*$E$1*A14^3/1000	635	=F14/E14
15	13	=0,5*1,225*$E$1*A15^3/1000	714	=F15/E15
16	14	=0,5*1,225*$E$1*A16^3/1000	740	=F16/E16
17	15	=0,5*1,225*$E$1*A17^3/1000	750	=F17/E17
18	16	=0,5*1,225*$E$1*A18^3/1000	750	=F18/E18
19	17	=0,5*1,225*$E$1*A19^3/1000	750	=F19/E19
20	18	=0,5*1,225*$E$1*A20^3/1000	750	=F20/E20
21	19	=0,5*1,225*$E$1*A21^3/1000	750	=F21/E21
22	20	=0,5*1,225*$E$1*A22^3/1000	750	=F22/E22
23	21	=0,5*1,225*$E$1*A23^3/1000	750	=F23/E23
24	22	=0,5*1,225*$E$1*A24^3/1000	750	=F24/E24
25	23	=0,5*1,225*$E$1*A25^3/1000	750	=F25/E25
26	24	=0,5*1,225*$E$1*A26^3/1000	750	=F26/E26
27	25	=0,5*1,225*$E$1*A27^3/1000	750	=F27/E27
28	26	=0,5*1,225*$E$1*A28^3/1000	0	=F28/E28